FLOOD ROUTING IN UNGAUGED CATCHMENTS USING MUSKINGUM METHODS

MH Tewolde

Submitted in fulfillment of the requirements
for the degree of Master of Science in hydrology

School of Bioresources Engineering and Environmental Hydrology
University of KwaZulu-Natal
Pietermaritzburg

2005

ABSTRACT

River stage or flow rates are required for the design and evaluation of hydraulic structures. Most river reaches are ungauged and a methodology is needed to estimate the stages, or rates of flow, at specific locations in streams where no measurements are available. Flood routing techniques are utilised to estimate the stages, or rates of flow, in order to predict flood wave propagation along river reaches. Models can be developed for gauged catchments and their parameters related to physical characteristics such as slope, reach width, reach length so that the approach can be applied to ungauged catchments in the region.

The objective of this study is to assess Muskingum-based methods for flow routing in ungauged river reaches, both with and without lateral inflows. Using observed data, the model parameters were calibrated to assess performance of the Muskingum flood routing procedures and the Muskingum-Cunge method was then assessed using catchment derived parameters for use in ungauged river reaches. The Muskingum parameters were derived from empirically estimated variables and variables estimated from assumed river cross-sections within the selected river reaches used.

Three sub-catchments in the Thukela catchment in KwaZulu-Natal, South Africa were selected for analyses, with river lengths of 4, 21 and 54 km. The slopes of the river reaches and reach lengths were derived from a digital elevation model. Manning roughness coefficients were estimated from field observations. Flow variables such as velocity, hydraulic radius, wetted perimeters, flow depth and top flow width were determined from empirical equations and cross-sections of the selected rivers. Lateral inflows to long river reaches were estimated from the Saint-Venant equation.

Observed events were extracted for each sub-catchment to assess the Muskingum-Cunge parameter estimation method and Three-parameter Muskingum method. The extracted events were further analysed using empirically estimated flow variables. The performances of the methods were evaluated by comparing both graphically and statistically the simulated and observed hydrographs. Sensitivity analyses were undertaken using three selected events and a 50% variation in selected input variables was used to identify sensitive variables.

The performance of the calibrated Muskingum-Cunge flood routing method using observed hydrographs displayed acceptable results. Therefore, the Muskingum-Cunge flood routing method was applied in ungauged catchments, with variables estimated empirically. The results obtained shows that the computed outflow hydrographs generated using the Muskingum-Cunge method, with the empirically estimated variables and variables estimated from cross-sections of the selected rivers resulted in reasonably accurate computed outflow hydrographs with respect to peak discharge, timing of peak flow and volume.

From this study, it is concluded that the Muskingum-Cunge method can be applied to route floods in ungauged catchments in the Thukela catchment and it is postulated that the method can be used to route floods in other ungauged rivers in South Africa.

DECLARATION

I declare that the work reported in this thesis is my own original and unaided work except where specific acknowledgement is made.

Signed:  Date: 26 / 10 / 2005

Mesfin H Tewolde

ACKNOWLEDGEMENTS

I would like to express my sincere gratitude for the assistance given by the following:

Prof. Jeff Smithers, School of Bioresources Engineering and Environmental Hydrology, University of KwaZulu-Natal, for his supervision and guidance throughout this study as well as his full support to accomplish the research;

Prof. Roland Schulze, School of Bioresources Engineering and Environmental Hydrology, University of KwaZulu-Natal, for his co-supervision and guidance throughout this study;

Mrs Tinisha Chetty, School of Bioresources Engineering and Environmental Hydrology, University of KwaZulu-Natal, for her co-operation and support in this work;

Mr Mark Horan, School of Bioresources Engineering and Environmental Hydrology, University of KwaZulu-Natal, for assistance with the GIS mapping software package;

Mrs Manjulla Maharaj, School of Bioresources Engineering and Environmental Hydrology, University of KwaZulu-Natal, for her assistance in FORTRAN programming;

Dr Fethi Ahmed, School of Applied Environmental Sciences, University of KwaZulu-Natal, for teaching me GIS, providing reference materials and for his friendly guidance;

Mr Riyad Ismail, School of Applied Environmental Sciences, University of KwaZulu-Natal, for providing information of hydrology related GIS sources and reference material;

The librarians of the University of KwaZulu-Natal for making books available and for their assistance;

The Department of Water Affairs and Forestry for providing flow data on their World Wide Web site;

The office of the Ministry of Agriculture, Eritrea and the Eritrean Human Resource Development Program office of University of Asmara, Eritrea for awarding the scholarship for this study;

The Eritrean Human Resource Development Program office of the University of Asmara, Eritrea and the Water Resources Commission, South Africa for funding the study;

The School of Bioresources Engineering and Environmental Hydrology, University of KwaZulu-Natal, for assistance and financial support;

Thanks to my parents who instilled in me the value of hard work and who supported me in all of my endeavours and achievements; and

The staff and postgraduate students of School of Bioresources Engineering and Environmental Hydrology, University of KwaZulu-Natal for their encouragement and friendly support.

TABLE OF CONTENTS

LIST OF TABLES

Page

LIST OF FIGURES

Page

LIST OF ABBREVIATIONS

ACRU	=	Agricultural Catchment Research Unit
ASAE	=	American Society of Agricultural Engineers
ASCE	=	American Society of Civil Engineers
AWRA	=	American Water Research Association
BEEH	=.	School of Bioresources Engineering and Environmental Hydrology
Catch	=	Catchment
DEM	=	Digital Elevation Model
DWAF	=	Department of Water Affairs and Forestry
EHRDP	=	Eritrean Human Resource Development Program
GIS	=	Geographical Information System
G.Sta.	=	Gauging Station
HIS	=	Hydrological Information System
IAHR	=	International Association of Hydrological Sciences
KZN	=	KwaZulu-Natal
M-Ma	=	Muskingum Matrix method
M-Cal	=	Muskingum-Cunge Calibrated
MC-E	=	Muskingum-Cunge with Empirical Equation
MC-X	=	Muskingum-Cunge with assumed Cross-sections
MAP	=	Mean Annual Precipitation
MAR	=	Mean Annual Rainfall
MTU	=	Michigan Technological University
NERC	=	Natural Environment Research Council
NRCS	=	Natural Resources Conservation Service
RMSE	=	Root Mean Square Error
RSA	=	Republic of South Africa
SAICEHS	=	Science Applications International Corporation Environmental & Health Science
USSCS	=	United States Soil Conservation Service
UK	=	United Kingdom
USA	=	United States of America
TASAE	=	Tsukuba Asian Seminar on Agricultural Education
TASCE	=	Transaction American Society of Civil Engineers

1. INTRODUCTION

As defined by Fread (1981) and Linsley *et al.* (1982), flood routing is a mathematical method for predicting the changing magnitude and celerity of a flood wave as it propagates down rivers or through reservoirs. Numerous flood routing techniques, such as the Muskingum flood routing methods, have been developed and successfully applied to a wide range of rivers and reservoirs (France, 1985). Generally, flood routing methods are categorised into two broad, but somewhat related applications, namely reservoir routing and open channel routing (Lawler, 1964). These methods are frequently used to estimate inflow or outflow hydrographs and peak flow rates in reservoirs, river reaches, farm ponds, tanks, swamps and lakes (NRCS, 1972; Viessman *et al.*, 1989; Smithers and Caldecott, 1995).

Flood routing is important in the design of flood protection measures in order to estimate how the proposed measures will affect the behaviour of flood waves in rivers so that adequate protection and economic solutions can be found (Wilson, 1990). In practical applications, the prediction and assessment of flood level inundation involves two steps. A flood routing model is used to estimate the outflow hydrograph by routing a flood event from an upstream flow gauging station to a downstream location. Then the flood hydrograph is input to a hydraulic model in order to estimate the flood levels at the downstream site (Blackburn and Hicks, 2001).

Flood routing procedures may be classified as either hydrological or hydraulic (Choudhury *et al.*, 2002). Hydrological methods use the principle of continuity and a relationship between discharge and the temporary storage of excess volumes of water during the flood period (Shaw, 1994). Hydraulic methods of routing involve the numerical solutions of either the convective diffusion equations or the one–dimensional Saint–Venant equations of gradually varied unsteady flow in open channels (France, 1985).

Several factors should be considered when evaluating which routing method is the most appropriate for a given situation. According to the US Army Corps of Engineers (1994a), the factors that should be considered in the selection process include, *inter alia*, backwater effects, floodplains, channel slope, hydrograph characteristics, flow network, subcritical and supercritical flow. The selection of a routing model is also influenced by other factors such as

the required accuracy, the type and availability of data, the available computational facilities, the computational costs, the extent of flood wave information desired, and the familiarity of the user with a given model (NERC, 1975; Fread, 1981).

The hydraulic methods generally describe the flood wave profile more adequately when compared to hydrological techniques, but practical application of hydraulic methods are restricted because of their high demand on computing technology, as well as on quantity and quality of input data (Singh, 1988). Even when simplifying assumptions and approximations are introduced, the hydraulic techniques are complex and often difficult to implement (France, 1985). Studies have shown that the simulated outflow hydrographs from the hydrological routing methods always have peak discharges higher than those of the hydraulic routing methods (Haktanir and Ozmen, 1997). However, in practical applications, the hydrological routing methods are relatively simple to implement and reasonably accurate (Haktanir and Ozmen, 1997). An example of a simple hydrological flood routing technique used in natural channels is the Muskingum flood routing method (Shaw, 1994).

Among the many models used for flood routing in rivers, the Muskingum model has been one of the most frequently used tools, because of its simplicity (Tung, 1985). As noted by Kundzewicz and Strupczewski (1982), the Muskingum method of flood routing has been extensively applied in river engineering practices since its introduction in the 1930s. The modification and the interpretation of the Muskingum model parameters in terms of the physical characteristics, extends the applicability of the method to ungauged rivers (Kundzewicz and Strupczewski, 1982). Most catchments are ungauged and thus a methodology to compute the flood wave propagation down a river reach or through a reservoir is required. One option is to develop models for gauged catchments and relate their parameters to physical characteristics (Kundzewicz, 2002). The approach for flood routing then can be applied to ungauged catchments in the region (Kundzewicz, 2002).

In this study, the Muskingum-Cunge method is adopted to estimate the model parameters because of its simplicity as well as its ability to perform flood routing in ungauged catchments by estimating the model parameters from flow and channel characteristics. The Muskingum-Cunge parameter estimation method utilises catchment variables such as flow top width (W), slope (S), average velocity (V_{av}), discharge (Q_0), celerity (V_w), and catchment length (L) to estimate the parameters of the Muskingum method.

When performing flood routing in ungauged catchments, the model parameters have to be estimated without observed hydrographs. The inflow hydrograph could be generated using a hydrological model such as the ACRU model (Schulze, 1995). For this study, the observed hydrographs are used to simulate an outflow hydrograph.

The objectives of this study are thus to:

(i) Assess the performance of the Muskingum method, both with and without lateral inflow, using calibrated parameters.

(ii) Assess the performance of the Muskingum-Cunge method in ungauged catchments using derived parameters, derived by:

(a) using variables estimated from empirical equations developed for different river reaches, and

(b) using variables estimated from assumed cross-sections within the river reach.

To understand the Muskingum flood routing methods, relevant literature was reviewed and is presented in Chapter 2. The literature review contained in Chapter 2 includes the basic Muskingum method, the Muskingum-Cunge method, the Three-Parameter Muskingum method, the Non-Linear Muskingum method, and the SCS Convex method as well as channel discharge relationships. Catchment selection and location, gauge selection, catchment descriptions and flow data analyses are included in Chapter 3. Details of assumptions made in the flow analysis, calculation steps to estimate the Muskingum flood routing parameters and methodology adopted in the study are contained in Chapter 4. The performance of the Muskingum method, both with calibrated parameters and in ungauged river reaches, and the sensitivity of the Muskingum flood routing parameters to different catchment variables are presented in Chapter 5. Discussion of the different Muskingum flood routing methods and conclusions are contained in Chapter 6. Finally, recommendations for further research are presented in Chapter 7.

2. MUSKINGUM CHANNEL ROUTING METHODS

The Muskingum model was first developed by McCarthy (1938, cited by Mohan, 1997), for flood control studies in the Muskingum River basin in Ohio, USA. As perceived by Choudhury *et al.* (2002) and Singh and Woolhiser (2002), this method is still one of the most popular methods used for flood routing in several catchment models.

2.1 The Basic Muskingum Flood Routing Method

Generally, the inflow hydrograph used in flood routing is obtained by converting a measured stage into discharge using a steady state rating curve (Mutreja, 1986; Perumal and Raju, 1998; Moramarco and Singh, 2001).

As depicted by Shaw (1994), storage in a river reach may be explained in three possible forms as shown in Figure 2.1. During the rising stage of a flood in the reach, when inflow is greater than outflow, the wedge storage must be added to the prism storage. During the falling stage when inflow is less than the outflow, the wedge storage is negative and it has to be subtracted from the prism storage to obtain the total temporary storage in the reach. In a reach when the outflow and inflow are equal, the only storage present in the channel is the prism storage.

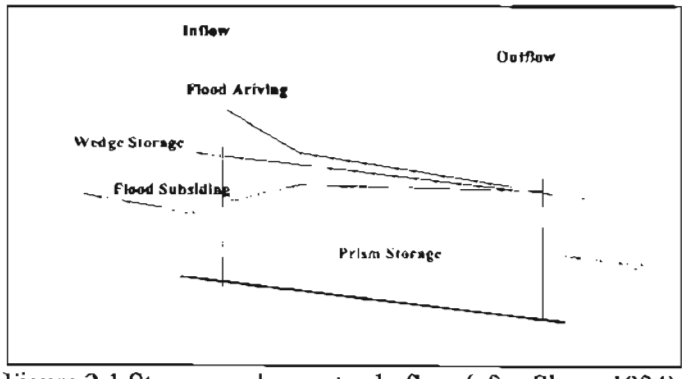

Figure 2.1 Storage and non-steady flow (after Shaw, 1994)

An example of inflow and outflow hydrographs to and from a reach at prism storage is shown in Figure 2.2. In a river reach with a uniform cross-section and an unvarying slope there is no

change in velocity, implying that the flow is a uniform flow (Chow, 1959). In such reaches the outflow hydrograph peak lies on the recession curve of the inflow hydrograph (Shaw, 1994).

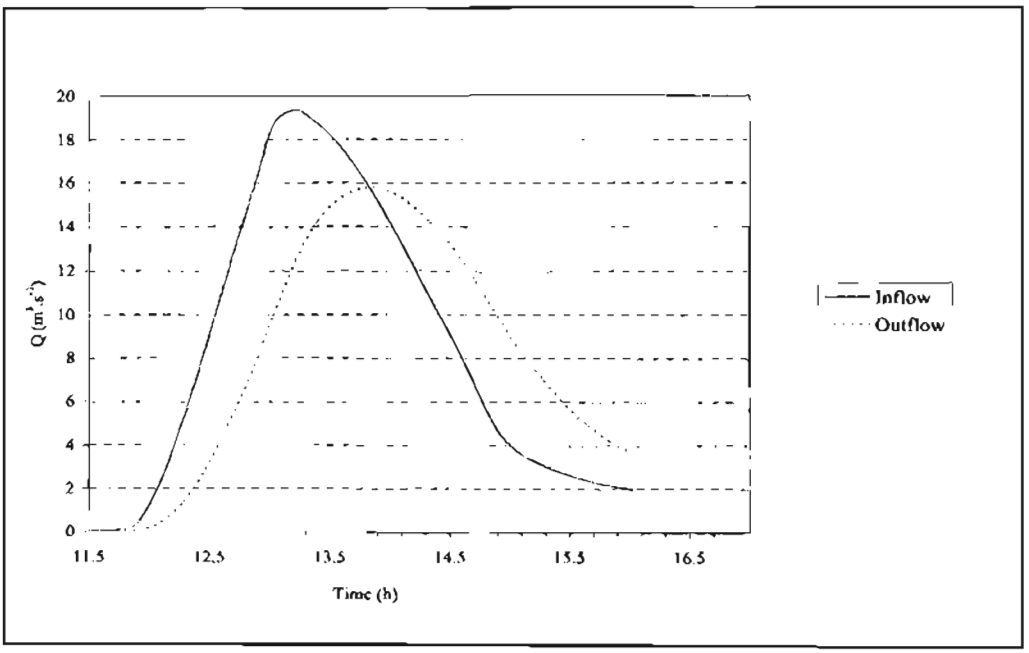

Figure 2.2 Example of inflow and outflow hydrographs

According to Tung (1985) and Fread (1993), the most common form of the linear Muskingum model is expressed as the following equations:

$$S_p = KQ_t \tag{2.1}$$

$$S_w = K\,(I_t - Q_t)\,X \tag{2.2}$$

where

S_p = temporary prism storage [m^3],

S_w – temporary wedge storage [m^3],

I_t = the rate of inflow [$m^3.s^{-1}$] at time = t,

Q_t = outflow [$m^3.s^{-1}$] at time = t,

K – the storage time constant for the river reach which has a value close to the wave travel time within the river reach [s], and

X = a weighting factor varying between 0 and 0.5 [dimensionless].

By combining Equations 2.1 and 2.2, the basic Muskingum equation is attained as given in Equations 2.3a and 2.3b:

$$S_t = S_p + S_w \tag{2.3a}$$

$$S_t = K\,[XI_t + (1 - X)\,Q_t] \tag{2.3b}$$

where

S_t = temporary channel storage in [m^3] at time t,

S_p = prism storage at a time t, and

S_w = wedge storage at a time t.

When X = 0, Equation 2.3 reduces to $S_t = KQ_t$, indicating that storage is a function of only outflow. When X = 0.5, equal weight is given to inflow and outflow, and the condition is equivalent to a uniformly progressive wave that does not attenuate (US Army Corps of Engineers, 1994a). Thus, 0.0 and 0.5 are limits on the value of X, and within this range the value of X determines the degree of attenuation of a flood wave as it passes through the routing reach (US Army Corps of Engineers, 1994a).

Fread (1993) explained that a simplified description of unsteady flow along a routing reach may be depicted as being a lumped process, in which the inflow at the upstream end, and the outflow at the down stream end of the reach are functions of time. In Muskingum flood routing, it is assumed that the storage in the system at any moment is proportional to a weighted average inflow and outflow from a given reach (Bauer, 1975).

Based on the continuity equation (Equation 2.4), the rate of change of storage in a channel with respect to time is equal to the difference between inflow and outflow (Shaw, 1994):

$$\frac{\Delta S_t}{\Delta t} = I_t - Q_t \tag{2.4}$$

where

$\frac{\Delta S_t}{\Delta t}$ = the rate of change of channel storage with respect to time.

The combination and solution of Equations 2.3 and 2.4 in finite difference form results in the well known Muskingum flow routing equations presented in Equations 2.5 and 2.6.

$$Q_{j+1}^{t+1} = C_0 I_j^t + C_1 I_j^{t+1} + C_2 Q_{j+1}^t \tag{2.5}$$

where

Q_j^t = outflow at time [t] of the j th sub-reach, and

I_j^t = inflow at time [t] of the j th sub-reach.

The three coefficients (C_0, C_1, and C_2) are calculated as:

$$C_0 = (\Delta t + 2KX)/m \tag{2.6a}$$

$$C_1 = (\Delta t - 2KX)/m \tag{2.6b}$$

$$C_2 = (2K(1-X) - \Delta t)/m \tag{2.6c}$$

$$m = 2K(1-X) + \Delta t \tag{2.6d}$$

where C_0, C_1 and C_2 are coefficients that are functions of K and X, and a discretised time interval Δt. The sum of C_0, C_1 and C_2 is equal to one, thus when C_0 and C_1 have been calculated then C_2 may be derived as $1\text{-}C_0\text{-}C_1$. Thus, the outflow at the end of a time step is the weighted sum of the starting inflow and outflow as well as the ending inflow (Shaw, 1994). The three coefficients (C_0, C_1, and C_2) are constant throughout the routing procedures (Fread, 1993).

As Viessman *et al.* (1989) suggested, negative values of C_1 must be avoided. Negative values of C_1 are avoided when Equation 2.7 is satisfied. Negative values of C_2 do not affect the flood-routed hydrographs (Viessman *et al.* 1989).

$$\frac{\Delta t}{K} > 2X \tag{2.7}$$

where

Δt = change in time [s],

K = the storage time constant for the river reach, which has a value close to the wave travel time within the river reach [s], and

X = a weighting factor varying between 0 and 0.5 [dimensionless].

After the X parameter is determined, the routing time interval should be checked again using the relationship shown in Figure 2.3 (Cunge, 1969; cited by NERC, 1975).

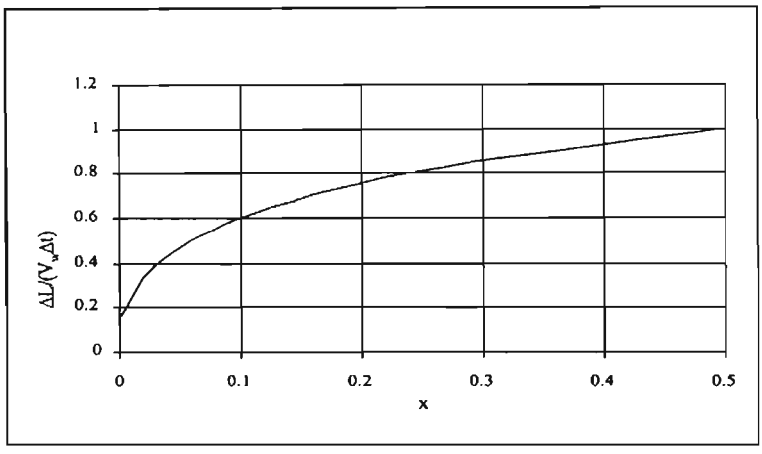

Figure 2.3 Cunge curve (Cunge, 1969 cited by NERC, 1975)

The time Δt is called the routing period and it must be chosen sufficiently small such that the assumption of flow rate linearity over time interval Δt is approximated (Gill, 1992). In particular, if Δt is too large, it is possible to miss the peak of the inflow curve, so the period should be kept smaller than 1/5 of the travel time of the flood peak through the reach (Wilson, 1990). According to Viessman *et al.* (1989), theoretical stability of the numerical method is accomplished if Equation 2.8 is fulfilled:

$$2KX \leq \Delta t \leq 2K(1-X) \qquad (2.8)$$

Viessman *et al.* (1989) and Fread (1993) noted that the routing time interval (Δt) is frequently assigned any convenient value between the limits of $(K/3) \leq \Delta t \leq K$. The analysis of many flood waves indicates that the time required for the centre of mass of the flood wave to pass from the upstream end of the reach to the down stream end is equal to K (Viessman *et al.*,

1989). The value of K can thus be estimated using gauged inflow and outflow data and with much greater ease and certainty than that of the X parameter (Viessman *et al.*, 1989; Wilson, 1990). Among other factors in a catchment that influence the travel time (K), the most important are: drainage pattern, surface geology, soil type, catchment shape and vegetal cover (Bauer and Midgley, 1974). None of these are readily expressible numerically, but to a large extent the factors are interdependent and can be generalised on a regional basis (Bauer and Midgley, 1974). Most researchers agree that the effectiveness of the Muskingum flood routing method depends on the accuracy of estimation of the K and X parameters (Singh and McCann, 1980; Wilson and Ruffin, 1988).

In order to determine the K and X parameters using observed inflow and outflow hydrographs, Equation 2.5 is used (Shaw, 1994). If observed inflow and outflow hydrographs are available for the reach, and since S_t and $[XI_t + (1-X)\ Q_t]$ are assumed to be related via Equation 2.3, a graphical procedure to estimate K and X parameters may be implemented by assuming different values of X (Chow *et al.*, 1988). The accepted value of X will then be that value of X that gives the best linear and narrowest loop (Gill, 1978; Fread, 1993). For example, in Figure 2.4, K is taken as the slope of the straight line of the narrowest loop (X = 0.3) (Heggen, 1984). The shortcomings of the graphical method include the time required to construct the plots for alternative Xs, visual subjectivity and the sensitivity of X in short reaches (Heggen, 1984; O'Donnell *et al.*, 1988; Gelegenis and Sergio, 2000).

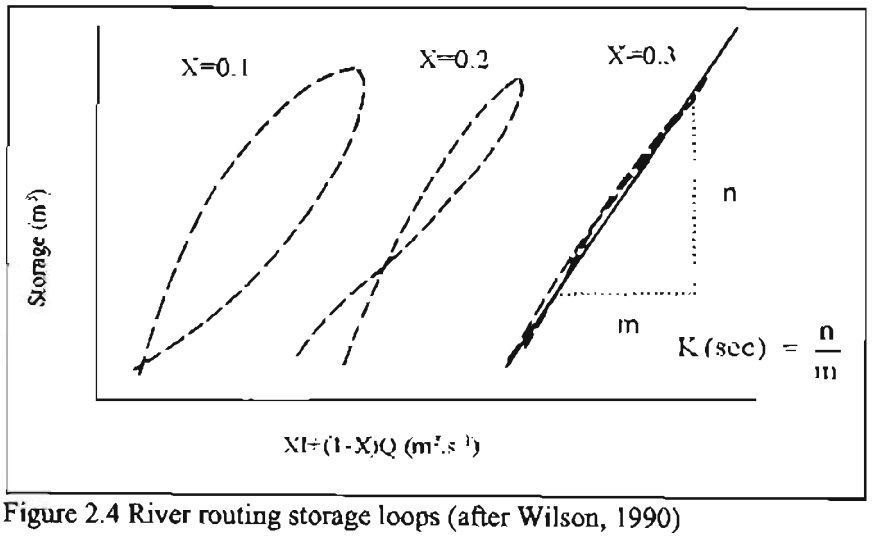

Figure 2.4 River routing storage loops (after Wilson, 1990)

The peak outflow does not lie on the inflow recession curve due to the effect of the wedge storage in streams (Shaw, 1994). As shown in Figure 2.5, the simulated outflow hydrograph is not a good reconstruction of the observed outflow. This may happen when the relationships shown in Equation 2.8 between K, X and Δt are not satisfied (Gill, 1992).

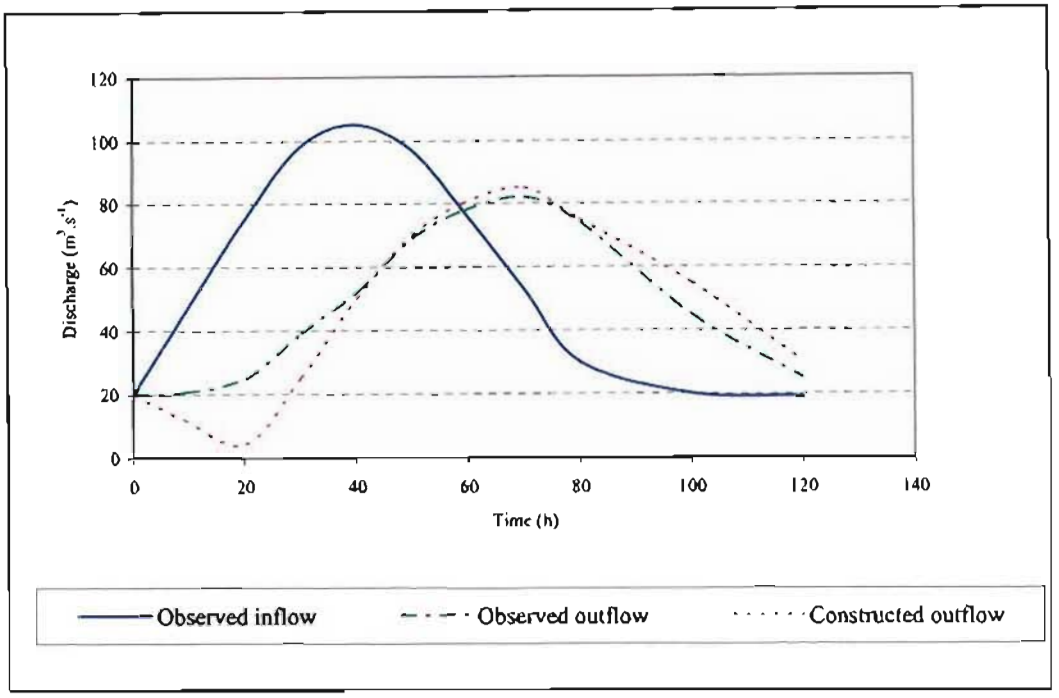

Figure 2.5 Muskingum routed hydrographs (after Shaw, 1994)

The basic Muskingum equation formulation is applicable to a single reach having no lateral inflow into the routing reach (Choudhury *et al.*, 2002). In most rivers, this constrains the routing reaches to be rather short, generally terminating at tributaries, and requires gauged or estimated tributary inflows to be added to the main channel flow (O'Donnell, 1985). If there is lateral inflow in the form of substantial tributaries, the routing reaches may be chosen to terminate at a confluence, augmenting the main channel flow by the tributary flow for the next reach (O'Donnell, 1985). As explained by Fread (1993) and the US Army Corps of Engineers (1994a), the original Muskingum method is limited to moderate to slow rising hydrographs being routed through mild to steep sloping channels. The method is not applicable to steeply rising hydrographs such as dam breaks and ice breaks, where acceleration and momentum predominate, and the method neglects variable backwater effects such as downstream dams, constrictions, bridges and tidal influences (O'Donnell *et al.*, 1988; Gelegenis and Sergio, 2000).

One of the disadvantages with hydrological methods of flow routing is that they assume a unique relationship between stage and discharge along the reach, even though the same discharge may have different flood levels at rising and falling stages (NERC, 1975). This phenomenon is indicated graphically in the well-known loop-rating curve as shown in Figure 2.6.

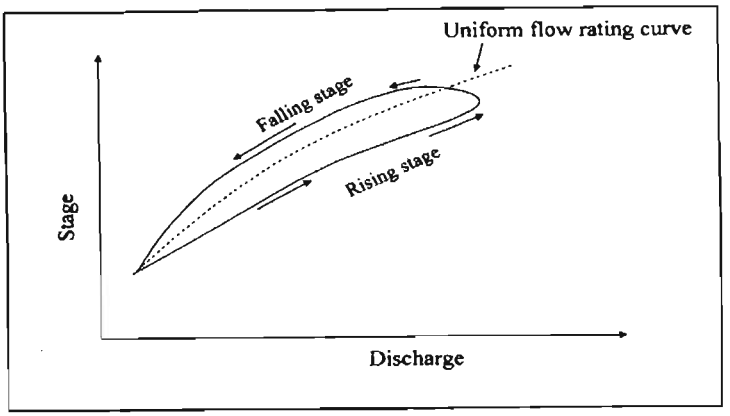

Figure 2.6 Loop-rating curve (after NERC, 1975)

2.2 The Muskingum–Cunge Parameter Estimation Method with Lateral Inflow

The original Muskingum method is based on the storage equation with the coefficients K and X derived by trial and error (O'Donnell *et al.*, 1988; Gelegenis and Sergio, 2000). Unlike the basic Muskingum method where the parameters are calibrated using observed stream flow data, in the Muskingum-Cunge method parameters are calculated based on flow and channel characteristics (Ponce, 1989). Hence, in the absence of observed flow data, the Muskingum-Cunge method may be used for parameter estimation (Smithers and Caldecott, 1993).

Equations 2.9 and 2.10 are used in the physically-based Muskingum-Cunge method to estimate the K and X parameters (Chow, 1959; Fread, 1993):

$$K = \frac{\Delta L}{V_w} \tag{2.9}$$

$$X = \frac{1}{2} - \frac{Q_0}{2SWV_w\Delta L} \tag{2.10}$$

where

Q_0 = reference discharge [$m^3.s^{-1}$],

S = dimensionless channel bottom slope [$m.m^{-1}$],

V_w = kinematic wave celerity [$m.s^{-1}$],

ΔL = routing reach length [m],

W = water surface width [m],

K = the storage time constant for the river reach, which has a value close to the wave travel time within the river reach [s], and

X = a weighting factor varying between 0.0 and 0.5 [dimensionless].

As evident from Equations 2.9 and 2.10, the Muskingum-Cunge K and X parameters are obtained using variables such as the top width of the river, wave celerity, reach cross-section area, reach length and reach slope. The relation of the Muskingum K and X parameters to the catchment characteristics makes the Muskingum-Cunge method suitable to be applied to ungauged streams (Ponce, 1989). The Muskingum-Cunge method can simulate the celerity and diffusion of flood waves in a practical and accurate manner (Ponce and Yevjevich 1978; Ponce *et al.*, 1996). The Muskingum flood routing models do not consider backwater effects, nor are they well suited for very mild sloping waterways where looped stage-discharge rating may exist (Fread, 1981; Feng and Xiaofang, 1999).

According to Wilson and Ruffin (1988), the reference discharge may be estimated as:

$$Q_0 = Q_b + 0.5\,(Q_p - Q_b) \tag{2.11}$$

where

Q_0 = reference discharge [$m^3.s^{-1}$],

Q_b = base flow taken from the inflow hydrograph [$m^3.s^{-1}$], and

Q_p = peak inflow [$m^3.s^{-1}$].

The kinematic wave celerity, defined as the slope of the discharge-area rating curve, may be estimated using Equation 2.12 (Chow, 1959):

$$V_w = \left(\frac{\Delta Q}{\Delta A}\right) \tag{2.12}$$

where

ΔA = change in cross-sectional area [m^2].

In large catchments, where there is a lateral inflow to the main stream, the volume of the outflow hydrograph may be larger than the inflow volume. Hence, lateral inflow should be considered and added to the main flow as follows (NERC, 1975):

$$Q_{j+1}^{l+1} = C_0 I_j^l + C_1 I_j^{l+1} + C_2 Q_{j+1}^l + C_3 \qquad (2.13)$$

Equation 2.13 is an extension of Equation 2.5, once the K and X parameters are determined the C_0, C_1 and C_2 coefficients can be determined from Equation 2.6.

The C_3 coefficient, calculated using Equation 2.14, is added as a lateral inflow term in Equation 2.13 (NERC, 1975):

$$C_3 = \frac{q * \Delta t * \Delta L}{2K(1-X) + \Delta t} \qquad (2.14)$$

Flows associated with lateral inflow that are not routed in the main channel, may be added using Equations 2.14 and 2.15 (Fread, 1993). The total lateral flow, per unit length, has an assumed time distribution along the reach and specified at intervals of Δt (NERC, 1975). Backwater effects are ignored and lateral flows are assumed to enter proportionally along the main reach (Fread, 1993).

The Saint-Venant Equation for gradually varying flow in open channels is given as follows (NERC, 1975):

$$q = \frac{\Delta A}{\Delta t} + \frac{\Delta Q}{\Delta L} \qquad (2.15a)$$

where

q = lateral inflow [$m^2.s^{-1}$] per unit length (m) at time t [s],
ΔQ = change in discharge [$m^3.s^{-1}$],
Δt = change in time [s], and
ΔL = change in length [m].

Fread (1998) approximated the terms in Equation 2.15a as:

$$\frac{\Delta A}{\Delta t} \cong \frac{\frac{A_j^{t+1} + A_{j+1}^{t+1}}{2} - \frac{A_j^t + A_{j+1}^t}{2}}{\Delta t} \qquad (2.15b)$$

$$\frac{\Delta Q}{\Delta L} \cong \frac{\beta(Q_{j+1}^{t+1} - I_j^{t+1}) + (1-\beta)(Q_{j+1}^t - I_j^t)}{\Delta L} \qquad (2.15c)$$

where

β = weighing factor, which is between 0.5 – 1 (Fread, 1998), and

A_j^t = cross sectional area [m^2] at time [t] of the j th sub-reach.

Hence, lateral flow per unit (q) can be calculated from:

$$q = \frac{\frac{A_j^{t+1} + A_{j+1}^{t+1}}{2} - \frac{A_j^t + A_{j+1}^t}{2}}{\Delta t} + \frac{\beta(Q_{j+1}^{t+1} - I_j^{t+1}) + (1-\beta)(Q_{j+1}^t - I_j^t)}{\Delta L} \qquad (2.15d)$$

When the ratio of lateral inflow to the main flow is too large, numerical difficulties in solving Equation 2.15c may arise. Increasing the routing length (ΔL_j) of the specified reach may solve the numerical difficulties (Fread, 1993).

In channel routing, the travel time through a river reach may be larger than the routing interval Δt selected to meet the limits in Equation 2.8. When this occurs, the channel must be broken down into sub-reaches with smaller routing steps to simulate the flood wave movement and changes in hydrograph shape (US Army Corps of Engineers, 1994a). An initial estimate of the number of routing steps may be obtained by dividing the total travel time (K) by the routing interval time (Δt). According to the US Army Corps of Engineers (1994a), a general rule of thumb is that the computation interval should be less than 1/5 of the time of rise of the inflow hydrograph. As noted by Reed (1984), the space and time steps chosen should approximate Equation 2.16a:

$$\Delta t \geq 1.625\mu / V_w \text{ and } 2.6\mu / V_w \leq \Delta L \leq 1.6 V_w \Delta t \qquad (2.16a)$$

where

$$\mu = \frac{Q_0}{2WS}$$

μ = hydraulic diffusivity [$m^2.s^{-1}$],

Q_0 = reference discharge [$m^3.s^{-1}$],

W = top flow width in [m], and

S = bottom slope [$m.m^{-1}$].

Fread (1993) also suggested that the length can be estimated from Equation 2.16b.

$$\Delta L \cong 0.5 V_w \Delta t \left[1 + \left(1 + 1.5 \frac{Q_0}{V_w^2 S \, \Delta t} \right)^{1/2} \right] \qquad (2.16b)$$

2.3 The Three–parameter Muskingum Procedure with Lateral Inflow

The Three–parameter Muskingum procedure is a method based upon the three-parameter Muskingum model, where the two conventional parameters are augmented by a third parameter to account for lateral inflow into the reach (O'Donnell *et al.,* 1988). O'Donnell (1985) incorporated a third parameter (α) assuming direct relationship between lateral inflow and main channel flow. Figure 2.7 shows the lateral inflow model. In the Three-parameter Muskingum method, the α parameter is multiplied by the stream inflow term and added as a lateral inflow to the main flow as shown in Equation 2.17:

$$I_t(1+\alpha) = Q_t + \frac{dS}{dt} \qquad (2.17)$$

and

$$S_t = K[X(1+\alpha)I_t + (1-X)Q_t] \qquad (2.18)$$

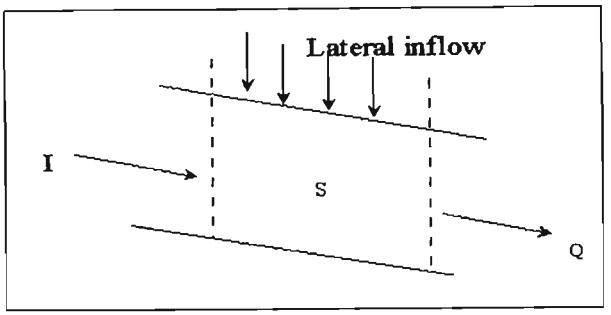

Figure 2.7 Lateral inflow model (after O'Donnell *et al.*, 1988)

In matrix formulation, the basic Muskingum routing Equation 2.5 may be written as (O'Donnell, 1985):

$$|Q_{t+1}| = |I_t, I_{t+1}, Q_t| * |d_i| \tag{2.19}$$

where

Q_{t+1} = outflow in [$m^3.s^{-1}$] for time step t+1,
I_t = inflow for time step t [$m^3.s^{-1}$],
I_{t+1} = inflow for time step t+1 [$m^3.s^{-1}$], and
d_i = the i th coefficient [dimensionless], $0 < i \leq 3$.

The matrix inversion using the least squares solution of Equation 2.19 yields the three d_i coefficients, and hence the K and X parameters (O'Donnell *et al*, 1988). The d_i coefficients are sufficient for reconstruction of an outflow hydrograph using Equation 2.19.

As O'Donnell *et al.* (1988) noted, the three parameters K, X and α can be derived from equations where the two sets (d_0, d_1, d_2 and K, X, α) of parameters are directly linked as shown in Equation 2.20.

$$d_0 = (1+\alpha)(\Delta t + 2KX)/N = (1+\alpha)C_0 \tag{2.20a}$$

$$d_1 = (1+\alpha)(\Delta t - 2KX)/N = (1+\alpha)C_1 \tag{2.20b}$$

$$d_2 = (2K(1-X) - \Delta t)/N = C_2 \tag{2.20c}$$

$$N = 2K(1-X) + \Delta t \tag{2.20d}$$

and

$$K = \Delta t\left(\frac{d_0 + d_1 d_2}{(1-d_2)(d_0 + d_1)}\right) \tag{2.21a}$$

$$X = \frac{1}{2}\left(1 - \frac{d_1 + d_0 d_2}{d_0 + d_1 d_2}\right) \tag{2.21b}$$

$$\alpha = \frac{(d_0 + d_1 + d_2 - 1)}{(1-d_2)} \tag{2.21c}$$

where

K = wave travel time [s],

X = weighting parameter [dimensionless],

Δt = time step[s],

α = the third extended parameter [dimensionless],

d_i = the i th coefficient [dimensionless], $0 < i \leq 3$, and

C_i = the i th coefficient [dimensionless], $0 < i \leq 3$.

As noted by O'Donnell (1985), if there is no lateral inflow, then α is equal to zero; when there is a lateral outflow α would have a negative value.

This modified method has three further advantages (O'Donnell, 1985):

(i) It replaces the tedious and subjective graphical trial and error estimation of the K and X parameter values with a numerical and direct best-fit solution technique.

(ii) By treating the whole river as a single reach, it avoids the need for multiple routings and multiple parameter determinations over many sub-reaches.

(iii) It allows for lateral inflow (if any), and it finds the routing coefficients directly.

The matrix analysis and simple lateral inflow model was applied by O'Donnell (1985), to a standard test event and to several events on two rivers in the United Kingdom, with reasonably encouraging success (O'Donnell, 1985). A summary of this study is contained in Section 2.4.

Aldama (1990) introduced in O'Donnell's method by eliminating C_0 in the Muskingum routing Equation 2.5 and the estimated outflow is computed as:

$$Q_{j+1} = I_{j+1} + C_1(I_j - I_{j+1}) + C_2(Q_j - I_{j+1}) \tag{2.22a}$$

The least square solution derived by Aldama (1990) is:

$$C_1 = D^{-1}\left\{\begin{array}{l}\left[\sum_{j=1}^{N}(Q_j - I_{j+1})^2\right]\left[\sum_{j=1}^{N}(I_j - I_{j+1})(Q_{j+1} - I_{j+1})\right] \\ -\left[\sum_{j=1}^{N}(I_j - I_{j+1})(Q_j - I_{j+1})\right]\left[\sum_{j=1}^{N}(Q_j - I_{j+1})(Q_{j+1} - I_{j+1})\right]\end{array}\right\} \tag{2.22b}$$

$$C_2 = D^{-1}\left\{\begin{array}{l}\left[\sum_{j=1}^{N}(I_j - I_{j+1})^2\right]\left[\sum_{j=1}^{N}(Q_j - I_{j+1})(Q_{j+1} - I_{j+1})\right] \\ -\left[\sum_{j=1}^{N}(I_j - I_{j+1})(Q_j - I_{j+1})\right]\left[\sum_{j=1}^{N}(I_j - I_{j+1})(Q_{j+1} - I_{j+1})\right]\end{array}\right\} \tag{2.22c}$$

where

$$D = \left\{\begin{array}{l}\left[\sum_{j=1}^{N}(I_j - I_{j+1})^2\right]\left[\sum_{j=1}^{N}(Q_j - I_{j+1})^2\right] \\ -\left[\sum_{j=1}^{N}(I_j - I_{j+1})(Q_j - I_{j+1})\right]^2\end{array}\right\} \tag{2.22d}$$

Reducing the C_o term in the above equations of Aldam (1990) reduce variables so that K and X parameters may be determined from C_1 and C_2 only as shown below:

$$K = \frac{C_1 + C_2}{1 - C_2}\Delta t \tag{2.22e}$$

and

$$X = 1 - \frac{1 + C_2}{2(C_1 - C_2)} \tag{2.22f}$$

2.4 Application of the Three-parameter Muskingum Model (Matrix)

In a study conducted on two British rivers, the Wye (75 km reach length) and the Wyre (25 km reach length), O'Donnell *et al.* (1988) showed the dependency of the α parameter on individual flood events and recommended that further studies should investigate the α values in relation to storm rainfall distribution. The very different ranges of α values for different hydrographs imply radically different catchment drainage behaviour and/or spatial storm distribution patterns. Other observations from the study include the following:

(i) For small flood events, the three-parameter method would seem to have a flood routing mechanism quite different from that operating for large floods.
(ii) The timing of the peak discharge and magnitude of the reconstructed outflow hydrograph for the bankfull river flow was poor compared to hydrographs with flow within the banks.

A possible reason for this difference in (ii) is that the travel time for flood peaks are frequently much longer for out of bank events than for those within banks (O'Donnell *et al.*, 1988). For the three-parameter model fitted to each of the individual events, the reconstructed hydrographs peak outflow was less than the observed peak values and in most of the cases the timing of the reconstructed peak outflow was earlier than that of the observed one.

The following procedure is necessary to apply the three-parameter model (O'Donnell *et al.*, 1988):

(i) Estimate the best routing coefficients (d_0, d_1 and d_2) using Equation 2.20 for observed inflow and outflow data.
(ii) Reconstruct the outflow hydrographs based on the estimated coefficients.
(iii) Estimate the model parameters (K, X and α) using Equation 2.21.
(iv) Evaluate the model using the calibrated parameters on events not used in the calibration procedure.

Application of the Three-parameter method requires observed inflow and outflow hydrographs to estimate the model parameters (K, X and α) initially. The K, X and α parameters of a

catchment in the Three-parameter Muskingum method should be calibrated using different events needing many years of observed inflows and outflows hydrographs, since calibrating with specific events might give erroneous parameters for a given catchment (O' Donnell *et al.*, 1988).

2.5 The Non-linear Muskingum Method

It is recognised that the storage versus weighted flow relationship is not always linear as is implied in Equation 2.3. If the relationship is non-linear, use of Equation 2.3 introduces considerable error (Gill, 1978).

Mohan (1997) proposed Equations 2.23 and 2.24, which utilise a non-linear Muskingum model in situations when the storage versus weighted flow relationship is non-linear:

$$S = K[XI_t + (1-X)Q_t]^n \tag{2.23}$$

$$S = K[XI_t^m + (1-X)Q_t^m] \tag{2.24}$$

where

n = exponent [dimensionless], and.

m = exponent [dimensionless].

Equations 2.23 and 2.24 have more degrees of freedom compared to Equation 2.3 and hence should yield a closer fit to the non-linear relation between storage and discharge. However, owing to the presence of non-linearity in the equation, the calibration procedure is complex (Gill, 1978; Mohan, 1997).

2.6 The SCS Convex Method

The US Soil Conservation Service (SCS) developed a coefficient channel routing technique similar to the Muskingum method. It has had widespread use in project planning and is used successfully even when limited storage data for the reach is available (Viessman *et al.*, 1989).

The theory of the SCS Convex method is based on the following principle: when a flood passes through a natural stream that has negligible local inflows or transmission losses, there is a reach length (ΔL) and a time interval (Δt) such that discharge (Q_{t+1}) falls between inflow (I_t) and outflow (Q_t), as shown in Figure 2.8 (NRCS, 1972; Viessman *et al.*, 1989). Equations 2.25 and 2.26 are algorithms for hydrograph rising and falling stages respectively (NRCS, 1972):

$$\text{If } I_t \geq Q_t \text{ then, } I_t \geq Q_{t+1} \geq Q_t \tag{2.25}$$

$$\text{If } I_t \leq Q_t \text{, then } I_t \leq Q_{t+1} \leq Q_t \tag{2.26}$$

As explained by the NRCS (1972) and Viessman *et al.* (1989), the working equation for the Convex Method is derived from Figure 2.8. The total inflow and outflow volumes are equal, hence, the area under the inflow and outflow hydrographs are equal. The peak outflow is smaller and occurs later than the peak inflow and the curves cross at some point, A, as shown in Figure 2.8. This means that as Q_{t+1} falls between I_t and Q_t at any time, the vertical distance of Q_{t+1} above Q_t or below Q_t on the right hand side of A is a fraction (C_t) of the difference (I_t-Q_t), as shown in the inset of Figure 2.8. From triangle similarity relations, Equations 2.27 and 2.28 can be derived:

$$Q_{t+1} = Q_t + C_t (I_t - Q_t) \tag{2.27}$$

and

$$C_t = \frac{Q_{t+1} - Q_t}{I_t - Q_t} \tag{2.28}$$

where

Q_t = outflow at time t [$m^3.s^{-1}$],
Q_{t+1} = outflow at time t+1 [$m^3.s^{-1}$],
I_t = inflow at time t [$m^3.s^{-1}$],
C_t = $\Delta t/K$ [dimensionless],
Δt = change in time [s], and
K = storage constant [s].

According to NRCS (1972) and Viessman *et al.* (1989), K is a constant storage parameter with time units and may be approximated from the Muskingum method. Similarly, C_t is approximately twice the Muskingum X

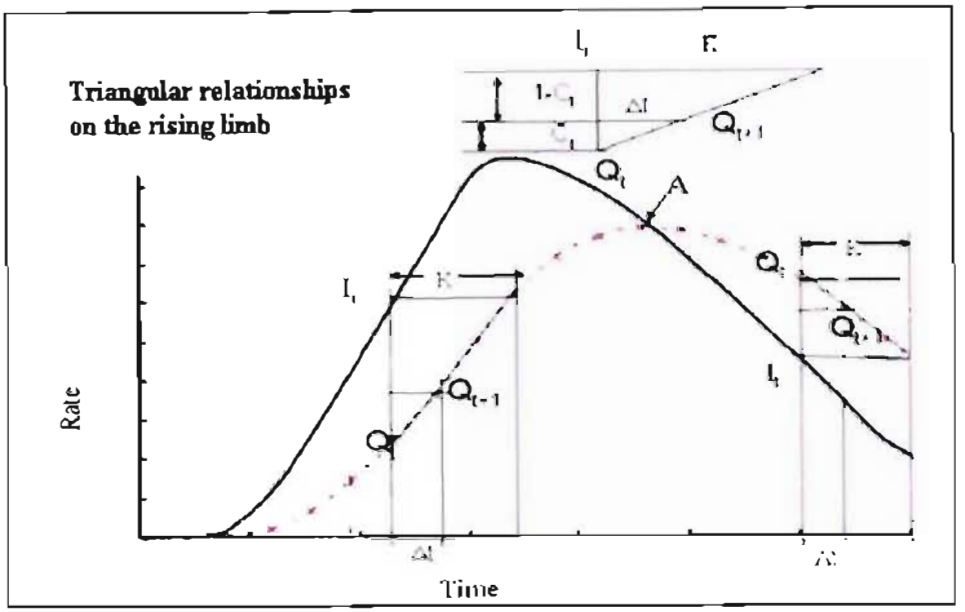

Figure 2.8 Channel routing using the Convex method (after NRCS, 1972)

Equation 2.27 is thus a working equation to route the entire inflow hydrograph once C_t is established using Equation 2.28.

The Convex method of routing is valid only if C_t falls between 0.0 and 1.0 and, more importantly, Q_{t+1} should always be between outflow Q_t and inflow I_t. The former can be controlled by selection of Δt, and the latter requirement is satisfied by the mathematical theory arising from analysis of convex sets (NRCS, 1972; Viessman *et al.*, 1989).

Unlike other routing methods, the convex method equation for Q_{t+1} is independent of I_{t+1}. Thus, the procedure can be used to forecast outflow from a reach without knowing the concurrent inflow. This provides a method for flood warning with a lead-time of at least the routing time Δt (Viessman *et al.*, 1989).

2.7 Discharge and Channel Relationships

As suggested by Clark and Davies (1988), rivers have a unique relationship between flow and channel dimensions, although close similarities are found for rivers in the same region with similar bed and bank materials and similar sediment loads. When there are limited data, relationships to relate channel dimensions to available variables are necessary. Of the many regime type equations that have been proposed, those relating channel width (b), to the dominant discharge have generally been found to be the most robust in application to rivers for which they were developed. These are mainly of the form as in Equation 2.29:

$$b = zQ^m \tag{2.29}$$

where

b = base width [m], and

Q = bankfull discharge [$m^3.s^{-1}$].

The coefficients z and m are estimated empirically. The values of z and m for various studies for gravel bed rivers are listed in Table 2.1.

Table 2.1 Coefficients of Equation 2.29 (after Clark and Davies, 1988)

References	z	m
Nixon (1959)	2.99	0.50
Simons and Albertson (1963)	2.85	0.50
Kellerhals (1976)	3.26	0.50
Charlton *et al.* (1979)	3.74	0.45
Bray (1982)	4.75	0.53
Hey and Thorne (1987)	3.67	0.45

Clark and Davies (1988) derived a relationship between slope and bankfull discharge for wadi channels in desert conditions given in Equation 2.30.

$$S = 0.012Q^{-0.44} \tag{2.30}$$

where

S = slope of the reach [m/m], and

Q = bankfull discharge [$m^3.s^{-1}$].

The relation between wetted perimeter (P) and discharge (Q) was developed for wide stable channels in Punjab, India by Lacey (1930, 1947, cited by Punmia and Pande, 1981). As noted by Klaassen and Vermeer (1988) and Garg (1992) the formula was applied in river schemes in part of India and Pakistan. Regime theory has been relatively successful in India and Pakistan in the design of stable irrigation channels under natural regimes (Savenije, 2003).

The Lacey equation is given by Lacey (1930, 1947; cited by Punmia and Pande, 1981), as

$$R = 0.47(\frac{Q}{f})^{1/3} \tag{2.31a}$$

$$P = c\sqrt{Q} \tag{2.31b}$$

where

P = wetted perimeter [m],

R = hydraulic radius [m],

f = silt factor [mm], usually ~1,

Q = discharge [$m^3.s^{-1}$], and

c = coefficient [between 4.71- 4.81].

As suggested by Chow (1959), channel dimensions for the section factor shown in Equation 2.32a can be determined from a normal depth curve developed for rectangular, trapezoidal and circular sections as shown in Figure A.1 (Appendix A). For a given bottom width (b), the corresponding flow depth, area and hydraulic radius can be calculated from the curve.

$$AR^{2/3} = \frac{Qn}{\sqrt{S}} \tag{2.32a}$$

where

A = flow area [m^2],

n = Manning's roughness coefficient [dimensionless],

R = hydraulic radius [m],

Q = discharge [$m^3.s^{-1}$], and

S = riverbed slope [m/m].

Manning's equation is given as (Chow, 1959):

$$V_{av} = \frac{1}{n} R^{2/3} \sqrt{S} \qquad (2.32b)$$

where

V_{av} = average velocity [$m.s^{-1}$].

Equation 2.33 is an empirical relationship recommended by US Reclamation Service (Etcheverry, 1915, cited by Chow, 1959):

$$y = 0.5\sqrt{A} \qquad (2.33)$$

where

y = depth of flow [m], and

A = area of flow [m^2].

2.8 Flood Routing in Ungauged Rivers

As noted by the US Army Corps of Engineers (1994a), various flood runoff models have been developed based on the laws of thermodynamics and laws of conservation of mass, momentum and energy. Other models are empirical models which are numerical relationships derived from observed events. The Muskingum-Cunge routing model uses channel geometry, reach length, roughness coefficient, and slope to estimate the parameters of the model. Therefore, the Muskingum-Cunge method may be used for flood routing analysis in an ungauged catchment.

The problem of estimating flood magnitudes for ungauged catchments is one that arises frequently (Herbst, 1968). As explained by Kundzewicz (2002), ungauged catchments include catchments that are genuinely ungauged, poorly gauged, or those previously gauged and where monitoring has been discontinued. If there are no flow records from a catchment, methods that do not require the availability of observed hydrological record have to be used to estimate model parameters (Linsley *et al.,* 1982).

According to the US Army Corps of Engineers (1994a), in channels with mild slopes and out of bank flows, X will be closer to 0.0. For steeper streams, with well-defined channels and

flows within the banks, X will be closer to 0.5. Most natural channels lie somewhere in between these two limits.

2.9 Factors that Influence Flood Routing

The factors that have an effect on the practical application of the Muskingum flood routing method and its limitations should be accounted for in parameter estimation techniques. The following sections summarise the effect of variables such as the slope, backwater effect and Manning roughness coefficient (n) in flood routing applications.

2.9.1 Slope

From Manning's Equation (2.32b) it is evident that a change in the slope of a channel affects flow velocity. This, in turn affects the lag time and shape of the hydrographs. Hence, the use of these variables in flood routing techniques has to be considered for different flow conditions in order to derive reliable estimates of the routing parameters.

According to Chow (1959), Fread (1993) and the US Army Corps of Engineers (1993), a river slope is classified as mild, steep, or critical. A critical slope is a slope where a critical velocity occurs by means of a change in potential energy rather than flow head. Slopes are classified as mild when they are less than the critical slope. They are classified as steep when they are greater than the critical slope for a given flow. A negative slope occurs when the riverbed rises in a downstream direction. For slopes greater than 95 $x10^{-5}$ $m.m^{-1}$, steady flow analysis is usually adequate (US Army Corps of Engineers, 1993). Depending on the magnitude of the Froude number, defined in Equation 2.34, the state of flow can be divided as either subcritical, critical, or supercritical (Chow, 1959; Fread, 1993; US Army Corps of Engineers, 1993; Koegelenberg *et al.*, 1997).

Froude number is estimated as follows,

$$F = \frac{V_{av}}{\sqrt{gc}} \tag{2.34}$$

where

F = Froude number [dimensionless],

V_{av} = mean flow velocity in the channel [$m.s^{-1}$],

g = acceleration due to gravity [$m.s^{-1}$], and

c = characteristics length [m].

The characteristics length (c) is often taken as the perpendicular cross-sectional area of the flow divided by the top width of flow surface. The denominator term in Equation 2.34 is the expression of celerity of a shallow water wave (Fread, 1993; US Army Corps of Engineers, 1993).

The simplest and most widely used method for defining the main slope of a channel is calculated as shown in Figure 2.9 (Linsley *et al.*, 1988). As indicated in Figure 2.9, the maximum elevation point used in the calculation is chosen to obtain a representative slope along the total reach.

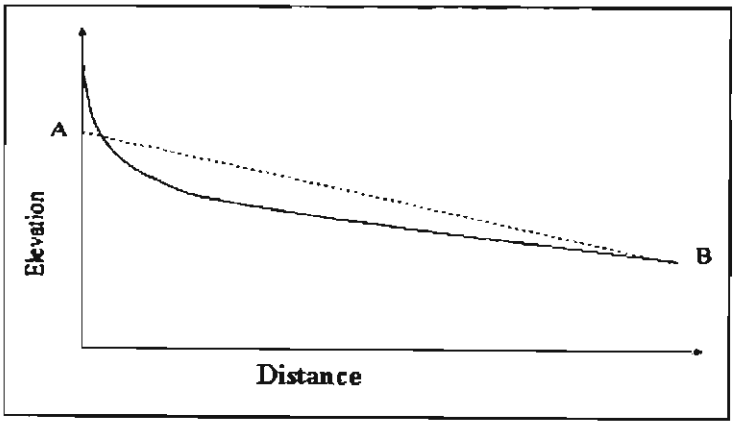

Figure 2.9 Mean stream slope (after Linsley *et al.*, 1988)

Alternatively, conveyance slope measured at 10% and 85% of stream length from mouth of the river can be used (US Army Corps of Engineers, 1994a).

2.9.2 Backwater and inundation effects

Hydrological flood routing methods ignore variable backwater effects such as downstream dams, constrictions, bridges, and tidal influences (O'Donnell, 1985). In addition, as noted by the US Army Corps of Engineers (1993), backwater effects attenuate the dynamics of flow strongly, which in turn negate the linearity assumption in the Muskingum method.

2.9.3 Manning roughness coefficient

Roughness coefficients represent the resistance to flood flows in channels and flood plains (Arcement and Schneider, 1989). As noted by Chow (1959) and Koegelenberg *et al.* (1997), there is no precise method to estimate roughness coefficients and therefore practical estimation of the Manning roughness coefficient is subjective. The roughness coefficients vary with the flow depth and the seasonal physical change in the river bed and bank. Hence, in design practice, the worst scenarios are usually considered. Surface roughness, plant growth along the river, sediment load, irregularity in channels and wind blowing against the direction of flow increase the value of resistance significantly. When there is less plant growth and less irregularity just above the surface of the flow depth, the resistance value decreases with an increase in discharge (Chow, 1959; Arcement *et al.*, 1989; Koegelenberg *et al.*, 1997). The base roughness coefficient values (n_b) of different river conditions are contained in Table 2.2.

Table 2.2 Base roughness coefficient values (Arcement and Schneider, 1989) [Modified from Aldridge and Garret, 1973]

Base roughness coefficient value			
Bed material	**Median size of bed material [mm]**	**Straight Uniform Channel**	**Smooth Channel**
Sand Channels			
Sand	0.2	0.012	—
	0.3	0.017	—
	0.4	0.020	—
	0.5	0.022	—
	0.6	0.023	
	0.8	0.025	—
	1.0	0.026	—
Stable Channels and Flood Plains			
Concrete	–	0.012-0.018	0.011
Rock cut	–	–	0.025
Firm Soil	–	0.025-0.032	0.020
Coarse Sand	1-2	0.026-0.035	—
Fine Gravel	--	--	0.024
Gravel	2-64	0.028-0.035	-
Coarse Gravel	–	–	0.026
Cobble	64-256	0.030-0.050	—
Boulder	>256	0.040-0.070	—

In the selection of a base roughness coefficient (n) value for a channel, the channel must be classified as a stable channel or as a sand channel. A stable channel remains relatively unchanged throughout most of the range inflow (Arcement and Schneider, 1989).

The flow in a river may be confined to one or more channels and, especially during floods, the flow may occur both in the channel and in the flood plain. The coefficient of roughness (n) value is determined from the values of the factors that affect the roughness of channels and flood plains (Arcement and Schneider, 1989).

As noted by Shen and Julien (1993) and Fread (1993), the best results are obtained when the roughness coefficient (n) is calibrated against historical observations of stage and discharge. The Manning roughness coefficient (n) is also related to the Darcy friction factor *f*, and the prevailing sediment size condition of the bed materials as shown in Equations 2.35 and 2.36 (Shen and Julien, 1993 and Fread, 1993):

$$n = \mu f^{0.5} D^{0.17} \tag{2.35}$$

where

$\mu = 0.113$ [When other variables are in SI units],

f = Darcy friction factor [dimensionless], and

D = hydraulic depth [m].

and

$$n = \frac{(d_{50})^{1/6}}{21} \tag{2.36}$$

where

d_{50} = the median sediment size [m].

As shown by Chow (1959), in applying the Manning formula to channels with composite roughness, it is sometimes necessary to compute an equivalent roughness coefficient value for the entire perimeter and use this value for the computation of the flow in the whole section.

Limerinos (1970, cited by Arcement and Schneider, 1989), related the base roughness coefficient value to hydraulic radius (R) and particle size (d_{84}) having bed material ranging from small gravel to medium-sized boulders. Limerinos (1970) related n to particles which

have minimum diameter which equals or exceeds the diameter of 84 % of the particles, as shown in Equation 2.37:

$$n_b = \frac{(0.8204)R^{1/6}}{1.16 + 20\log\left[\frac{R}{d_{84}}\right]} \tag{2.37}$$

where

n_b = roughness coefficient base value [dimensionless],

R = hydraulic radius [m], and

d_{84} = particle diameter (m) that equals or exceeds the diameter of 84 % of the particles [determined from a sample of about 100 randomly distributed particles].

Arcement and Schneider (1989), recommend Equation 2.37 to estimate the base roughness (n_b) value for a stable channel. The base roughness coefficient (n_b) values contained in Table 2.2 are for straight channels of nearly uniform cross-sectional shape. Hence, adjustments for channel irregularities, alignment, obstructions, vegetation, and meandering corrections may be made to account for particular channel characteristics using Equation 2.38 and the information contained in Table 2.3.

As noted by Arcement and Schneider (1989), projecting points or exposed trees increase the resistance coefficient. An increase of the resistance coefficient is also associated with a change in cross-sectional area.

The degree of meandering, (m), depends on the ratio of the total length of the meandering channel in the reach being considered to the straight length of the channel reach (Arcement and Schneider, 1989).

Cowan (1956, cited by Chow, 1959), Arcement and Schneider (1989) and Land & Water Australia (2004) proposed that Manning's resistance value for open channel flow could be determined by considering all the factors that contribute to flow resistance. Hence, the value may be computed by considering all the channel characteristics as shown in Equation 2.38:

$$n = (n_b + n_1 + n_2 + n_3 + n_4)\, m \qquad (2.38)$$

where

n_b = a base value for a straight, uniform, smooth channel in natural channels,

n_1 = a value for the effect of surface channel irregularities,

n_2 = a value for variations in shape and size of the channel cross-section,

n_3 = a value for obstructions,

n_4 = a value for vegetation and flow conditions, and

m = a correction factor for channel meandering.

First the river reach should be classified as a sand channel or stable channel, then the bed materials and the uniformity of the channel should be identified. Based on the channel type and characteristics, the base roughness value (n_b) is assigned from Table 2.2. Since the base value is for smooth and straight reaches, the base value should be adjusted using Table 2.3 for the site condition with regards to the degree of channel irregularity, variation in channel cross-section, effect of obstruction, amount of vegetation cover and degree of meandering.

Table 2.3 Adjustment for channel roughness values (after Arcement and Schneider, 1989) [Modified from Aldridge and Garrett, 1973]

Channel conditions	**n values adjustment**	**Example**
Degree of irregularity (n_1)		
Smooth	0.000	Smoothest channel attainable in a given bed material.
Minor erosion	0.001-0.005	Degraded channels in good condition having slightly eroded side slopes.
Moderate erosion	0.006-0.010	Degraded channels having moderately eroded side slopes
Severe erosion	0.011-0.020	Badly eroded unshaped, jagged and irregular surface of channel.
Variation in channel cross-section (n_2)		
Gradual	0.000	Size and shape of channel cross-section change gradually.
Alternating occasionally	0.001-0.005	Large and small cross-sections alternate occasionally.
Alternating frequently	0.010-0.015	Large and small cross-sections alternate frequently.

Table 2.3 (Continued)…

Channel conditions	n values adjustment	Example
Effect of obstruction (n_3)		
Negligible	0.000-0.004	A few scattered obstructions, which include debris deposits or isolated boulders that occupy less than 5 % of the cross-sectional area.
Minor	0.040-0.050	Obstruction occupies less than 15 % of cross-sectional area.
Appreciable	0.020-0.030	Obstructions occupy from 15% to 50% of cross-sectional area.
Severe	0.005-0.015	More than 50% of cross-sectional area.
Amount of vegetation (n_4)		
Small	0.002-0.010	Dense growth of flexible turf grass, such as Bermuda or weeds growing where the average depth of flow is at least two times the height of the vegetation.
Medium	0.010-0.025	Turf grass growing where the average depth of flow is from one to two times the height of the vegetation, moderately dense grass, weeds or brushy, moderately dense vegetation.
Large	0.025 -0.050	Turf grass growing where the average depth of flow is about equal to the height of the vegetation.
Very Large	0.050-0.100	Turf grass growing where the average depth of flow is less than half the height of the vegetation.

Table 2.3 (Continued)...

Channel conditions	n values adjustment	Example
Degree of meandering (m)		
Minor	1.00	Ratio of the channel length to valley length is 1.0 to 1.2.
Appreciable	1.15	Ratio of the channel length to valley length is 1.2 to 1.5.
Severe	1.30	Ratio of the channel length to valley length is greater than 1.5.

In this chapter the Muskingum flood routing methods, the relationship between discharge and channel, flood routing method applications in ungauged rivers, and factors that influence the practical application of flood routing methods have been discussed. In the next chapter, the catchment and event selection procedure are detailed.

3. CATCHMENT AND EVENT SELECTION

The selection of suitable gauge sites, river reaches, and event for analysis are presented in this chapter.

3.1 Catchment Selection

As noted by Thukela Basin Consultants (2001), the Department of Water Affairs and Forestry (DWAF) initiated the Vaal Augmentation Planning Study (VAPS) in 1994 to determine alternative development options to meet the increased demand for water in South Africa. DWAF has found that inter-basin transfer schemes, together with other strategic actions, offer a possible and affordable means for augmenting water supplies to the Vaal River system. The Thukela River, among others, is one of the options investigated for a further inter-basin transfer scheme.

According to Thukela Basin Consultants (2001) and Encyclopaedia of Nationmaster (2004), the Thukela River has its source in the Drakensberg Mountains near Bergville, where mountain peaks rise to over 3000 m. The river falls rapidly 947 m down to the Thukela falls. The mean annual rainfall (MAR) in the Thukela catchment ranges from 1500 mm or more in the Drakensberg, to 50 mm and less in the dry central regions of the catchment where the MAR is lower than 700 mm.

The Thukela catchment was selected to conduct flood routing studies as it has numerous gauging stations, long records of flow and long rivers and tributaries. Additionally, the research would supplement other current research activities in the School of Bioresources Engineering and Environmental Hydrology.

3.2 Suitable Gauging Sites and River Reach Selection

The factors considered when selecting suitable gauging stations for streamflow records are the availability of data, the quality of data, and the suitability of the river reach to estimate flood routing parameters, i.e. whether there are not any constrictions, dams, backwater effects due to

inundations and the appropriateness of the reaches to apply the Muskingum flood routing methods, as outlined previously. Usually the data required to analyse flood routing includes the recorded inflow and outflow hydrographs, length of reach, river slope, channel network, channel roughness and ice jam conditions (Fread, 1993). Reaches of different lengths were selected to assess the influence of river length in the application of flood routing methods.

River reach length (ΔL), slope of the river reach (S) and the longitudinal profile of each river reach was extracted from a 200 m Digital Elevation Model used by the South African Atlas of Agro hydrology and Climatology (Schulze *et al.*, 1997). The slope and length of selected reaches were derived using the ArcView 3.2a (ESRI, 2000) software package. Base values for Manning's roughness coefficient were estimated from Table 2.2 (Section 2.9.3) and from field observations. The catchment area and location of gauging weirs were obtained from the Department of Forestry and Water Affairs (DWAF) (2003) internet hydrology link at the URL of www.dwaf.gov.za/hydrology/cgi-bin/his/cgihis.exe/station.

3.3 Catchment Location

As shown in Figures 3.1 and 3.2, the Thukela catchment extends latitudinaly from 27.41^0 to 29.40^0 S and longitudinally from 28.96^0 to 31.44^0 E and has a catchment area of 29 036 km^2. The catchment is made up of 86 interlinked and cascading Quaternary Catchments as defined by the DWAF (Schulze and Taylor, 2002).

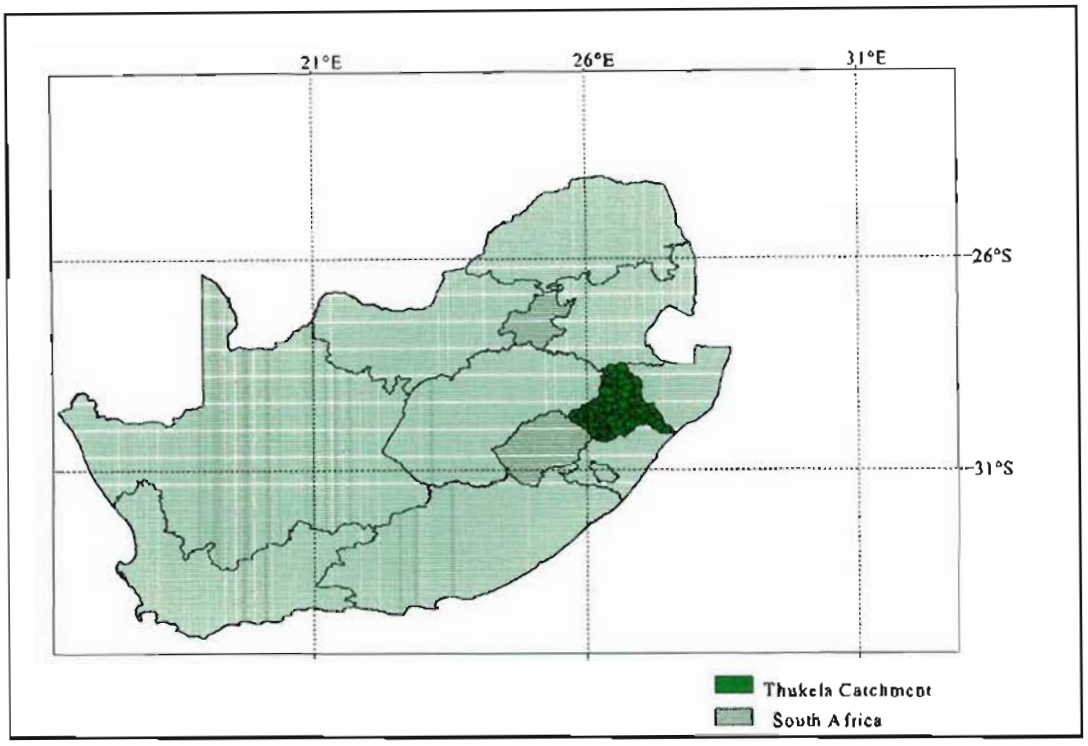

Figure 3.1Thukela location map

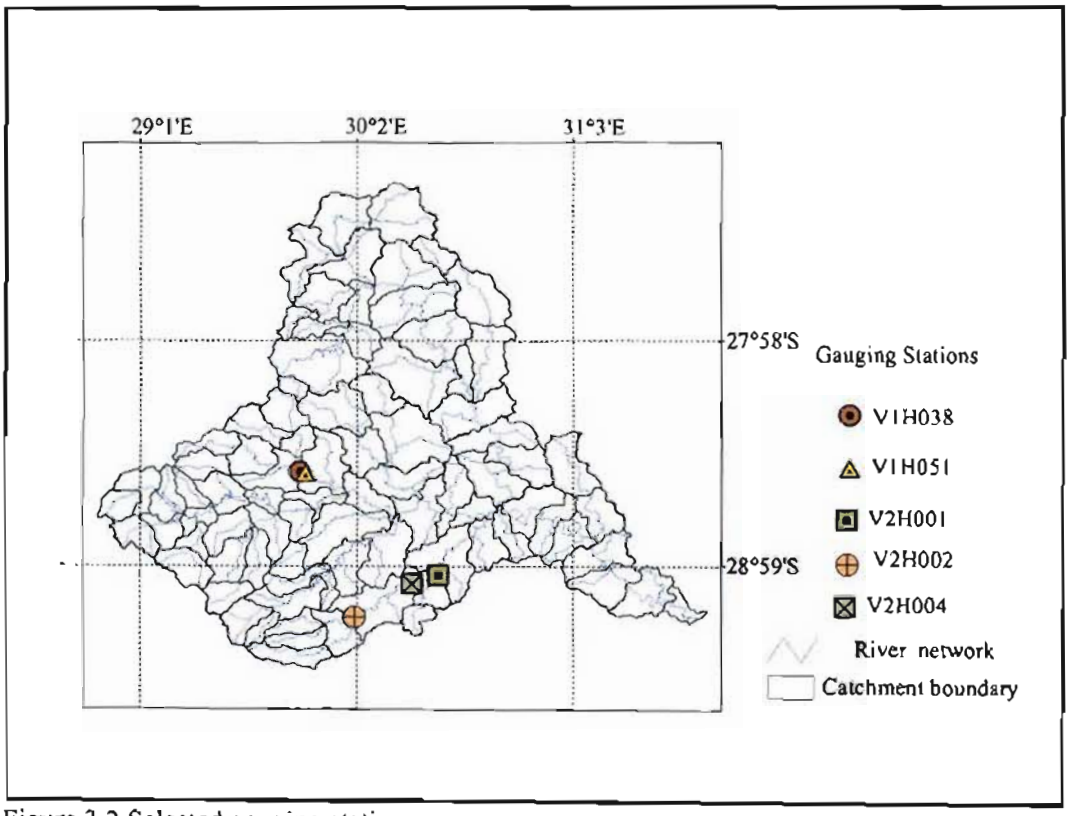

Figure 3.2 Selected gauging stations

Figures 3.3, 3.4 and 3.5 illustrate selected sub-catchments, gauging stations and river networks. Owing to the limitation of Muskingum methods as stated in Sections 2.1 and 2.2, as well as the lack of good data for many of the gauging weirs in the Thukela catchments, only three of the sub-catchments are considered for this study.

A summary of weir site locations and other relevant information for each gauging station are included in Table 3.1.

Table 3.1 Summary of reaches and gauging stations used

Reach	Upstream and downstream Gauging Stations	Location	River	Elevation [m]	Catch. area [km^2]	Sub-Catch. area [km^2]	Reach Length [km]	Average Channel Slope [%]
I	V1H038	Dorpsgronde	Klip	1042	1644	10	4.09	0.70
	V1H051	Ladysmith	Klip	1007	1654			
II	V2H002	Mooi	Mooi	1390	937	609	54.40	0.55
	V2H004	Doornkloof	Mooi	1099	1546			
III	V2H004	Doornkloof	Mooi	1099	1546	44	20.00	0.12
	V2H001	Scheepersdaal	Mooi	1075	1950			

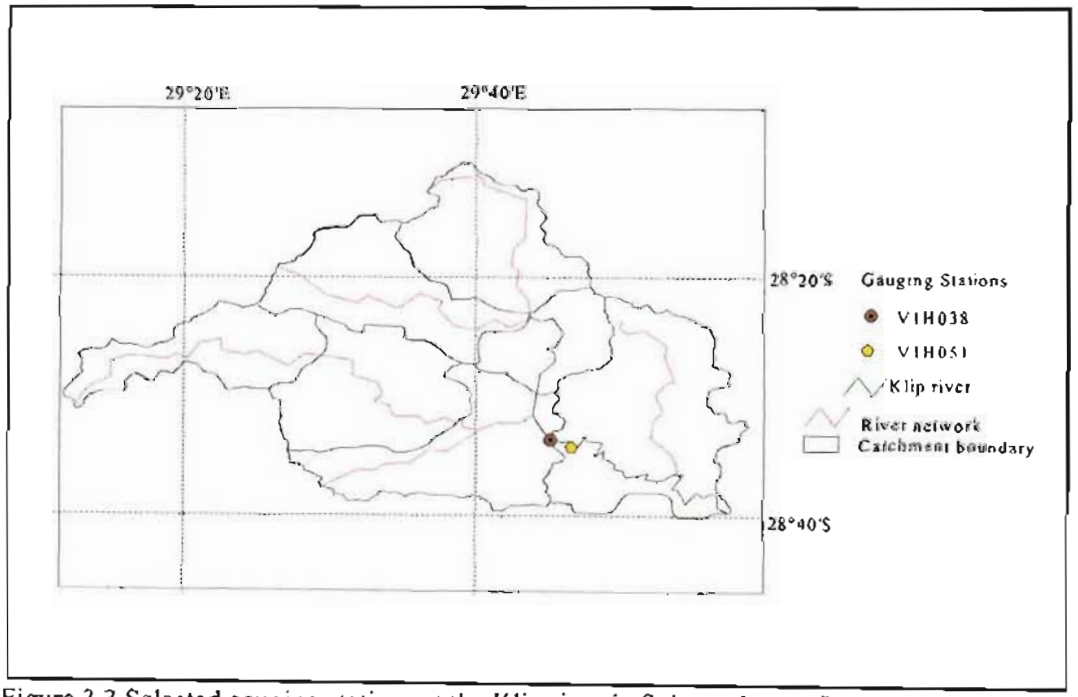

Figure 3.3 Selected gauging stations at the Klip river in Sub-catchment-I

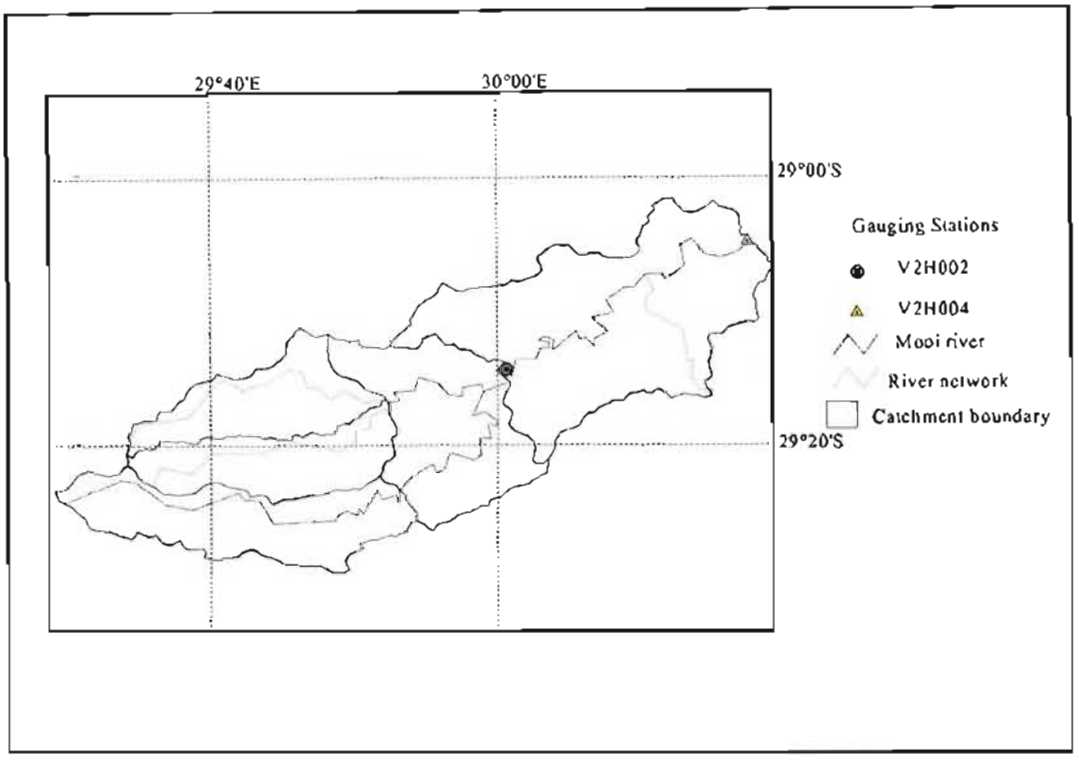

Figure 3.4 Selected gauging stations at the Mooi River in Sub-catchment-II

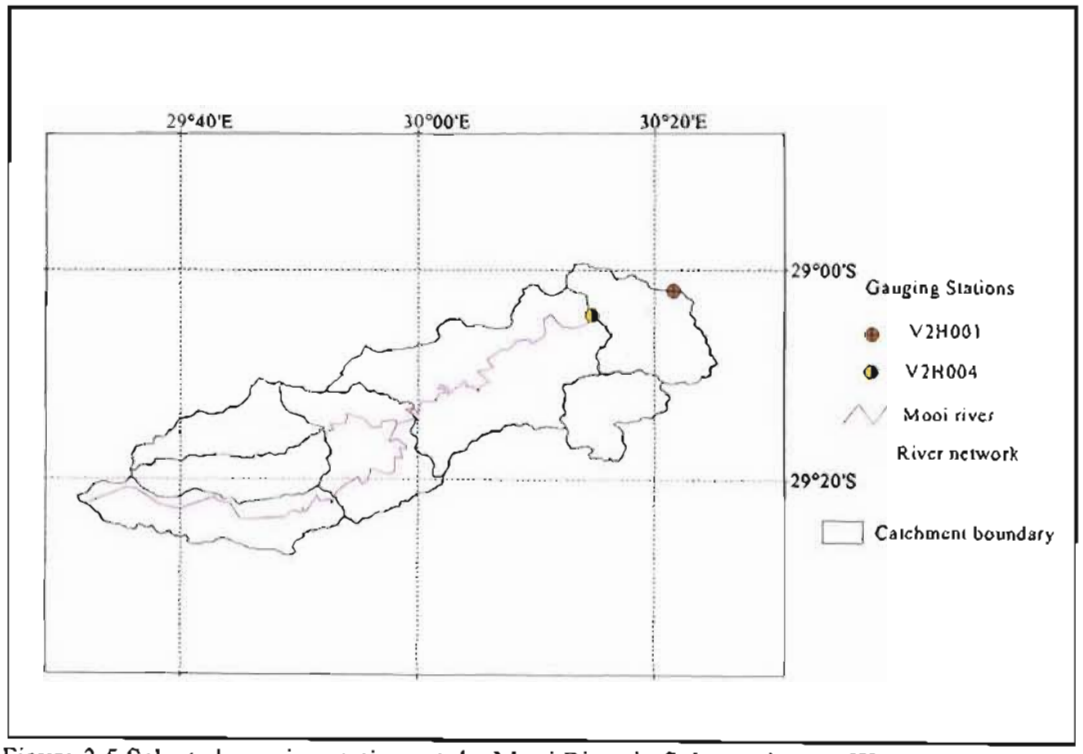

Figure 3.5 Selected gauging stations at the Mooi River in Sub–catchment-III

3.4 Characteristics of River Reaches

In order to observe the site conditions and estimate factors affecting Manning roughness coefficient (n) and the maximum bankfull top flow width (W), the reaches in the selected catchments were visited during June 2004. The river reach information for all sub-catchments was collected during the field visit, and additional information was derived from the 1:50 000 South Africa Map (1989) and the 1:100 000 KZN Tourist Map (2003). The interpretation of information collected from the field survey is contained in Table 3.2. The average bankfull top width and maximum flow depth observed in the field were used to set the maximum bankfull river flow. All the channels were assumed to be stable channels. The approximate general top widths are between 50-70m and the maximum flow depths are between 2-4 m..

Assumed cross-sectional dimensions of maximum top width (W) and maximum section depth (y) observed during the field visit are contained in Table 3.2.

Table 3.2 Field observed data for assumed cross-sections

Reach	Top flow width (m)	Maximum depth (m)
I	70	2.5
II	30	2
III	50	5

Table 3.3 Field survey data

Reach	Channel Shape	Channel condition	Meanderness	Channel obstruction	Channel vegetation cover Size
I	Moderately Irregular	Occasionally alternating	Appreciable	Negligible	Small
II	Moderately Irregular	Occasionally alternating	Severe	Negligible	Small
III	Moderately Irregular	Occasionally alternating	Appreciable	Negligible	Small

3.4.1 Characteristics of Reach-I

The Klip River has a moderately irregular channel shape with occasionally alternating width of cross-sections. It has negligible obstructions and the ratio of channel length to its valley length is estimated to be 1.3. Hence, the river is categorised as an appreciable channel meandering condition from values contained in Table 2.3 (Section 2.9.3). The river has an alternating medium vegetation cover along the reach. An example of riparian vegetation in the river is shown in Figure 3.6.

Figure 3.6 The Klip River in Sub-catchment-I

The slope of the main Klip River changes drastically from a steep slope to a much flatter slope as shown in Figure 3.7. The upper 46% of the reach length has a slope of 2.1% and the downstream 54% of the reach has a slope of almost zero (flat). This implies that the reach has high velocity flows at the upstream and a very slow flow at the downstream side.

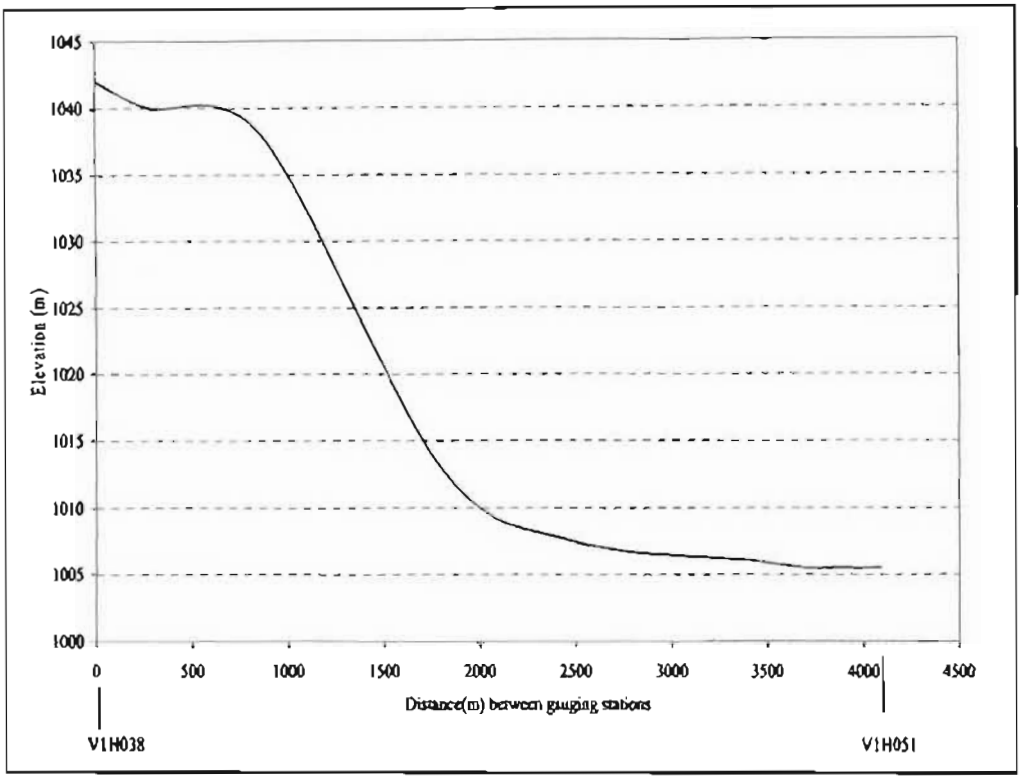

Figure 3.7 Longitudinal profile of the Klip River in Sub-catchment-I

3.4.2 Characteristics of Reach-II

In the Mooi River the ratio of meandering channel length to its valley length is estimated to be 1.8. Hence, the river is categorised as having a severely meandering condition from values contained in Table 2.3 (Section 2.9.3). The river has alternating bushy cover along the reach, and an example of riparian vegetation along the river is shown in Figure 3.8.

Figure 3.8 The Mooi River in Sub-catchment-II

The slope of the main river reach of the Mooi River is shown in Figure 3.9.

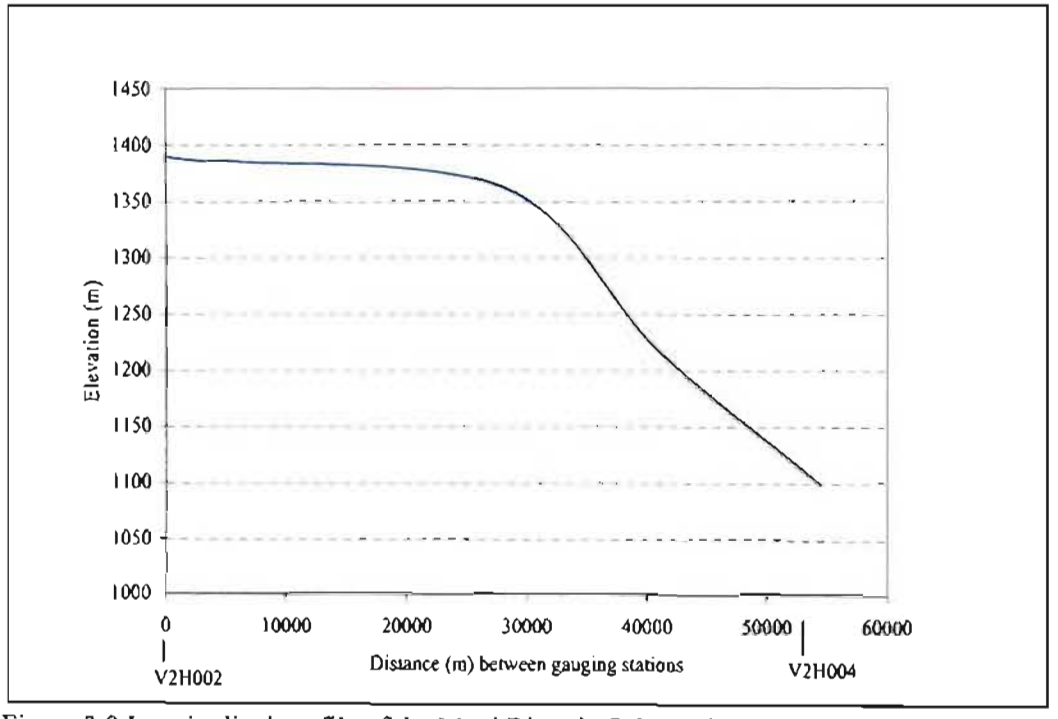

Figure 3.9 Longitudinal profile of the Mooi River in Sub-catchment-II

3.4.3 Characteristics of Reach-III

Reach-III is a continuation of the Mooi River downstream of Muden village and has a moderate irregular channel shape with occasionally alternating width of cross-sections. The

reach downstream of the Mooi River has negligible obstructions. The ratio of channel length to its valley is estimated to be 1.38. Hence, the river is categorised as having an appreciable meandering channel condition based on values contained in Table 2.3 (Section 2.9.3). The Mooi River has shorter riparian vegetation at the downstream reach than the upper reaches. An example of riparian vegetation along the river is shown as in Figure 3.10.

Figure 3.10 The Mooi River in Sub-catchment-III (Downstream)

The slope of Reach-III is shown in Figure 3.11.

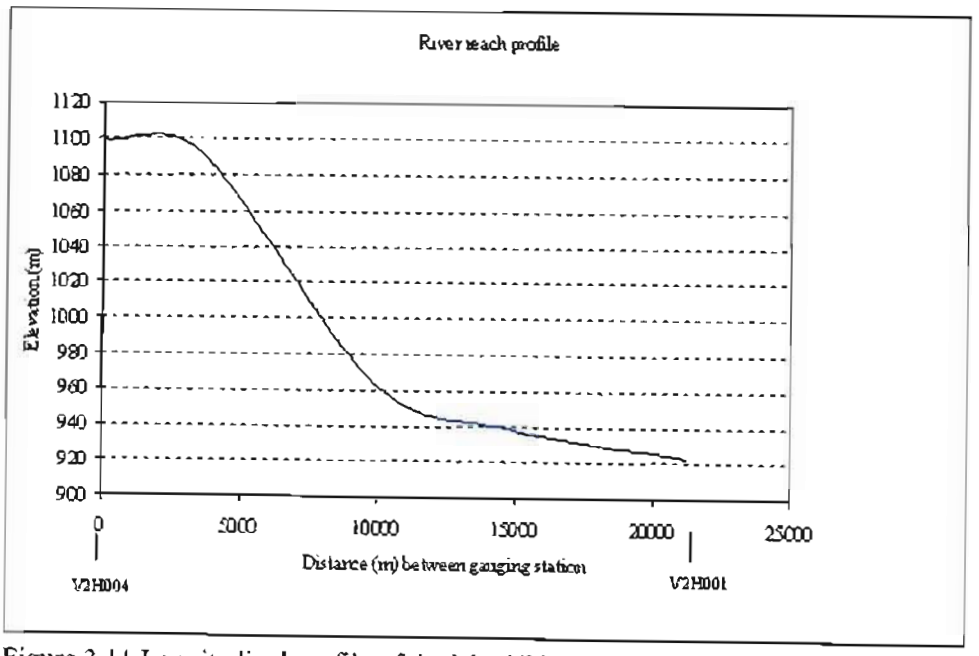

Figure 3.11 Longitudinal profile of the Mooi River in Sub-catchment-III

During the field visit as it was observed that the river bed has cobbles with stable river side banks, the base value (n_b) for each channel was taken from values contained in Table 2.2 for a stable bed material channel condition with gravel size 2-64 mm. The adjustments were done based on the observed channel condition and total values were estimated using the Cowan (1956) method. The results are contained in Table 3.4.

Table 3.4 Roughness coefficient values for the reaches

Reach.	n_b	Irregularity	Cross-Section	Obstruction	Vegetation Cover	Meandering	Final n
I	0.03	0.006	0.001	0	0.002	1.15	0.045
II	0.028	0.006	0.001	0	0.002	1.30	0.048
III	0.028	0.006	0.001	0	0.002	1.15	0.043

3.5 Analysis of Flow Data

The observed hydrograph data used in this study were downloaded from DWAF (2003). The break point digitised data (primary data), which have varying time steps, were converted to a constant time step using a program developed by Smithers (2003). The time step chosen was sufficiently small so that the assumption of flow rate linearity over the time interval was approximately satisfied. Both small and large flood events were chosen to ensure that various flow conditions were included in the analyses.

Flow records for the three selected reaches in Sub-catchments-I, II and III are shown in Figures 3.12, 3.13 and 3.14.

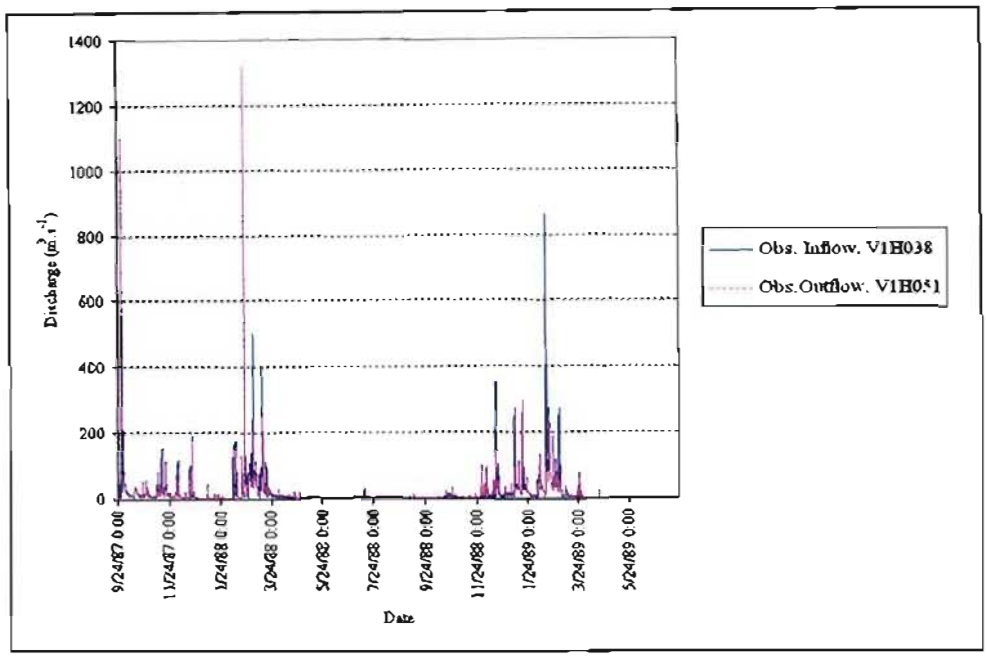

Figure 3.12 Observed inflows and outflows of Reach-I

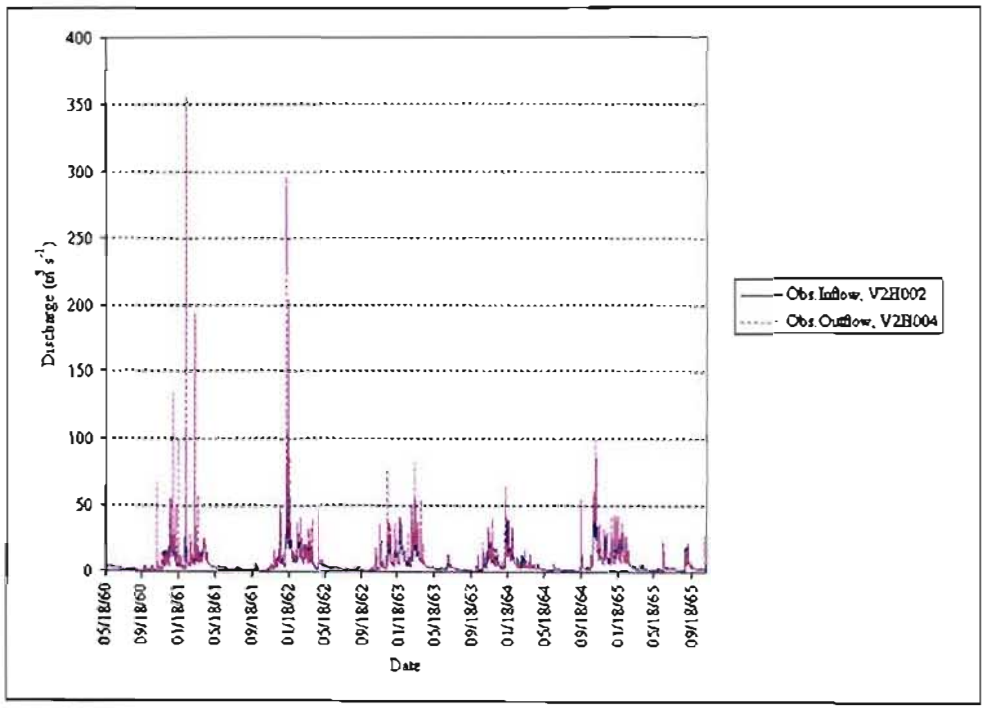

Figure 3.13 Observed inflows and outflows of Reach-II

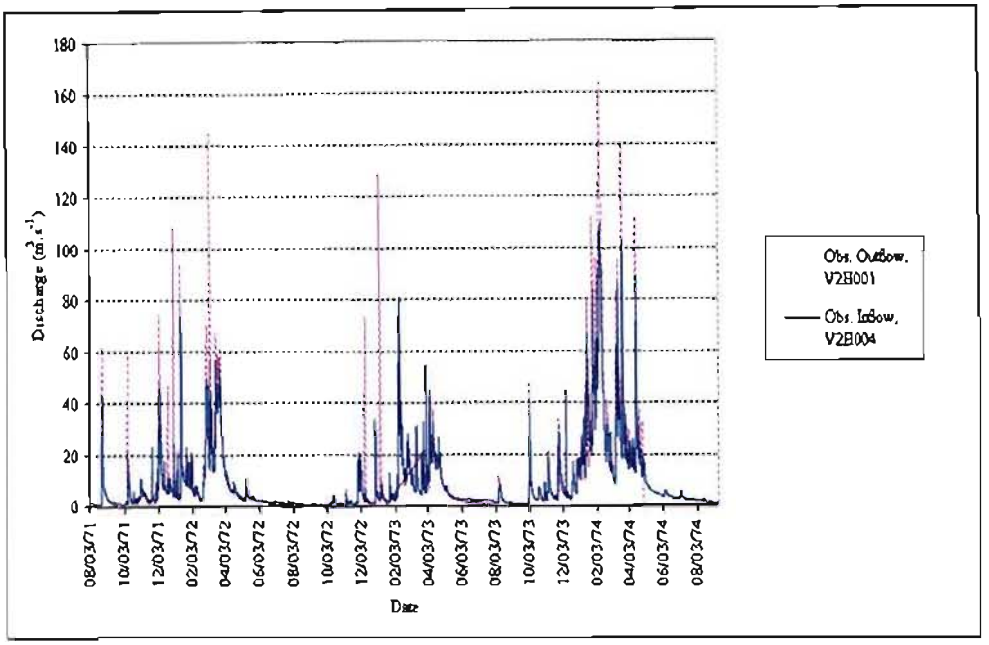

Figure 3.14 Observed inflows and outflows of Reach-III

The rating curves of the selected reaches are shown in Figures 3.15 to 3.17.

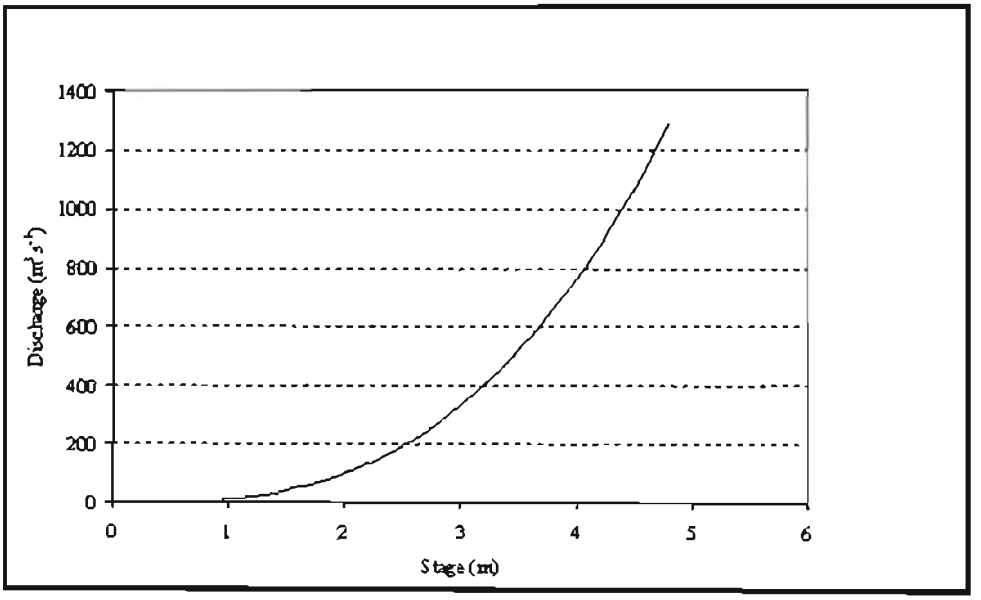

Figure 3.15 Observed rating curve at gauging station V1H038 (after DWAF, 2003)

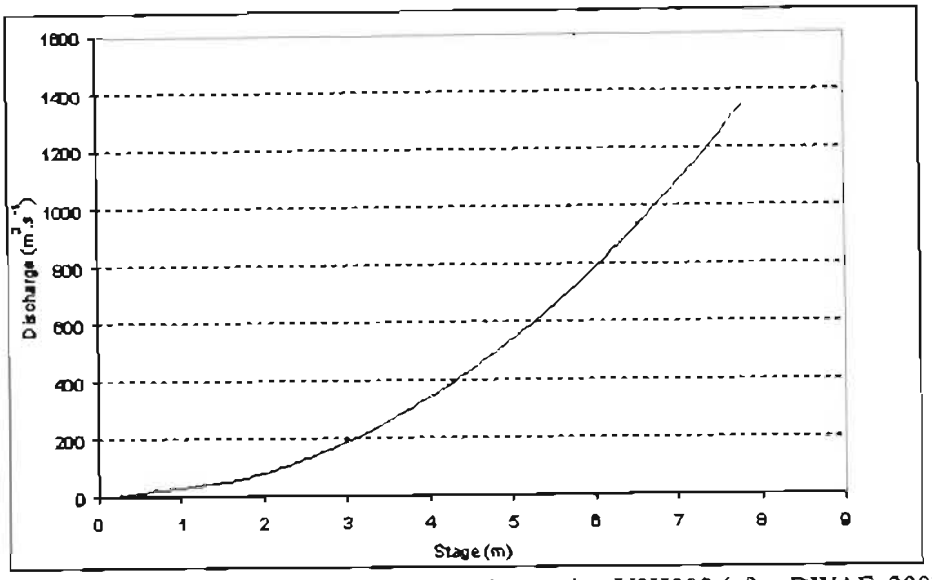

Figure 3.16 Observed rating curve at gauging station V2H002 (after DWAF, 2003)

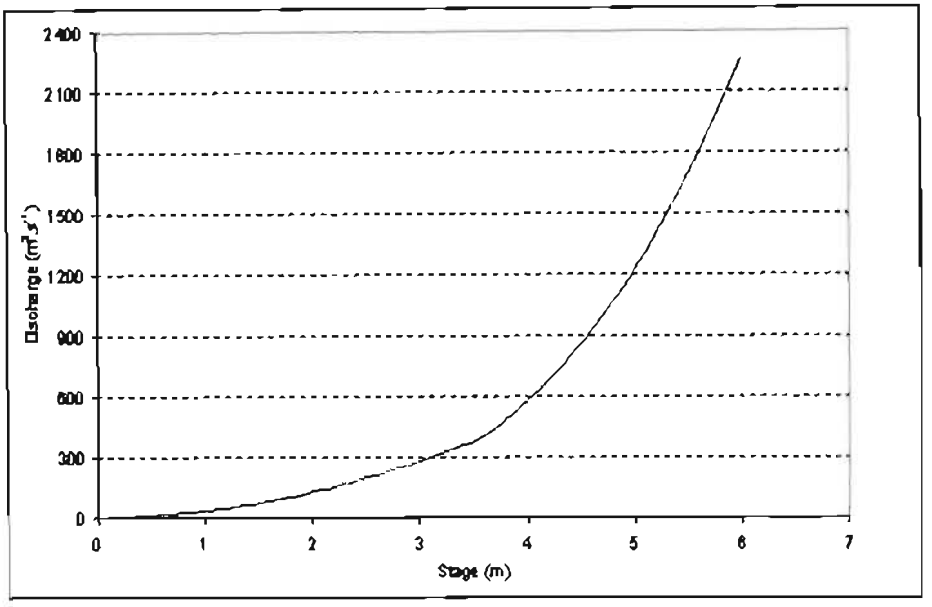

Figure 3.17 Observed rating curve at gauging station V2H004 (after DWAF, 2003)

From an inspection of the flow data, it was evident that some of the observed hydrographs had unrealistic records. The errors might be due to technical problems or incorrect data acquisition. For example, some of the events have earlier peaks at down stream reaches and some events have exceptionally high peak values, which are much larger than the other peaks at the gauge. Hence, the quality of data should be assessed before selecting events for flood routing analyses. The errors in some of the events can be clearly seen when a single event hydrograph is extracted and considered in large-scale as shown in Figure 3.18. It can be

suggested that the apparent error shown in Figure 3.18 may be due to incorrect digitisation of a pen reversal on the autographically recorded chart.

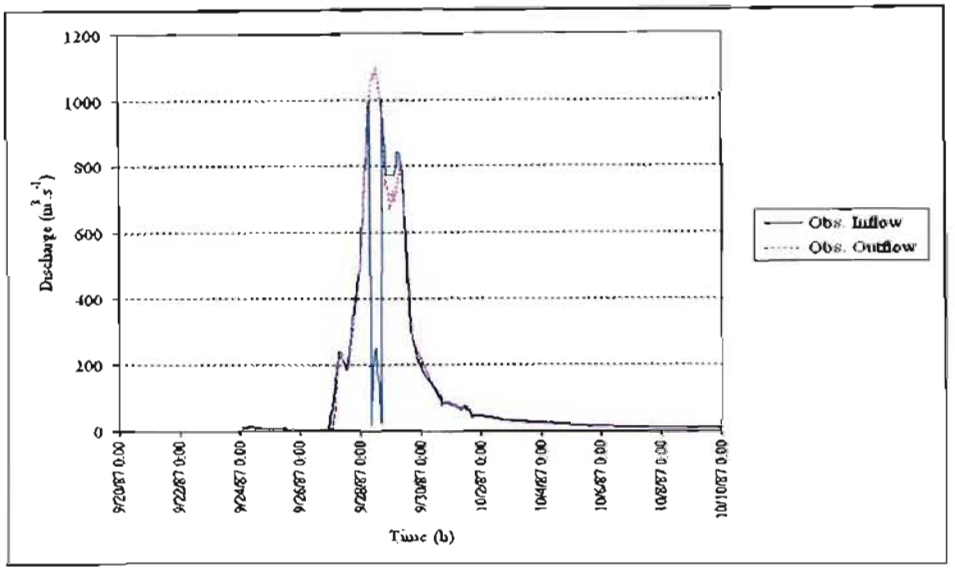

Figure 3.18 Example of poor data in Reach-I

Considering representative event sizes such as small, medium and large events, event selection was made. The selected events for all reaches are shown in Figures 3.19 to 3.26. Events selected from Reach-I are shown in Figures 3.19 to 3.20.

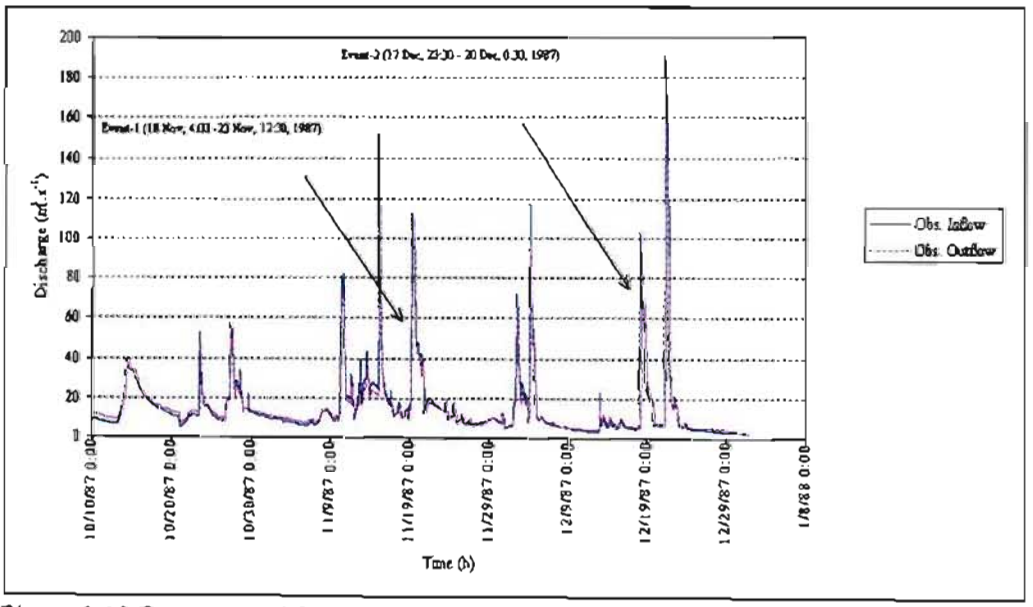

Figure 3.19 Events-1 and 2 selected from Reach-I

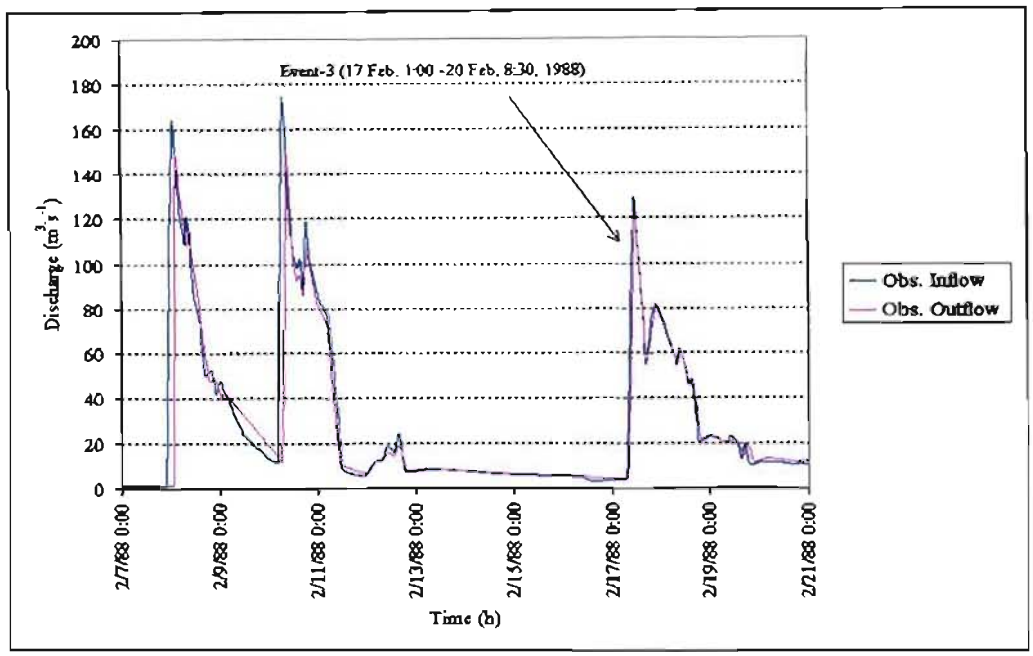

Figure 3.20 Event-3 selected from Reach-I

Selected events from Reach-II are shown in Figures 3.21 to 3.25.

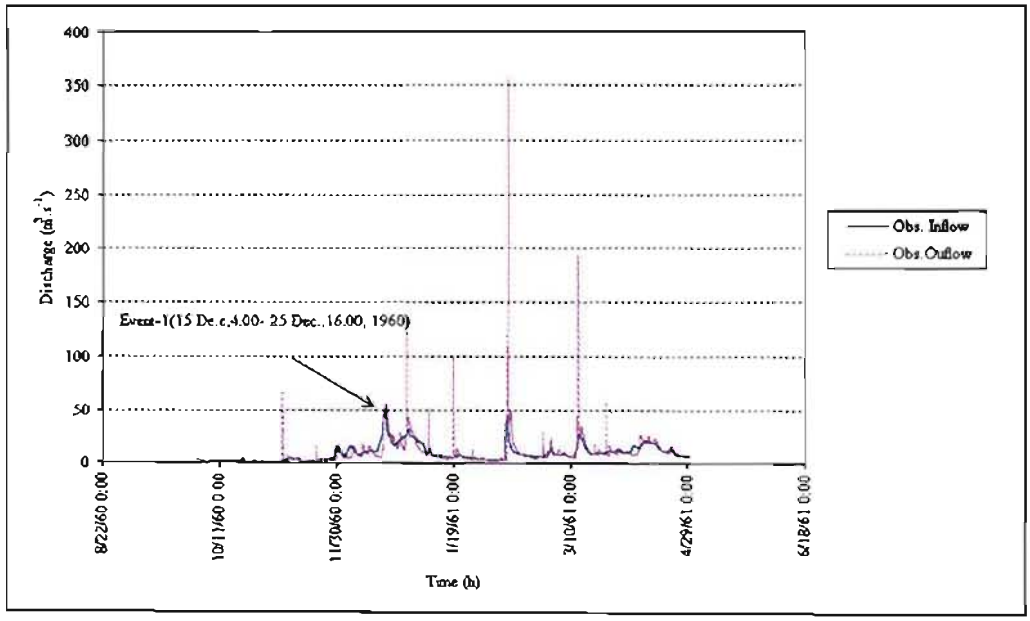

Figure 3.21 Event-I selected from Reach-II

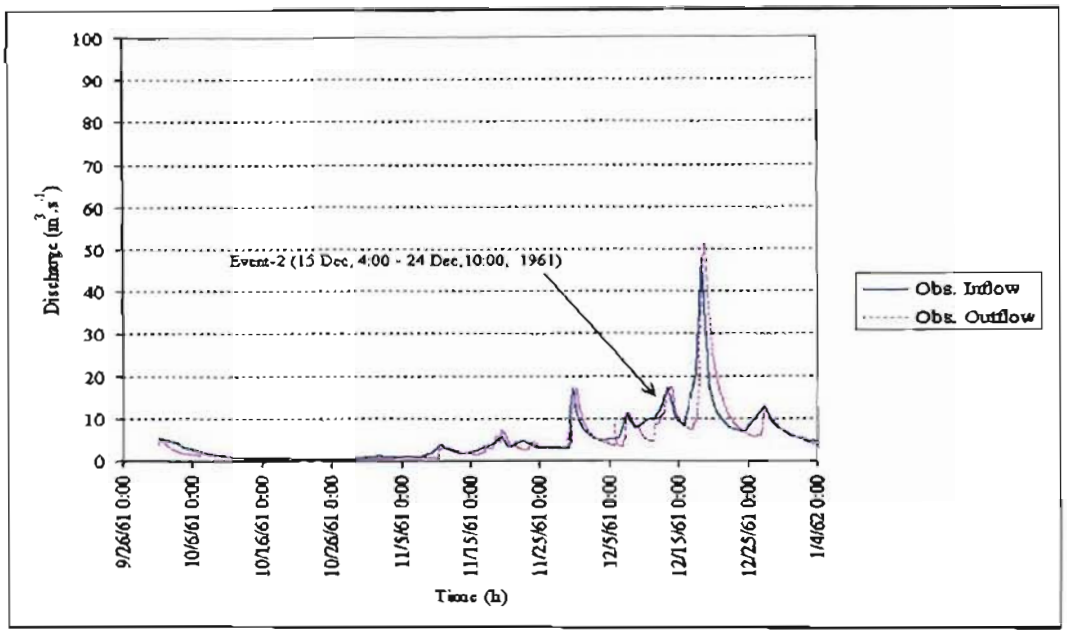

Figure 3.22 Event-2 selected from Reach-II

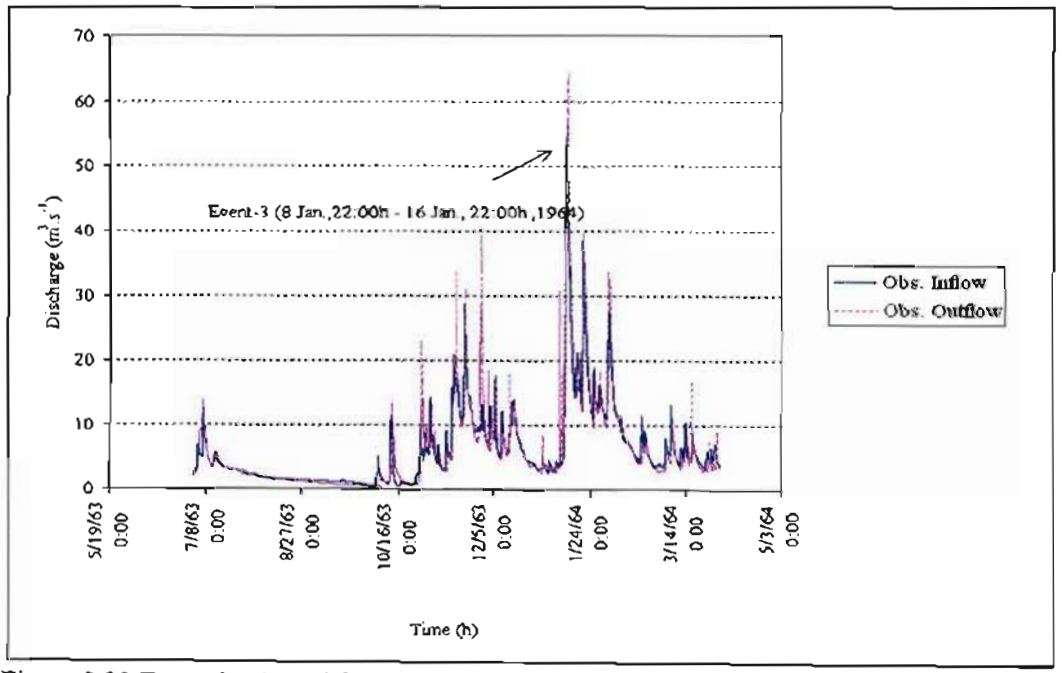

Figure 3.23 Event-3 selected from Reach-II

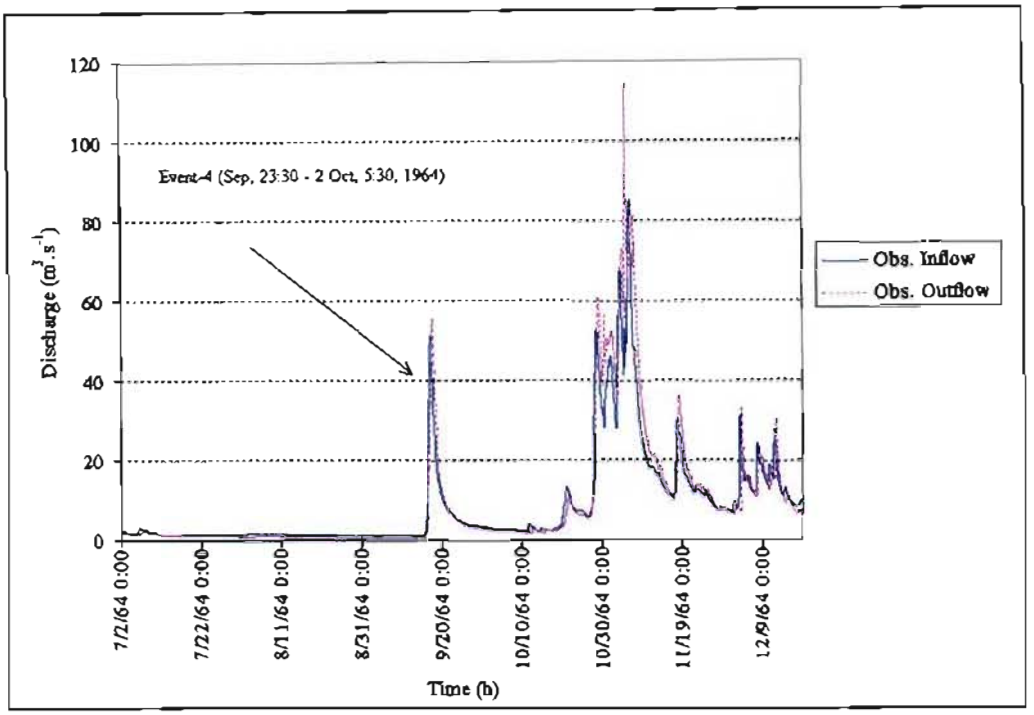

Figure 3.24 Event-4 selected from Reach-II

Selected events from Reach-III are shown in Figures 3.25 to 3.26.

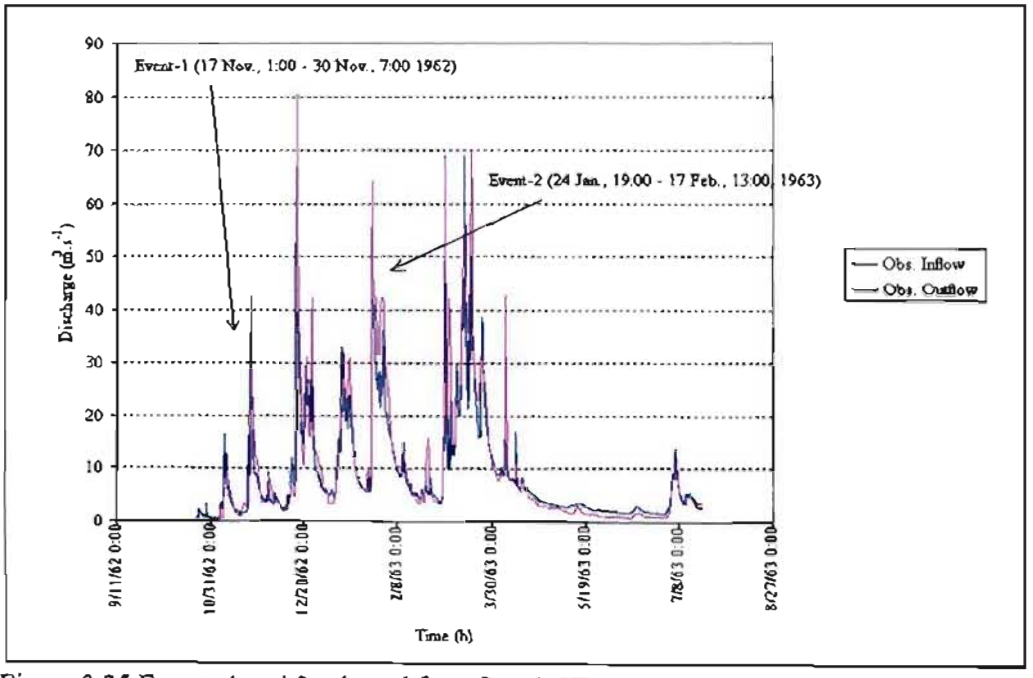

Figure 3.25 Events-1 and 2 selected from Reach-III

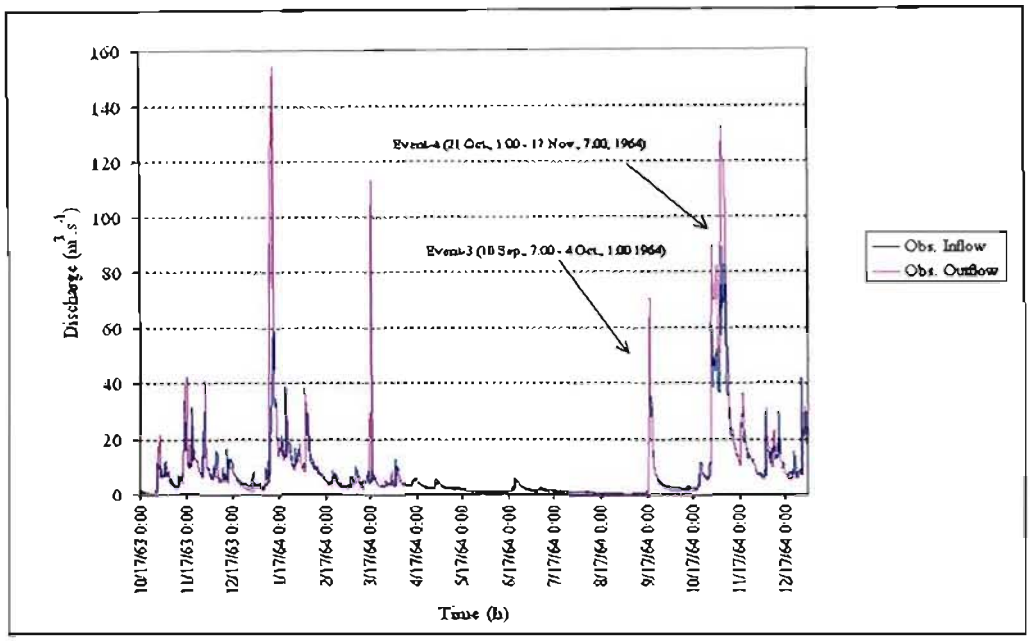

Figure 3.26 Event-3 and 4 selected from Reach-III

In this chapter the selection of river reaches, gauging sites and flood events have been made. In the next chapter, the methodology of the analyses applied to estimate K and X parameters in ungauged catchments is detailed.

4. METHODOLOGY

This chapter describes the methodologies utilised in the selection and analyses of stream flow data as well as the flood routing methods applied to selected events. The Muskingum K and X parameters were calibrated from observed inflow and outflow hydrographs using the Muskingum (M-Cal) and the Three-parameter Muskingum matrix (M-Ma) methods. At ungauged sites the Muskingum-Cunge equation was used, with flow variables estimated using both an empirical (MC-E) approach and by an assumed cross-section (MC-X) approach. The computed outflow hydrographs were compared statistically and graphically with the observed hydrographs. The methodology is detailed as follows:

(i) For selected sub-catchments, observed events were selected and the outflow hydrographs computed using calibrated Muskingum K and X parameters (M-Cal) as well as the Three-parameter Muskingum method (M-Ma). The computed hydrographs were compared to the observed hydrographs to assess the performance of the Muskingum method with calibrated parameters.

(ii) The Muskingum K and X parameters were estimated for each reach on the basis of empirically determined flow characteristics such as flow top width (W), wetted perimeter (P), flow depth (y), hydraulic radius (R) and average velocity (V_{av}) (Section 4.2.1). The method is referred to as MC-E.

(i) The Muskingum K and X parameters were estimated for each reach on the basis of assumed channel cross-sectional dimensions, as observed in the field, such as maximum flow depth (y) and maximum flow top width (W) (Section 4.2.2). The method is referred to as MC-X.

(ii) The computed hydrographs were compared to the observed hydrographs by statistical as well as visual analyses with regard to flood volume, peak flow magnitude and timing as well as hydrograph shape (Section 4.3).

(iii) Sensitivity analyses to different catchment variables such as routing reach length (ΔL), routing time step (Δt), Manning roughness coefficient (n), channel geometry, river slope (S) and Muskingum K and X parameters were performed (Section 4.3).

The details of the calculation steps are explained in the following sections.

4.1 Flood Routing Using Observed Inflow and Outflow

The Muskingum K and X parameters were calibrated from observed inflow and outflow hydrographs using the Muskingum-Cunge calibrated (M-Cal) and the Three-parameter Muskingum (M-Ma) methods. The detail of the procedure is discussed in Sections 4.1.1 and 4.1.2.

4.1.1 The M-Cal method

In the Muskingum method of flood routing, the river reach may be divided into sub-reaches (Section 2.2) and, according to the US Army Corps of Engineers (1994a), a general rule of thumb is that the computation interval should be less than 1/5 of the time of rise of the inflow hydrograph. This was used as an initial estimate of the routing time interval. Viessman *et al.* (1989) and Fread (1993) noted that the routing time interval Δt is frequently assigned any convenient value between the limits of $(K/3) \leq \Delta t \leq K$.

The Muskingum parameter (K) in Equation 2.9, which is equivalent to the wave travel time in the reach, may be estimated by the lag between the peak of inflow and outflow hydrographs, as shown in Figure 4.1.

The number of sub-reaches was determined by dividing the estimated total travel time (K) by routing time interval (Δt).

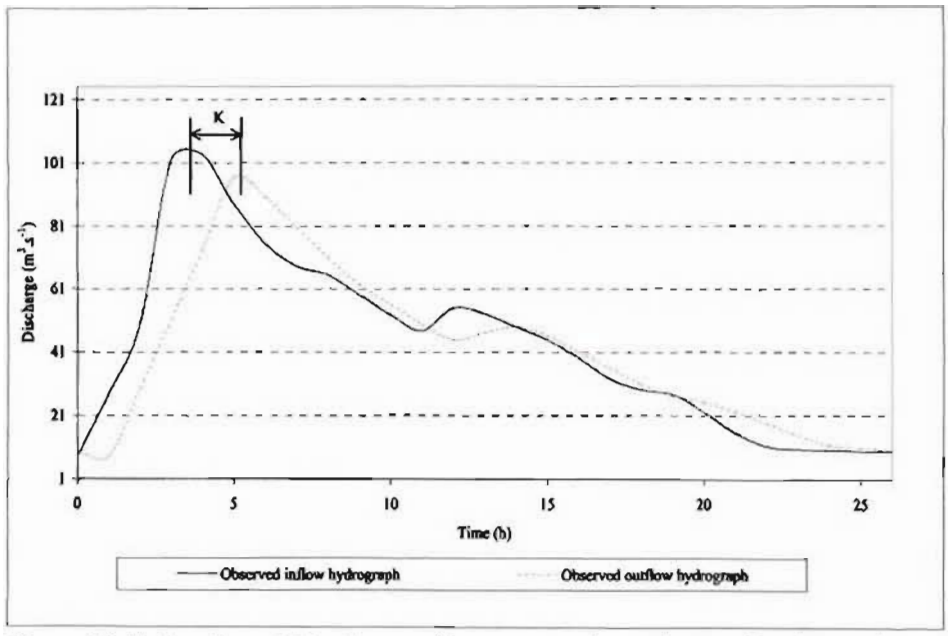

Figure 4.1 Estimation of Muskingum K parameter from observed hydrographs

Hence, the celerity may be estimated by substituting the value of K in Equation 2.9 as:

$$V_w = \frac{\Delta L}{K} \tag{4.1}$$

where

V_w = celerity [$m.s^{-1}$],

K = wave travel time [s], and

ΔL = reach length [m].

Alternatively, the celerity may be estimated from the average velocity, using Equation 4.2 and Table 4.1, for an assumed parabolic cross-section.

$$V_w = \frac{11}{9} V_{av} \tag{4.2}$$

Rearranging Equation 4.2, the average flow velocity for a parabolic cross-section can be calculated as:

$$V_{av} = \frac{9}{11} V_w \tag{4.3}$$

where

V_{av} = average velocity [$m.s^{-1}$].

Table 4.1 Estimation of celerity for various channel shapes (Viessman *et al.*, 1989)

Channel shape	Manning equations	Chezy equation
Wide rectangular	5/3 V_{av}	3/2 V_{av}
Triangular	4/3 V_{av}	5/4 V_{av}
Parabolic	11/9 V_{av}	7/6V_{av}

The average velocity calculated from Equation 4.3 was used to calculate cross-sectional flow area for a reference flow, computed as shown in Equation 4.4.

From Equation 2.11 (Section 2.2) the reference flow is estimated as:

$$Q_0 = Q_b + 0.5\,(Q_p - Q_b)$$

where

Q_0 = reference flow [$m^3.s^{-1}$],

Q_b = minimum discharge [$m^3.s^{-1}$], and

Q_p = peak discharge [$m^3.s^{-1}$].

Using the continuity equation (Chow, 1959; Linsley *et al.*, 1988; KenBohuslay, 2004) the cross-sectional area of flow obtained from Equation 4.4 is as follows:

$$A = \frac{Q_0}{V_{av}} \qquad (4.4)$$

where

A = cross-sectional area [m^2].

In a channel where top flow width (W) exceeds mean flow depth by a factor of 20, the mean flow depth (d) can approximate the hydraulic radius (R) (Barfield *et al.*, 1981 cited in SAICEHS, 2001). The hydraulic radius approximated from hydraulic mean depth (d) relationships for various cross-sectional shapes are shown in Table 4.2.

Table 4.2 Hydraulic mean depth (after Chow, 1959 and Koegelenberg *et al.*, 1997)

Cross-section	Hydraulic mean depth (d)
Parabolic section	(2/3) y
Rectangular	y
Triangular	0.5y

In this study and based on field observations, a parabolic cross section was assumed for all reaches.

The mean flow depth (d) for a parabolic cross-section is given by:

$$d = \frac{2}{3} y \qquad (4.5a)$$

where

d = mean flow depth [m], and

y = flow depth [m].

The hydraulic radius can thus be estimated from Equation 4.5b:

$$R = \frac{2}{3} y \qquad \text{where top flow width} > 20y \qquad (4.5b)$$

where

R = hydraulic radius for parabolic section [m].

The depth of flow was taken from rating curves shown in Figures 3.15 to 3.17.

The slope of the river reach was estimated from the DEM used by Agro hydrology and-Climatology Atlas of South Africa (Schulze *et al.*, 1997). The base roughness value (n_b) was estimated from values contained in Table 2.2 (Section 2.9.3) and based on field observations. The corrections for base roughness value for a particular site were taken from Table 2.3 (Section 2.9.3). Assuming a constant river cross-section along the river reach, the area (A) and the hydraulic radius (R) can be used to calculate the wetted perimeter (P) as shown in Equation 4.6:

$$P = \frac{A}{R} \tag{4.6}$$

where

P = wetted perimeter [m].

The formulae for geometrical cross-sectional area of various channels are illustrated in Table A.1 in Appendix A. The top flow width (W) for a parabolic river cross-sectional area may be estimated as shown in Equation 4.7 (Chow, 1959; Koegelenberg *et al.*, 1997):

$$W = \frac{3A}{2y} \tag{4.7}$$

where

A = cross-sectional area [m^2], and

y = depth of flow [m].

The Muskingum X parameter was calibrated by minimising the error between the peak discharge of the observed and computed hydrographs.

After the Muskingum K (Figure 4.1) and X parameters were calibrated, the routing coefficients were estimated using Equations 2.6a, 2.6b and 2.6c (Section 2.1).

As suggested by Viessman *et al.* (1989), negative values of C_1 must be avoided. Negative values of C_2 do not affect the routed hydrographs. The negative values of C_1 can be avoided by satisfying Equation 2.7 (Section 2.1), which is repeated below:

$$\frac{\Delta t}{K} > 2X$$

After the X parameter was determined, the routing time interval was adjusted using relationship given in Figure 2.3 (Section 2.1) (Cunge, 1969; cited by NERC, 1975).

Since Q_t, I_t and I_{t+1} are known for a given time increment, Q_{t+1} is computed using Equation 2.13 (Section 2.2) and repeated for successive time increments to estimate the outflow hydrograph. The lateral inflow per unit length (q) for longer river reaches was estimated using

Equation 2.15d (Section 2.2) and added to the computed outflow. It was assumed that the inflow was estimated from a single upstream catchment.

From the continuity equation,

$$Q = AV_w$$

where

Q = discharge [$m^3.s^{-1}$],

A = area [m^2], and

V_w = celerity [$m.s^{-1}$].

The area term in Equation 2.15d can be substituted by discharge as shown in the following Equation 4.8 (Fread, 1998).

$$q = \frac{\frac{1}{V_w}\left(\frac{I_j^{t+1} + Q_{j+1}^{t+1}}{2} - \frac{I_j^t + Q_{j+1}^t}{2}\right)}{\Delta t} + \frac{\beta(Q_{j+1}^{t+1} - I_j^{t+1}) + (1-\beta)(Q_{j+1}^t - I_j^t)}{\Delta L} \qquad (4.8)$$

The value of β is between 0.5-1 (Fread, 1998). Based on the results obtained, a value of 0.7 was used in this study for Reach-II and Reach-III.

Flow characteristics such as the magnitude and timing of peak flow, hydrograph shapes and flow volume were compared statistically against the observed events. Using this M-Cal method, the K and X parameters were calibrated for each event analysed.

The Three-parameter Muskingum estimation method (M-Ma) outlined in Section 2.3 was also applied.

4.1.2 The M-Ma method

The K, X and α parameters were estimated using the M-Ma method by treating the entire reach as single reach. The three coefficients (d_1, d_2 and d_3) in Equation 2.20 were estimated directly using the matrix method. After the primary flow data were reformatted into fixed time steps, the matrix inversion was performed, for each selected event, using the SPSS (Version 11.0.1) statistical software package to perform the matrix inversion (SPSS11, 2003).

Using the routing coefficients (d_1, d_2 and d_3) obtained directly from the matrix computation, and since I_t and I_{t+1} are known for every time increment, routing is accomplished by solving Equation 2.5 (Section 2.1) for successive time increments.

The three C_i coefficients in Equation 2.5 (Section 2.1) can be derived from the d_i coefficient of Equations 2.20a, 2.20b and 2.20c as indicated in Section 2.3. Computations were used to calculate the K, X and α parameters numerically from Equations 2.21a, 2.21b and 2.21c (Section 2.3).

4.2 Flood Routing in Ungauged River Reaches

When routing in ungauged catchments, the parameters of the model have to be estimated without observed hydrographs. Inflow hydrographs to downstream catchments can be simulated using a hydrological model such as the ACRU model (Schulze, 1995). For this study, the observed inflow hydrographs to the reaches are used.

4.2.1 The MC-E method

In ungauged catchments, where observed inflow and outflow hydrographs are not available, and a methodology to estimate inflow and outflow hydrographs has to be derived. As Angus (1987) noted, it is possible to estimate runoff from rainfall using the ACRU distributed model. Hence, the inflow hydrographs for ungauged catchments may be simulated using a hydrological model. The depth of flow and discharge can be derived from empirical relationships recommended by the US Reclamation Service (Chow, 1959), or other flow regime theories suited to rivers with similar characteristics (Section 2.8). Hence, the

Muskingum K and X parameters can be estimated in ungauged river reaches using inflow hydrographs and channel dimensions, which are estimated empirically. In this method, the observed primary flow data obtained from the Department of Water Affairs and Forestry (DWAF) and empirically estimated channel variables are used for the estimation of the Muskingum K and X parameters.

The Muskingum K parameter is estimated from Equation 2.9 as follows (Section 2.2):

$$K = \frac{\Delta L}{V_w}$$

For a parabolic cross-section, the celerity (V_w) may be estimated from Table 4.1 as follows:

$$V_w = \frac{11}{9} V_{av}$$

The average velocity (V_{av}) is calculated from the Manning Equation 2.32b as follows (Chow, 1959):

$$V_{av} = \frac{1}{n} R^{2/3} \sqrt{S}$$

The hydraulic radius (R) is estimated from Table 4.2 once the flow depth (y) has been estimated from empirical relationships shown in Equation 2.31b.

From Manning's Equation, a section factor, as shown in Equation 2.32a (Section 2.8) can be calculated as (Chow, 1959):

$$AR^{2/3} = \frac{Q_0 n}{\sqrt{S}}$$

From Equation 2.11 (Section 2.2) the reference flow is estimated as:

$$Q_0 = Q_b + 0.5 \left(Q_p - Q_b\right)$$

Since the reference flow, Q_0, roughness coefficient (n) and slope (S) are known for the river reach and events under consideration, the unknown variables in Equation 2.32a (Section 2.8) have to be estimated by known variables using either empirical rules that relate discharge and depth, slope or by using charts that relate section factor to depth of flow (Chow, 1959). The chart is shown in Figure A.1 in Appendix A.

Equation 2.31b relates the wetted perimeter with discharge for natural rivers as follows (Section 2.8):

$$P = 4.71\sqrt{Q_0} \qquad \text{for stable river channels}$$

where

P = wetted perimeter [m], and

Q_0 = reference flow [$m^3.s^{-1}$].

The hydraulic radius (R) and hydraulic mean depth (d) can be assumed to be equal when the top flow width exceeded mean flow depth by a factor of 20 (Section 4.1). From the flow area equations contained in Table A.1 (Appendix A), it is evident that for a parabolic section the wetted perimeter (P) can be assumed to be equal to the top flow width (W). Hence, top flow width (W) is substituted by wetted perimeter (P) as shown for a parabolic channel Equation 4.9

When the hydraulic radius is equated with the mean hydraulic depth, then from Table A.1 (Appendix A), width (W) and perimeter (P) can be proved to be equal for a parabolic equation as follows:

The area of a parabolic section is computed as:

$$A = \frac{2yW}{3} \qquad (4.9a)$$

For wide parabolic channels, the hydraulic radius may be estimated as:

$$R \cong d = \frac{2y}{3} \qquad (4.9b)$$

The wetted perimeter is computed as:

$$P = \frac{A}{R} \tag{4.9c}$$

Substituting Equations 4.9a and 4.9b into Equation 4.9c result in:

$$P = \left(\frac{2yW}{3}\right) \Big/ \left(\frac{2y}{3}\right) = W \tag{4.9d}$$

Equation 4.9d can then be substituted in the following equation as:

$$AR^{2/3} = \left(\frac{2yP}{3}\right) * \left(\frac{2y}{3}\right)^{2/3} = \frac{Qn}{\sqrt{S}} \tag{4.9e}$$

Then, solving for y in Equation 4.9e, the flow depth (y) may be estimated as:

$$y = \left(\frac{Q_0 n}{0.508\, P\sqrt{S}}\right)^{3/5} \tag{4.10}$$

For the MC-E method, Equation 4.10 was used to estimate the depth of flow in ungauged catchments in order to estimate the Muskingum K and X parameters.

A representative slope of the river reach may be estimated from the river profile as shown in Section 3.4.

The roughness coefficient (n), slope (S) and hydraulic radius (R) can be substituted in the Manning Equation 2.32b to estimate the average velocity (V_{av}).

The average velocity (V_{av}) is substituted in Equation 4.2 to calculate celerity (V_w) and then the celerity term substituted into Equation 2.9 (Section 2.2) to calculate the Muskingum K parameter.

The average velocity is calculated from Equation 2.32b. Manning's equation is used to calculate celerity and flow area of the reference flow (Chow, 1959; Linsley *et al.*, 1988; KenBohuslay, 2004), or the area of flow can be estimated using the geometrical parameters as shown in the following equation for a parabolic section:

$$A = \frac{2yP}{3} \tag{4.11}$$

where

A = cross-sectional area [m^2],

P = wetted perimeter (From Equation 2.29) [m], and

y = depth of flow [m].

From Equation 4.9d, the wetted perimeter (P) and top flow width (W) are assumed to be equal.

The top flow width (W), reference flow (Q_0), river slope (S), celerity (V_w) and sub-reach length (ΔL) are substituted in Equations 2.9 and 2.10 (Section 2.2) to estimate the Muskingum K and X parameters as follows:

$$K = \frac{\Delta L}{V_w}$$

$$X = \frac{1}{2} - \frac{Q_0}{2SWV_w\Delta L}$$

In this method, Equation 4.10 was used to estimate the channel flow depth.

4.2.2 The MC-X method

Another method of estimating flow depth in ungauged catchments is by developing a rating curve for an assumed section in the reaches (Smithers and Caldecott, 1995). Hence, flood routing can be applied using selected channel cross-sections. For the selected channel cross-section observed in the field, a rating curve was developed based on the maximum width and depth relationships.

The assumed cross-section is divided into incremental cross-sectional depths and the corresponding cumulative area is calculated from geometrical properties of a parabolic channel shape, as shown in Table A.1 (Appendix A). The parabolic shape is used to illustrate the calculation steps.

Assuming a linear relationship between width and depth of the river section, for each given depth, a corresponding top width can be proportioned from the observed maximum depth and width ratio contained in Table 3.2 (Section 3.4) as follows:

$$W_i = \frac{W_{Max}}{y_{Max}} y_i \qquad (4.12)$$

where

y_i = given depth [m],
W_i = top width [m],
W_{Max} = maximum top width [m] from Table 3.2, and
y_{Max} = maximum depth [m] from Table 3.2.

The wetted perimeter for each sub-section is calculated from geometrical equations as contained in Table A.1 (Appendix A). The parabolic section is used as example for showing the calculations:

$$P_i = W_i + \frac{8y_i}{3W_i} \qquad (4.13)$$

where

P_i = wetted perimeter for given sub-section [m],
W_i = top width for sub-sections [m], and

y_i = given depth for sub-section [m].

The flow area can be estimated from the continuity equation or geometrical properties for a parabolic shape illustrated in Table A.1 (Appendix A).

$$A = \frac{2Wy}{3}$$

where

A = flow area [m^2],
W = top flow width [m], and
y = flow depth [m].

The hydraulic radius is computed from the wetted perimeter and cumulative area as follows:

$$R = \frac{A}{P} \tag{4.14}$$

Then, the corresponding cumulative discharge is calculated from the Manning equation as follows:

$$Q = A \frac{1}{n} R^{2/3} \sqrt{S} \tag{4.15}$$

where

A = area [m^2], and
Q = discharge [$m^3.s^{-1}$].

Since the roughness coefficients (n), hydraulic radius (R), flow area (A) and slope (S) of each reach is known, the discharge can be calculated from Equation 4.15. Thus from the derived rating curve, the depth of flow can be estimated for a given discharge and the corresponding width and wave celerity can be computed using Equation 4.12 and Table 4.1 respectively. Equations 2.9 and 2.10 are then used to estimate the K and X parameters.

4.3 Model Performance and Sensitivity

It is generally accepted that the output of a hydrological simulation model will not be identical in every aspect to the real system it proposes to represent. However, it is required that the output be sufficiently close to the real system so that the model may be considered to be an acceptable model (Green and Stephenson, 1985).

As suggested by Green and Stephenson (1985), in order to compare a model output to the observed data, criteria for making such a comparison must first be identified. Visual comparison by plotting simulated and observed hydrographs provides a valuable means of assessing the accuracy of the model output. However, visual comparisons usually tend to be subjective and need additional statistical analysis. To overcome these difficulties, as well as to highlight certain model peculiarities, statistical goodness-of-fit procedures can be employed.

Although the reliability of a hydrological simulation model depends on the quality of input data provided, the accuracy of simulated hydrographs should be assessed by comparing the computed hydrographs against the observed hydrographs (Caldecott, 1989). In addition, the reliability of a runoff estimate made for an ungauged catchment is a function of the reliability of the flood runoff model, the type of the predictive equations and their parameters and coefficients as well as the wisdom and experience of the analyst (US Army Corps of Engineers, 1994a). Hence, the difference in the observed and computed hydrograph are analysed statistically by means of Root-Mean-Square Error (RMSE) and goodness-of-fit statistics. A statistical goodness-of-fit procedure implies a procedure employed to measure the deviation of simulated output from the observed input data set (Green and Stephenson, 1985).

Even though numerous goodness-of-fit criteria for assessing the accuracy of simulated output have been proposed, particular aspects may give more weight to certain output interests (Green and Stephenson, 1985). Hence, different goodness-of-fit statistics should be applied to assess different hydrograph components such as flood volume, hydrograph shape, peak flow magnitude and timing. Since, an objective of this research is to compute hydrographs in ungauged reaches, the criteria for assessments were selected as described below.

Equation 4.16 was used to estimate the actual errors in the computed hydrographs. RMSE computes the magnitude of error in the computed hydrographs (Schulze *et al.*, 1995).

$$RMSE = \sqrt{\frac{\sum_{i=0}^{n}(Q_{comp} - Q_{obs})^2}{n}} \qquad i = 1, 2, 3\ldots, n \qquad (4.16)$$

where

RMSE = Root-Mean-Square Error [$m^3.s^{-1}$ per event],

Q_{comp} = computed outflow [$m^3.s^{-1}$], and

Q_{obs} = observed outflow [$m^3.s^{-1}$].

As peak outflow is important in a single event model, a comparison of computed and observed peak flow rates, peak timing and volume were computed as shown in Equation 4.17 (Green and Stephenson, 1985):

$$E_{peak} = \frac{Q_{p\text{-}comp} - Q_{p\text{-}obs}}{Q_{p\text{-}obs}} 100 \qquad (4.17a)$$

where

E_{peak} = peak flow error [%],

$Q_{p\text{-}comp}$ = computed peak flows [$m^3.s^{-1}$], and

$Q_{p\text{-}obs}$ = observed peak flows [$m^3.s^{-1}$].

$$E_{time} = \frac{t_{p\text{-}comp} - t_{p\text{-}obs}}{t_{p\text{-}obs}} 100 \qquad (4.17b)$$

where

E_{time} = peak time error,

$t_{p\text{-}comp}$ = time when Q_{comp} occurs [s], and

$t_{p\text{-}obs}$ = time when Q_{obs} occurs [s].

$$E_{volume} = \frac{V_{comp} - V_{obs}}{V_{obs}} 100 \qquad (4.17c)$$

where

E_{volume} = peak volume error [%],

V_{comp} = computed total volume [m^3], and

V_{obs} = observed total volume [m^3].

Even though the RMSE, E_{peak}, E_{time} and E_{volume} statistics may appear to be reasonable, the shapes of the respective hydrographs may be different. Nash and Sutcliffe (1970, cited by Green and Stephenson, 1985) proposed a dimensionless coefficient of model efficiency (E). The computed hydrograph is a better fit to the observed hydrograph when the coefficient of model efficiency (E) approaches 1 (Green and Stephenson, 1985). Hence, the hydrograph shape comparison was estimated as follows:

$$E = \frac{F_0^2 - F^2}{F_0^2} \tag{4.18}$$

where

$$F^2 = \sum_{i=1}^{n} \left[Q_{obs}(t) - Q_{comp}(t) \right]^2 ,$$

$$F_0^2 = \sum_{i=1}^{n} \left[Q_{Obs.}(t) - Q_m \right]^2 ,$$

Q_m = mean of the observed flows [$m^3.s^{-1}$], and

n = number of data values.

In addition to the limitations of the Muskingum-Cunge method, uncertainties in estimation of catchment parameters such as reach slope, roughness coefficients and geometry of the channel are expected to affect the simulated hydrographs. Therefore, in addition to the results from the application of the methodology discussed in this chapter, sensitivity analysis of catchment parameters such as roughness coefficients, reach slope and reach geometry are contained in Chapter 5.

5. RESULTS

The results of applying the methodology outlined in Chapter 4 are contained in this chapter and include both results using calibrated parameters, to assess the performance of the Muskingum method, and results from using the Muskingum-Cunge method, to assess the performance of the method in ungauged catchments.

5.1 Flood Routing Using Observed Inflow and Outflow Hydrographs

Flood routing using calibrated parameters was undertaken and events that had good inflow and outflow hydrographs were considered for further sensitivity analysis. Single observed events were extracted from each sub-catchment, as detailed in Section 4.3. The extracted hydrographs were analysed using the M-Cal and M-Ma parameter estimation methods. The details of the results and plotted hydrographs are contained in the following sub-sections.

5.1.1 Reach–I

The estimated catchment characteristics and parameters for Reach-I are contained in Tables 5.1 to 5.3.

Table 5.1 Estimated parameters for Reach-I using the M-Cal method

Reach	Event	ΔL [m]	Δt [s]	A [m^2]	Q_0 [$m^3.s^{-1}$]	K[s]	X	C_0	C_1	C_2
I	1	2045	1800	65.90	61.26	1800	0.00	0.33	0.33	0.33
	2	2045	2520	82.21	54.58	2520	0.00	0.33	0.33	0.33
	3	4090	1800	35.73	66.43	1800	0.00	0.33	0.33	0.33

Table 5.2 Estimated parameters for Reach-I using the M-Ma method

Reach	Event	ΔL [m]	Δt [s]	A [m^2]	Q_0 [$m^3.s^{-1}$]	K [s]	X	C_0	C_1	C_2	α
I	1	4090	1800	65.90	61.26	4895	-0.26	-0.06	0.31	0.75	-0.07
	2	4090	2520	82.21	54.58	3700	-0.02	0.23	0.27	0.50	-0.12
	3	4090	1800	35.73	66.43	2748	-0.33	0.00	0.40	0.60	-0.03

The computed and observed hydrographs from the application of the M-Cal and M-Ma methods for events in Reach-I are shown in Figures 5.1 to 5.3.

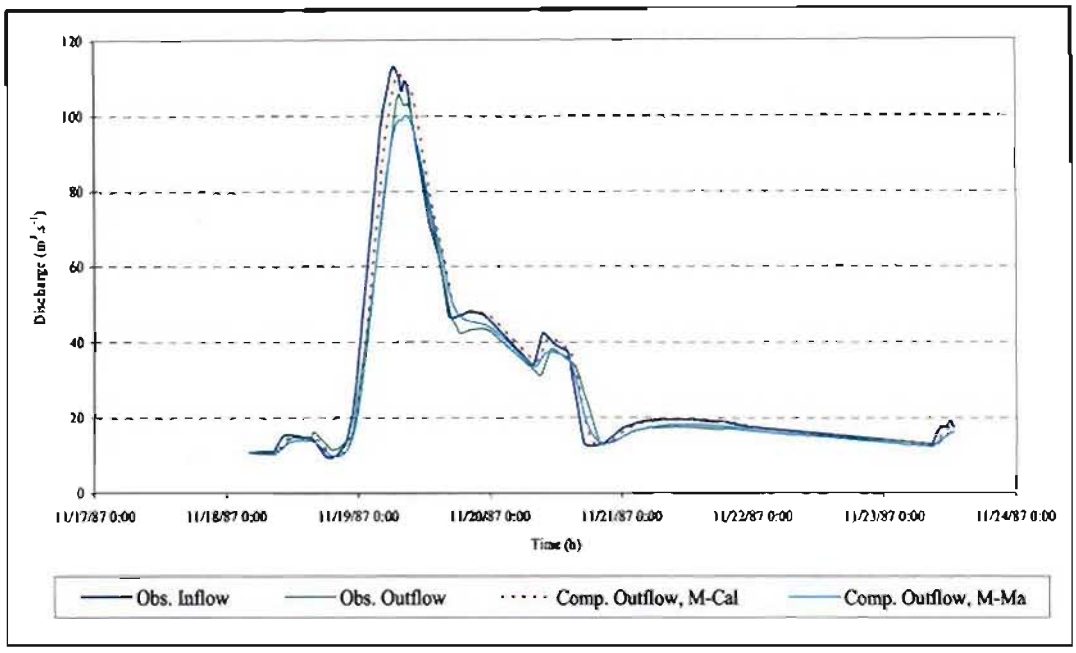

Figure 5.1 Observed and computed hydrographs of Event-1 in Reach-I

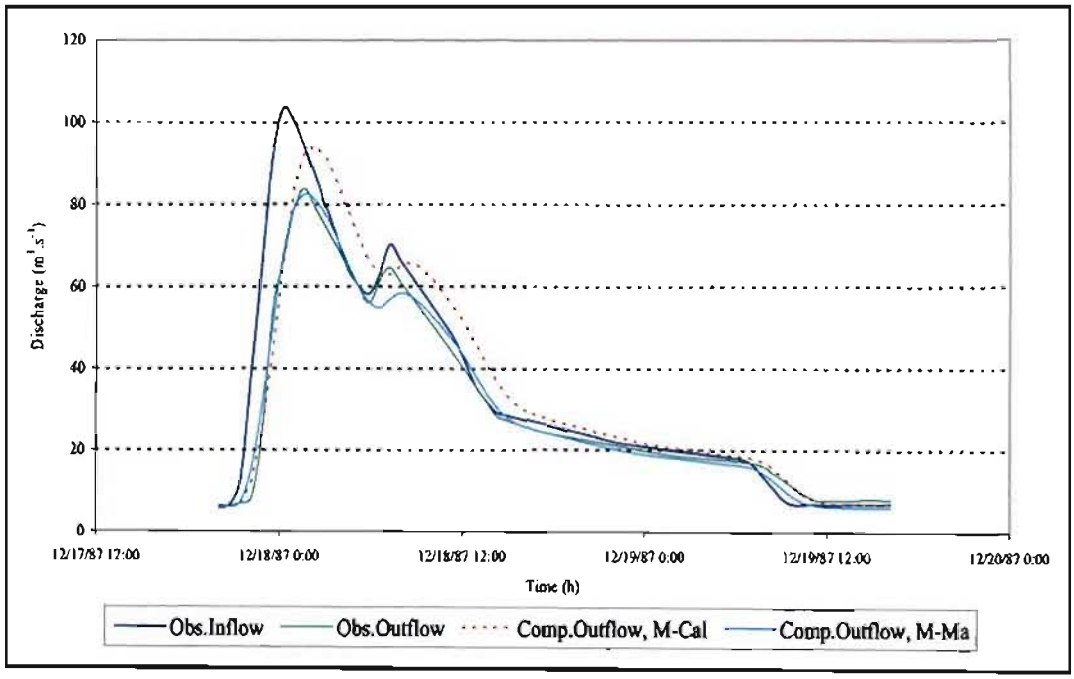

Figure 5.2 Observed and computed hydrographs of Event-2 in Reach-I

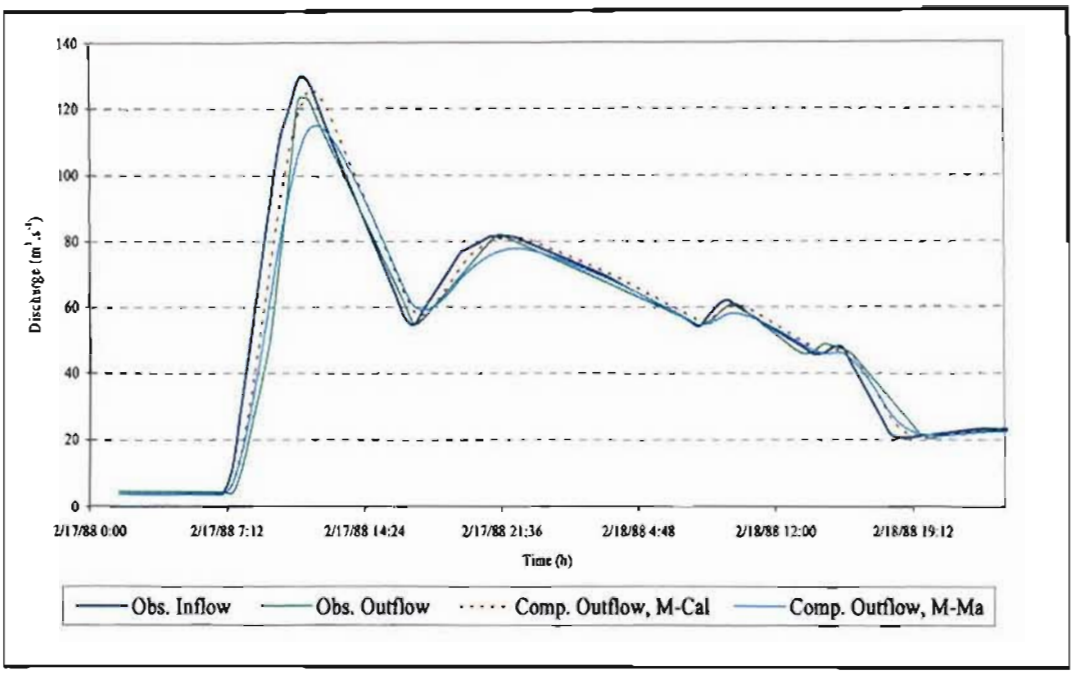

Figure 5.3 Observed and computed hydrographs of Event-3 in Reach-I

The results from using the M-Cal and M-Ma parameter estimation methods for Reach-I are contained in Tables 5.3 to 5.4.

Table 5.3 Results for Reach-I using the M-Cal method

Reach	Events	Obs Peak flow [$m^3.s^{-1}$]	Comp Peak flow [$m^3.s^{-1}$]	Peak flow Error [%]	Peak timing Error [%]	RMSE [$m^3.s^{-1}$]	E	Obs Volume [mcm]	Comp Volume [mcm]	Volume Error [%]
I	1	105.70	111.07	5.08	-1.59	3.34	0.98	12.63	13.44	6.44
	2	83.67	94.27	12.67	-5.47	6.42	0.92	4.88	5.49	12.58
	3	122.79	125.54	2.24	-5.00	3.80	0.98	10.72	11.00	2.61

mcm = million cubic meter

Table 5.4 Results for Reach-I using the M-Ma method

Reach	Events	Obs Peak outflow [$m^3.s^{-1}$]	Comp Peak Outflow [$m^3.s^{-1}$]	Peak flow Error [%]	Peak timing Error [%]	RMSE [$m^3.s^{-1}$]	E	Obs Volume [mcm]	Comp Volume [mcm]	Volume Error [%]
I	1	103.20	100.00	-3.10	1.59	1.69	0.99	12.63	12.57	0.52
	2	83.60	82.33	-1.52	0.00	2.37	1.00	4.88	4.84	0.81
	3	122.40	114.79	-6.22	0.00	2.97	0.99	10.72	10.62	0.96

From the analyses of events using the M-Cal and the M-Ma method shown in Tables 5.1 to 5.4, it is noted that the methods have different K and X values. The K parameter in the M-Cal and the M-Ma methods are different. The K parameters from the M-Ma method are for the whole reach, but the K parameters from the M-Cal method are for the sub-routing reaches (ΔL). The X values are negative in the M-Ma method. As noted by O'Donnell *et al.* (1988), the calibration procedure requires many events to be analysed to define the most appropriate X value for the selected reach. Since the M-Ma method cannot be applied in ungauged catchments as it requires observed inflow and outflow hydrographs, it is not necessary to analyse many events for the assessment of M-Ma method in the present study.

From the results for the M-Cal method for Reach-I, contained in Table 5.3, the computed peak outflow is larger than the observed peak discharge for all three events considered. This may be explained by the fact that the M-Cal equation does not consider any lateral outflows which might happen due to infiltration and activities such as irrigation or diversion for other purposes. In addition, incorrect estimation of the slope may have an effect, which in turn affects the computation of the outflow hydrographs.

The negative α value shown in Table 5.2 indicates that there is no lateral inflow but that there are outflows from the main reach. Both methods have small RMSE values and E values that are nearly equal to 1, which indicates a small error in the computed hydrographs and similar shape of observed and computed hydrographs.

For the M-Ma method (Table 5.4 and Figure 5.1), the computed outflow hydrographs are very similar to the observed outflow hydrograph except having a lower peak in Event 1 and 3. This may be explained by the calibration of parameters directly from the inflow and observed outflow hydrographs in the M-Ma method.

Although the K and X parameters are different in both the M-Cal and the M-Ma methods, the computed hydrographs are similar to the observed hydrograph in terms of peak flow, peak flow time, volumes and shapes of the hydrographs. The negative values of peak flow error, peak timing error and volume error indicates that the computed results are smaller than the observed values. The RMSE values obtained from the analyses indicates that the error are small. The X values in M-Cal method is 0.0 indicates that storage is a function of only outflow.

From the results of both methods, it can be concluded that the Muskingum method, with calibrated parameters, results in computed hydrographs in Reach-I which have reasonably similar volume and shape compared to the observed hydrographs. Of the two methods, and based on the E and volume error statistic, it evident that the M-Ma performed slightly better than the M-Cal method.

5.1.2 Reach-II

The catchment characteristics and parameters estimated for Reach-II are contained in Tables 5.5 to 5.8.

Table 5.5 Estimated parameters for Reach-II using the M-Cal method

Reach	Event	ΔL [m]	Δt [s]	A [m^2]	Q_0 [$m^3.s^{-1}$]	K [s]	X	C_0	C_1	C_2
II	1	7777	5400	23.18	27.32	5400	0.49	0.98	0.01	0.01
	2	7777	5400	26.64	31.39	5400	0.49	0.98	0.01	0.01
	3	7777	5400	20.50	30.26	5400	0.49	0.98	0.01	0.01
	4	7777	5400	22.10	26.04	5400	0.49	0.98	0.01	0.01

Table 5.6 Estimated parameters for Reach-II using the M-Ma method

Reach	Event	ΔL [m]	Δt [s]	A [m^2]	Q_0 [$m^3.s^{-1}$]	K [s]	X	C_0	C_1	C_2	α
II	1	54440	5400	23.18	27.32	59090	0.16	0.23	-0.13	0.90	0.20
	2	54440	5400	26.64	31.39	99491	0.23	0.32	-0.25	0.93	0.04
	3	54440	5400	20.50	30.26	32400	-0.37	-0.20	0.31	0.89	0.20
	4	54440	5400	22.10	26.04	9200	-4.09	-0.71	0.81	0.89	-0.06

The computed and observed hydrographs for events in Reach-II using both the M-Cal and the M-Ma method are shown in Figures 5.4 to 5.7.

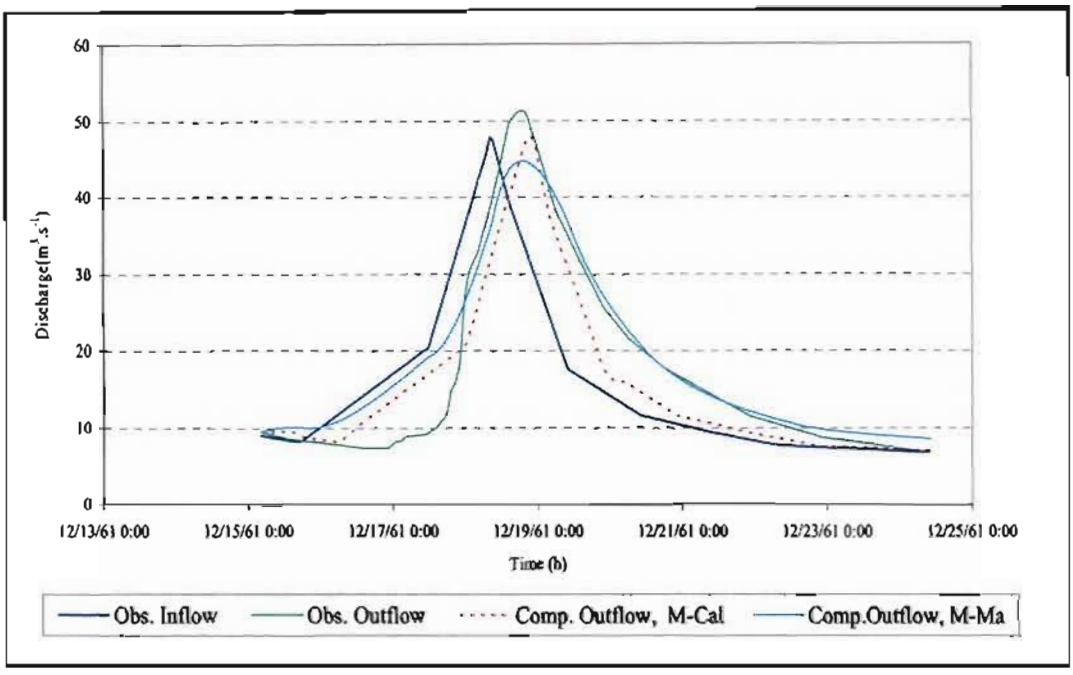

Figure 5.4 Observed and computed hydrographs of Event-1 in Reach-II

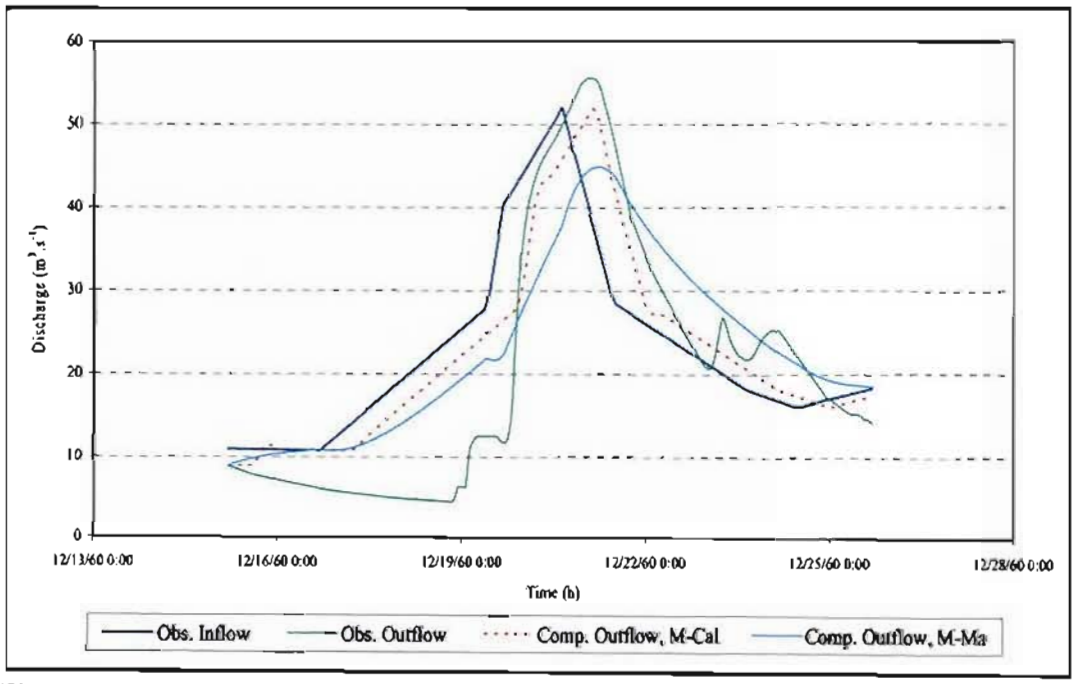

Figure 5.5 Observed and computed hydrographs of Event-2 in Reach-II

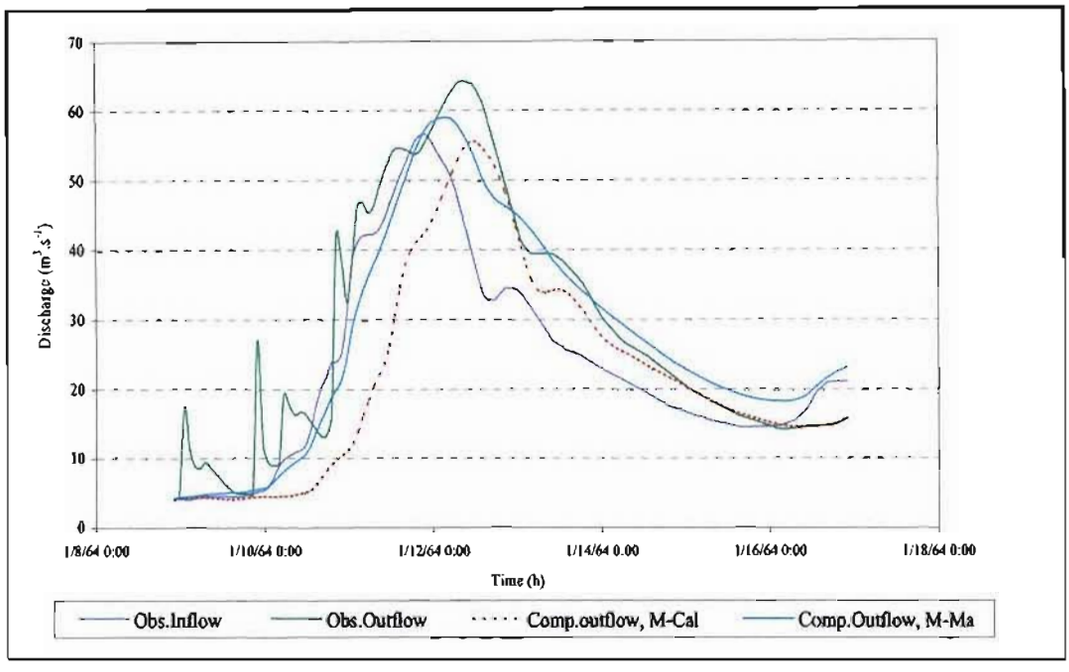

Figure 5.6 Observed and computed hydrographs of Event-3 in Reach-II

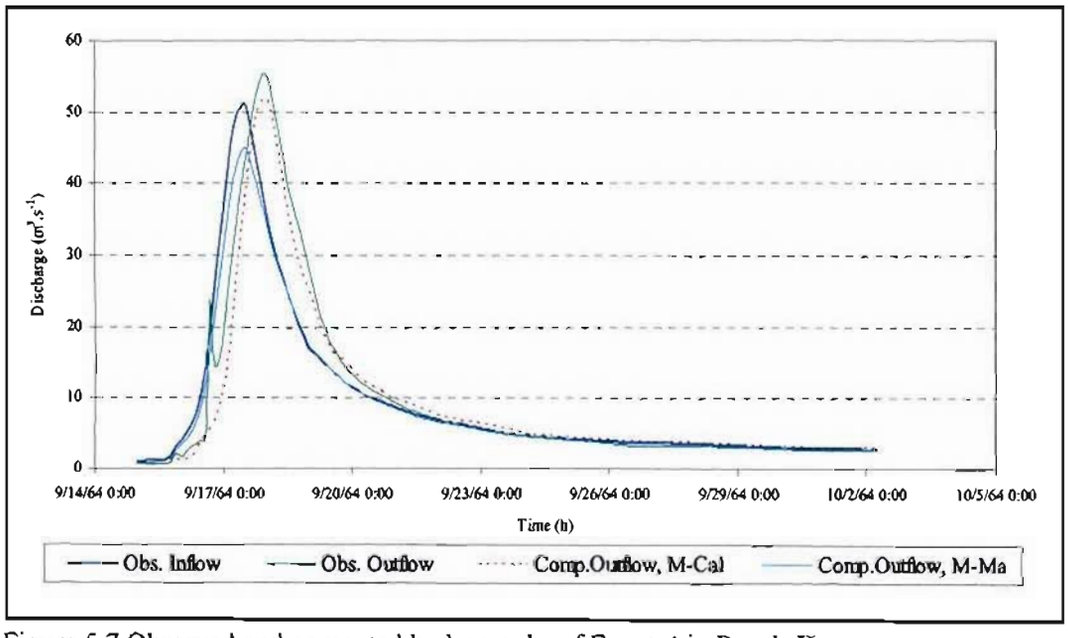

Figure 5.7 Observed and computed hydrographs of Event-4 in Reach-II

The results of flood routing analyses for Reach-II using the M-Cal method and the M-Ma method are contained in Tables 5.7 and 5.8.

Table 5.7 Results for Reach-II using the M-Cal method

Reach	Event	Obs Peak outflow [$m^3.s^{-1}$]	Comp Peak outflow [$m^3.s^{-1}$]	Peak flow Error [%]	Peak timing Error [%]	RMSE [$m^3.s^{-1}$]	E	Obs Volume [mcm]	Comp Volume [mcm]	Volume Error [%]
II	1	51.25	47.98	-6.38	3.30	4.39	0.88	13.63	12.39	-9.08
	2	55.52	51.85	-6.61	1.03	7.07	0.83	18.54	20.57	10.96
	3	64.22	55.53	-13.53	-2.87	10.50	0.65	19.87	15.45	-22.24
	4	55.40	51.87	-6.36	1.60	2.24	0.97	14.39	13.74	-4.52

Table 5.8 Results for Reach-II using the M-Ma method

Reach	Event	Obs Peak outflow [$m^3.s^{-1}$]	Comp Peak [$m^3.s^{-1}$]	Peak flow Error [%]	Peak timing Error [%]	RMSE [$m^3.s^{-1}$]	E	Obs Volume [mcm]	Comp Volume [mcm]	Volume Error [%]
II	1	51.25	44.67	-12.83	0.00	3.66	0.91	13.63	14.85	8.97
	2	55.52	44.85	-19.23	1.03	1.56	0.99	18.54	20.95	13.01
	3	64.22	58.96	-8.19	0.00	5.93	0.89	19.87	18.89	-4.92
	4	55.40	44.86	-19.03	1.60	5.14	0.84	14.39	12.91	-10.24

In Reach-II there is lateral inflow as a result of the length of the reach. Hence, the computation of the hydrographs includes the addition of lateral inflow into the main stream.

The volume errors are greater than 5% for Events 1, 2 and 3 using the M-Cal method. Similarly, the volume errors for Events 1, 2 and 4 are greater than 5% using the M-Ma method. Based on the hydrographs, RMSE and E values, it is evident that the shape of the computed hydrographs are similar to the observed outflow hydrographs for both methods.

Although the K and X parameters are different in both methods, the computed hydrographs are similar to the observed outflow hydrographs in terms of peak flow, peak flow time, volume and shape of the hydrographs. The value of X = 0.49 indicates that the equal weight is given to inflow and outflow hydrographs in the routing procedure.

5.1.3 Reach-III

The estimated catchment characteristics and parameters for Reach-III are contained in Tables 5.9 and 5.10.

Table 5.9 Estimated parameters for Reach-III using the M-Cal method

Reach	Event	ΔL [m]	Δt [s]	A [m^2]	Q_0 [$m^3.s^{-1}$]	K [s]	X	C_0	C_1	C_2
III	1	4000	9000	50.85	18.49	9000	0.49	0.98	0.01	0.01
	2	4000	9000	43.40	26.31	9000	0.49	0.98	0.01	0.01
	3	10000	9000	24.30	22.09	9000	0.50	1.00	0.00	0.00
	4	10000	9000	13.08	11.89	9000	0.39	0.80	0.10	0.10

Table 5.10 Estimated parameters for Reach-III using the M-Ma method

Reach	Event	ΔL [m]	Δt [s]	A [m^2]	Q_0 [$m^3.s^{-1}$]	K [s]	X	C_0	C_1	C_2	a
III	1	20000	9000	50.85	18.49	5462	0.1	0.22	-0.04	0.83	0.09
	2	20000	9000	43.40	26.31	5291	0.3	0.60	-0.36	0.77	0.00
	3	20000	9000	24.30	22.09	1857	0.5	1.09	-0.41	0.32	-0.05
	4	20000	9000	13.08	11.89	2625	0.4	0.81	-0.34	0.54	-0.09

The computed and observed hydrographs for events in Reach-III using both the M-Cal and the M-Ma method are shown in Figures 5.8 to 5.11.

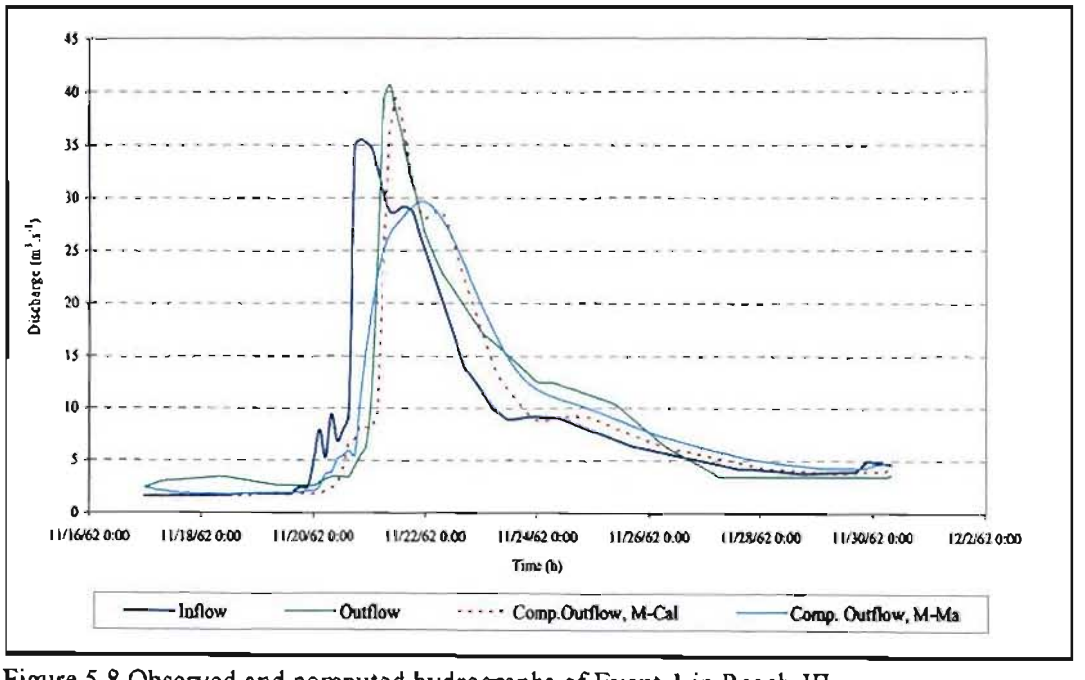

Figure 5.8 Observed and computed hydrographs of Event-1 in Reach-III

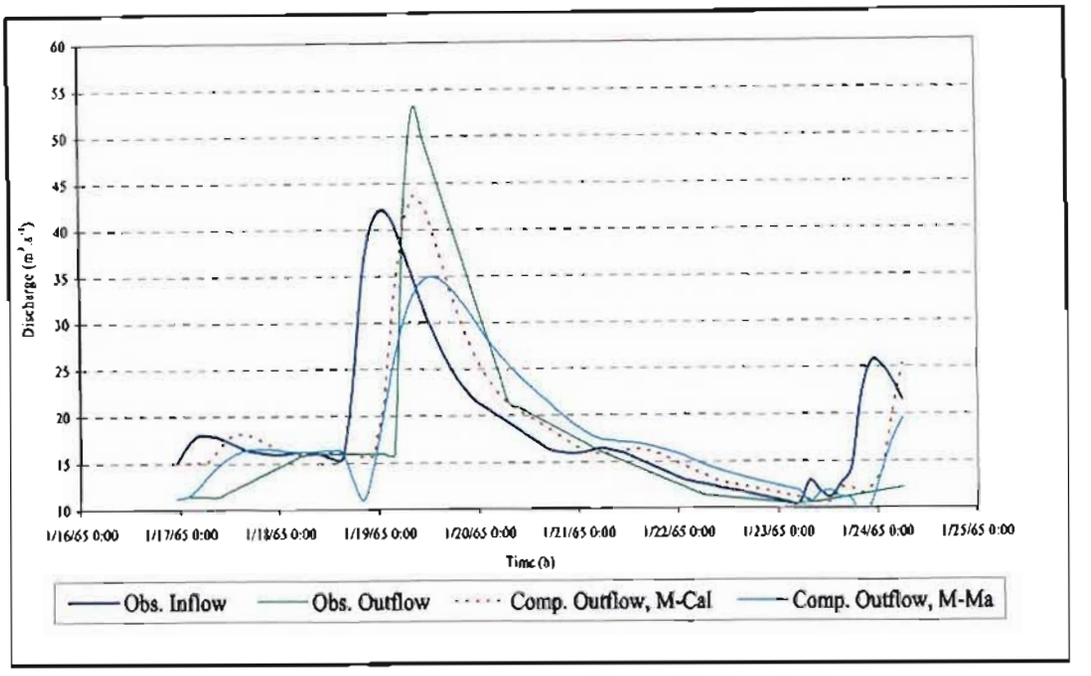

Figure 5.9 Observed and computed hydrographs of Event-2 in Reach-III

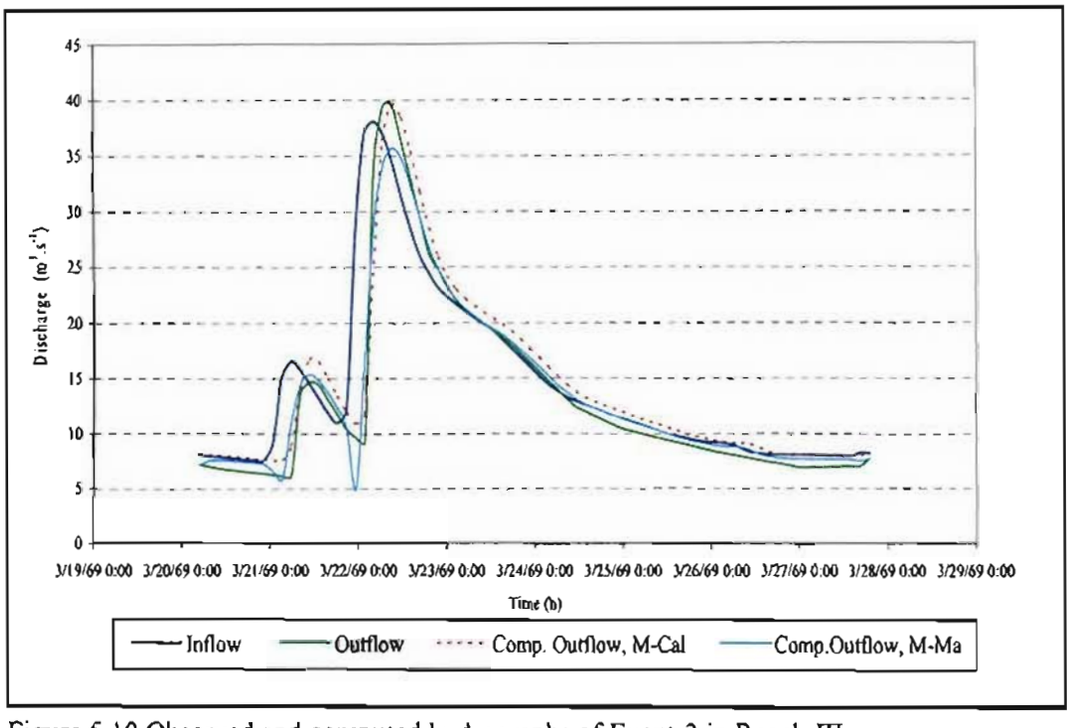

Figure 5.10 Observed and computed hydrographs of Event-3 in Reach-III

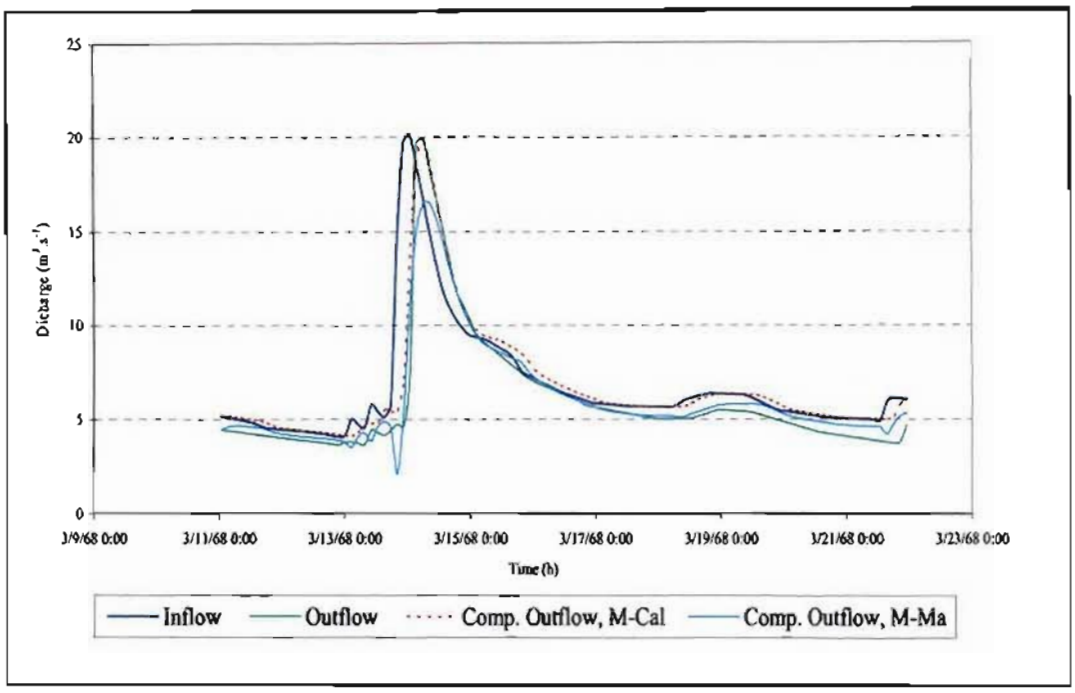

Figure 5.11 Observed and computed hydrographs of Event-4 in Reach-III

The results of flood routing analysis using the M-Cal and M-Ma methods in Reach-III are contained in Tables 5.11 and 5.12 following.

Table 5.11 Results for Reach-III using the M-Cal method

Reach	Event	Obs Peak outflow [$m^3.s^{-1}$]	Comp Peak outflow [$m^3.s^{-1}$]	Peak flow Error [%]	Peak timing Error [%]	RMSE [$m^3.s^{-1}$]	E	Obs Volume [mcm]	Comp Volume [mcm]	Volume Error [%]
III	1	40.65	39.40	-3.07	2.38	2.75	0.90	10.34	9.62	-6.97
	2	52.97	43.74	-17.41	0.00	4.14	0.82	11.08	11.56	4.36
	3	39.64	39.54	-0.27	0.00	1.69	0.96	8.72	9.45	8.37
	4	19.97	19.92	-0.26	0.00	0.99	0.91	5.67	6.36	12.31

Table 5.12 Results for Reach-III using the M-Ma method

Reach	Event	Obs Peak outflow [$m^3.s^{-1}$]	Comp Peak [$m^3.s^{-1}$]	Peak flow Error [%]	Peak timing Error [%]	RMSE [$m^3.s^{-1}$]	E	Obs Volume [mcm]	Comp Volume [mcm]	Volume Error [%]
III	1	40.65	29.61	-27.15	2.38	2.97	0.89	10.34	10.5	1.05
	2	52.97	34.87	-34.17	4.35	4.59	0.78	11.08	11.4	2.92
	3	39.64	35.64	-10.09	0.00	0.20	0.96	8.72	8.9	2.57
	4	19.97	16.54	-17.18	0.00	0.85	0.93	5.67	5.8	2.41

Reach-III is 20 km long and lateral inflows are considered in the simulated hydrographs. A significant decrease in the computed hydrographs of M-Ma method is observed this happens when there is a large change in the observed inflow between time steps (Δt) of the observed inflow hydrograph, with no corresponding change in the observed outflow hydrograph. The M-Ma method under performed in estimating peak flow of Event 1, 2, 3, and 4

In Reach-III, the statistics considered in Table 5.11 are generally less than 12% for the M-Cal method, with the exception of the peak flow error for Event 2 and the error in volume for Event 4. For the M-Ma method applied in Reach-III, the error in peak flows are generally larger than 20% and less than 5% for all other statistics considered in Table 5.12.

5.1.4 Section conclusions

For the M-Cal method, the X values are generally close to 0.5. As noted in Section 2.8, previous studies have shown that the X values for unconfined, wide natural rivers to be close to 0.0 and for natural rivers that are confined with well defined channels the X values are near to 0.5. Therefore, the computed X parameters contained in Tables 5.1 to 5.10 for Reach-I and Reach-II as well as Reach-III are acceptable.

From the analyses performed in the river reaches, it is noted that the computed hydrographs using the M-Ma method provide a better fit to the observed outflow hydrographs than the hydrographs computed using the M-Cal method, excluding the peak flow error observed in Reach III. However, both methods produced acceptable results with errors of less than 30% for most statistics considered. Both methods performed better for shorter reaches where the effect of lateral inflow is not significant.

The addition of lateral inflow to the computed hydrographs was not sufficient to obtain the observed peaks, but did result in outflow peak discharges, which were larger than the inflow peak discharges, as evident in the observed data. This under simulation of lateral inflow may be attributed to inflow water from other catchments. The lateral inflow addition considers only the flows that are derived from the same rainfall event that resulted in the hydrographs. However, in reality the tributaries that flow from other catchments also contribute to the increase in the observed outflow hydrographs. In addition, as the length of a reach increases so

does the possibility of tributary inflows increases. Hence, in long reaches the tributary flow should be added separately.

Considering the linearity assumption and other catchment characteristics such as the estimation of slope and Manning's roughness coefficient, it can be concluded from the results obtained that the M-Cal and M-Ma methods performed with in acceptable limits. The M-Ma method needs observed events to estimate the K and X parameters. The M-Ma method estimates the hydrographs well when the observed hydrographs have uniformly increasing data series. If the hydrograph has possible erroneous data among the other good data series, then the M-Ma method fails to compute the peak discharge well, as shown in Reach-III. Hence, the M-Ma method cannot be used in ungauged catchments. Since the Muskingum-Cunge method estimates the K and X parameters from the catchment and flow characteristics, it can be applied in ungauged catchments to estimate the K and X parameters.

5.2 Flood Routing in Ungauged Catchments

The outflow hydrographs for the selected events were computed using the Muskingum-Cunge method with both empirically estimated variables (MC-E) as well as variables estimated from assumed cross-sections (MC-X). The geometrical parameters of river reaches such as roughness coefficients (n), top flow width (W), cross-section area (A), wetted perimeter (P) and the hydraulic parameters such as celerity (V_w), average velocity (V_{av}), flow depth (y) were computed based on the observations made in the field. As detailed in Section 3.2, the rating curves for the MC-X method which were used to estimate the depths of reference flows (Q_0) in the routing procedure for each of the three reaches are shown in Figures 5.12, 5.13 and 5.14.

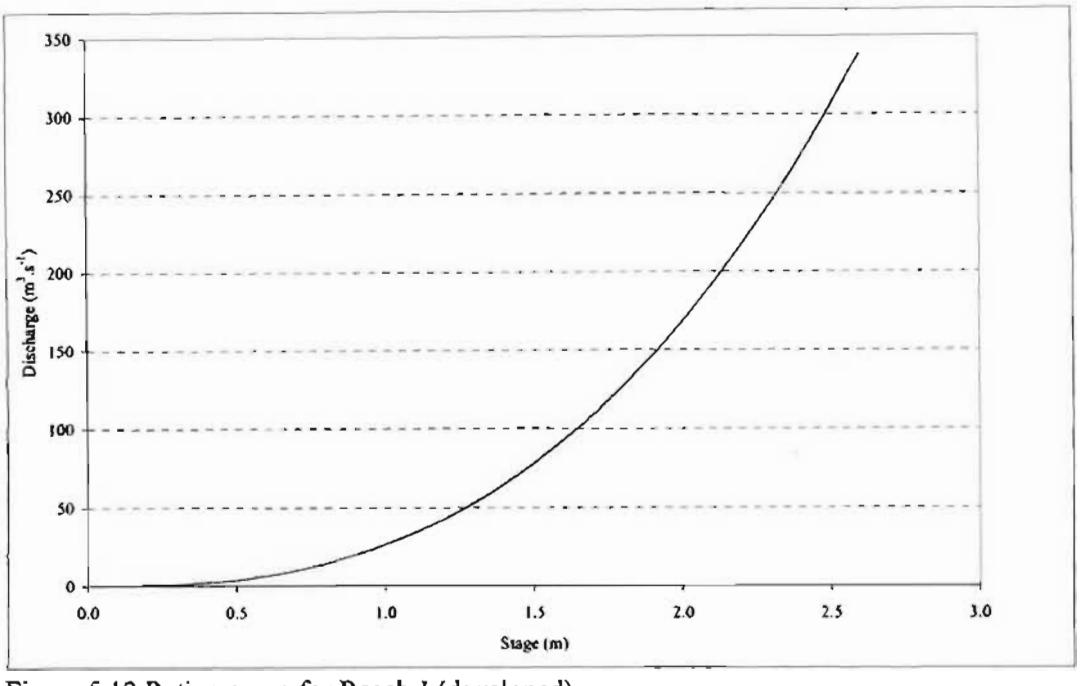

Figure 5.12 Rating curve for Reach-I (developed)

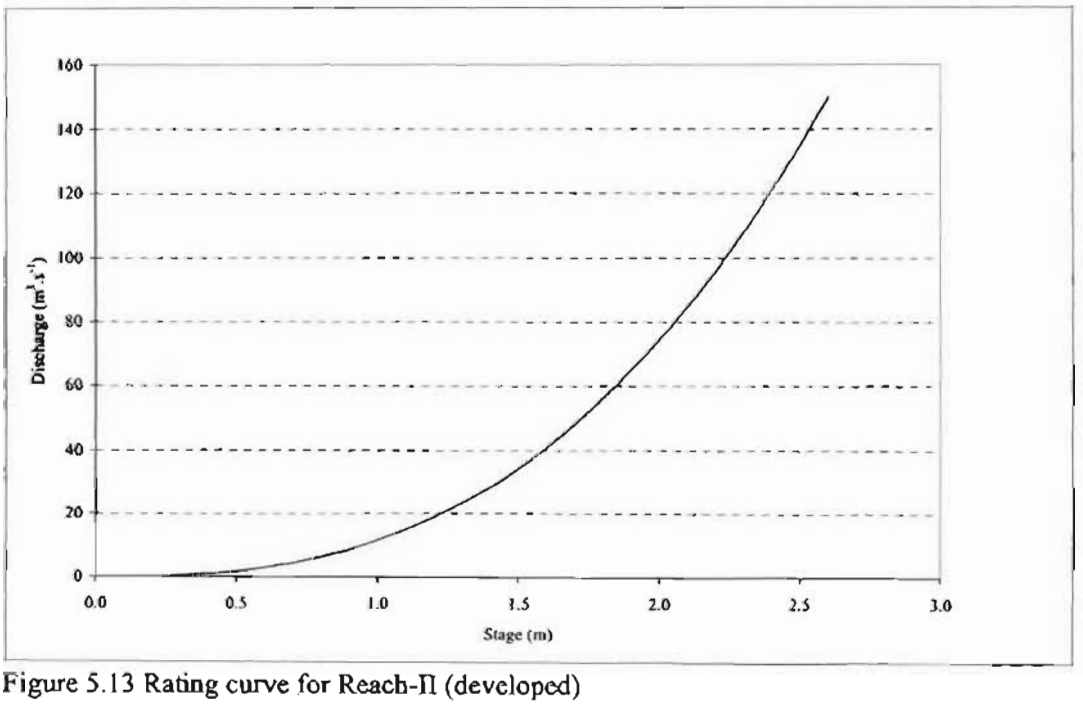

Figure 5.13 Rating curve for Reach-II (developed)

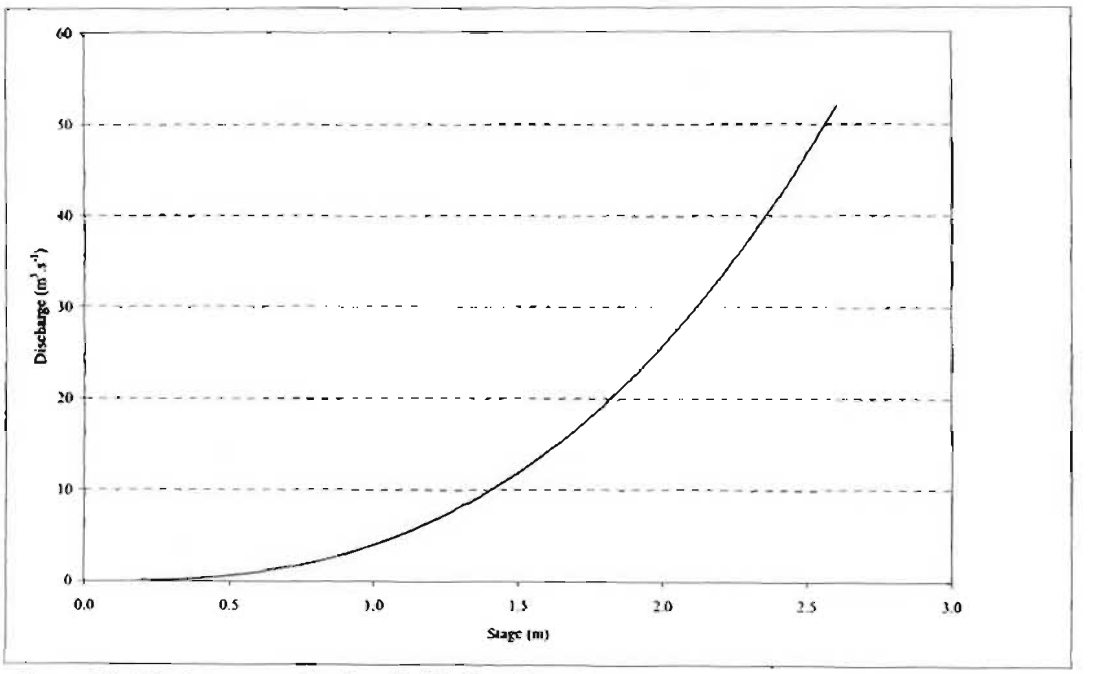

Figure 5.14 Rating curve for Reach-III (developed)

5.2.1 Reach-I

The estimated catchment characteristics and parameters for Reach-I are contained in Tables 5.13 to 5.16.

Table 5.13 Hydraulic parameters for Reach-I estimated using the MC-E method

Reach	Event	V_{av} [m.s^{-1}]	V_w [m.s^{-1}]	R [m]	y [m]	S [%]	n
I	1	2.02	2.47	1.13	1.70	0.70	0.045
	2	1.94	2.37	1.07	1.60	0.70	0.045
	3	2.25	2.75	1.33	2.00	0.70	0.045

Table 5.14 Hydraulic parameters for Reach-I estimated using the MC-X method

Reach	Event	V_{av} [m.s^{-1}]	V_w [m.s^{-1}]	R [m]	y [m]	S [%]	n
I	1	1.78	2.17	0.93	1.40	0.70	0.045
	2	1.69	2.07	0.87	1.30	0.70	0.045
	3	1.82	2.22	0.97	1.45	0.70	0.045

Table 5.15 Estimated parameters for Reach-I using the MC-E method

Reach	Event	ΔL [m]	Δt [s]	A [m^2]	W [m]	Q_0 [$m^3.s^{-1}$]	K [s]	X	C_0	C_1	C_2
I	1	2045	1800	30.31	26.74	61.26	828	0.47	0.96	0.38	-0.34
	2	2045	2520	28.12	26.36	54.58	862	0.47	0.97	0.50	-0.47
	3	4090	1800	29.49	22.12	66.43	1486	0.48	0.97	0.11	-0.08

Table 5.16 Estimated parameters for Reach-I using the MC-X method

Reach	Event	ΔL [m]	Δt [s]	A [m^2]	W [m]	Q_0 [$m^3.s^{-1}$]	K [s]	X	C_0	C_1	C_2
I	1	2045	1800	34.50	39.20	61.26	942	0.47	0.97	0.32	-0.29
	2	2045	2520	32.30	36.40	54.58	990	0.47	0.97	0.44	-0.42
	3	4090	1800	36.54	40.60	66.43	1841	0.49	0.97	0.00	0.02

The computed and observed hydrographs from the application of the MC-E and MC-X methods for Reach-I are shown as Figure 5.15 to 5.17.

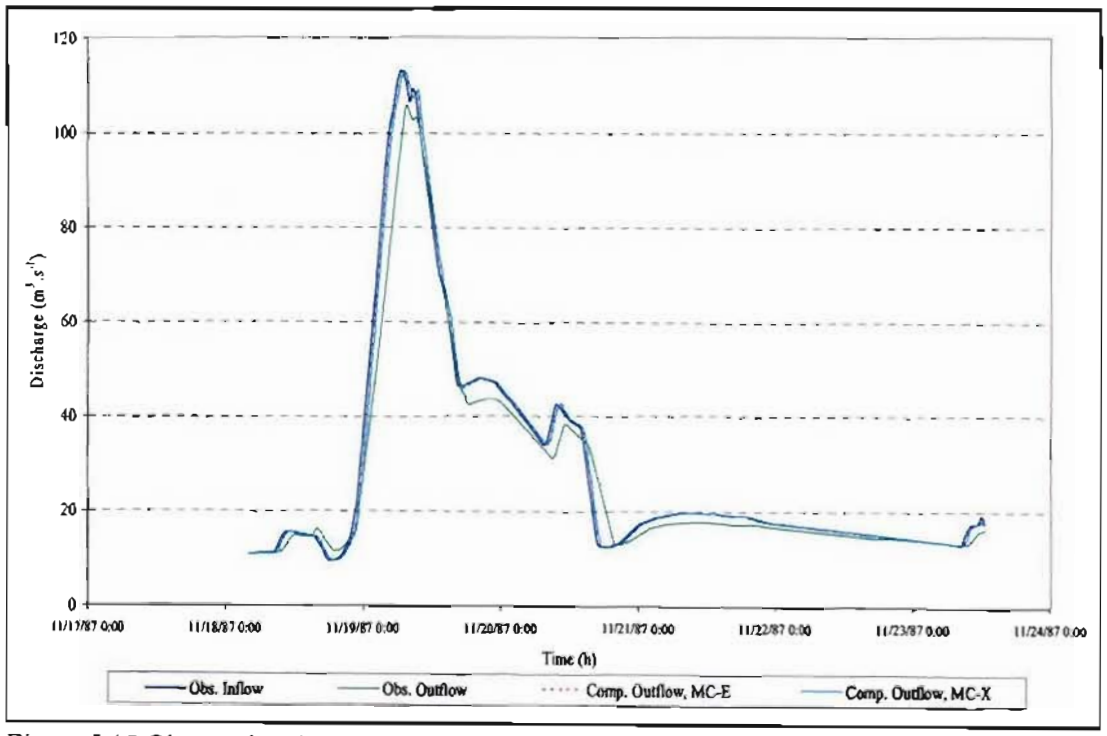

Figure 5.15 Observed and computed hydrographs for Event-1 in Reach-I

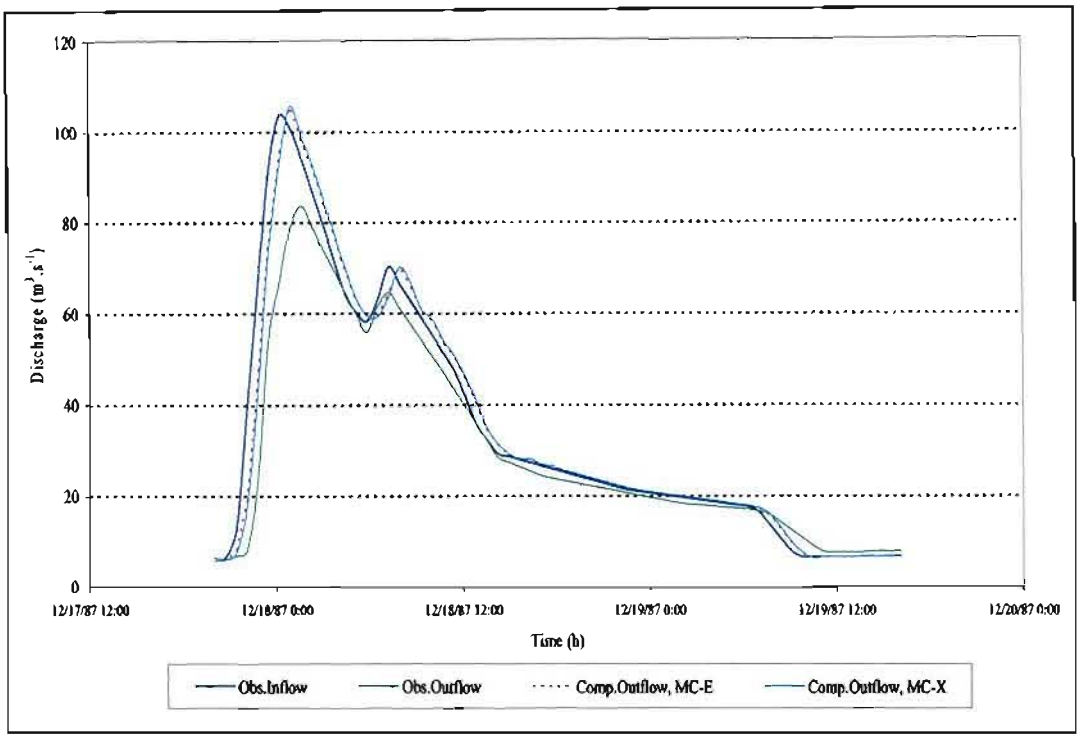

Figure 5.16 Observed and computed hydrographs for Event-2 in Reach-I

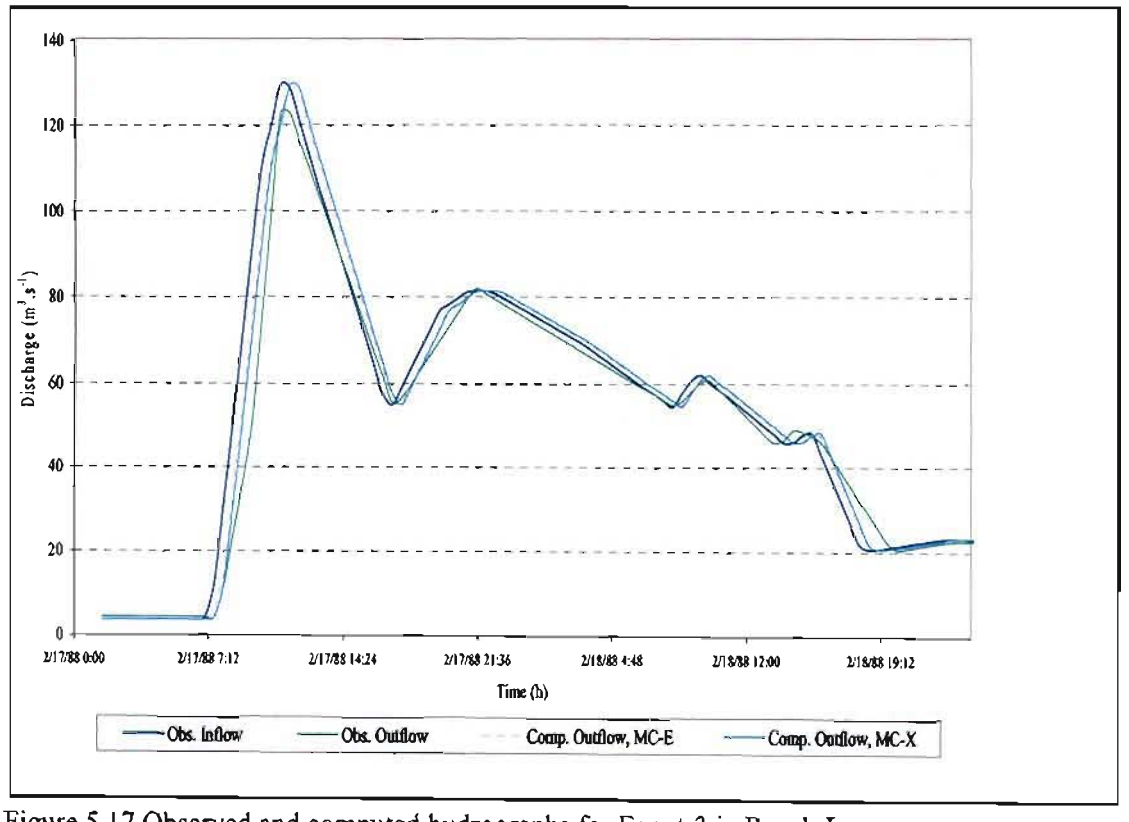

Figure 5.17 Observed and computed hydrographs for Event-3 in Reach-I

The results of flood routing analyses using the MC-E and MC-X methods for Reach-I are contained in Tables 5.17 and 5.18.

Table 5.17 Results for Reach-I using the MC-E method

Reach	Event	Obs Peak Outflow [$m^3.s^{-1}$]	Comp Peak outflow [$m^3.s^{-1}$]	Peak flow Error [%]	Peak timing Error [%]	RMSE [$m^3.s^{-1}$]	E	Obs Volume [mcm]	Comp Volume [mcm]	Volume Error [%]
I	1	105.70	113.05	6.95	-1.59	4.27	0.96	12.63	13.46	6.55
	2	83.67	105.59	26.20	-5.47	7.59	0.88	4.88	5.49	12.59
	3	122.79	129.77	5.68	-5.00	4.27	0.98	10.72	11.01	2.64

Table 5.18 Results for Reach-I using the MC-X method

Reach	Event	Obs Peak outflow [$m^3.s^{-1}$]	Comp Peak [$m^3.s^{-1}$]	Peak flow Error [%]	Peak timing Error [%]	RMSE [$m^3.s^{-1}$]	E	Obs Volume [mcm]	Comp Volume [mcm]	Volume Error [%]
I	1	105.70	112.98	6.89	-1.59	4.14	0.96	12.63	13.46	6.53
	2	83.67	105.45	26.04	-5.47	7.33	0.89	4.88	5.49	12.58
	3	122.79	129.03	5.08	-5.00	3.92	0.98	10.72	11.00	2.61

The flow depths shown in Table 5.13, derived using empirical relationships, and in Table 5.14, derived from an assumed cross-section, are similar. Hence the results from both methods show similar computed outflow hydrographs. The K and X parameters of both methods are nearly equal, showing no difference in the computed hydrographs.

As shown in Tables 5.17 and 5.18, Event 2 has a relatively large RMSE error and volume error. The other events generally have acceptable statistical results and these results are similar to those obtained using the calibrated methods (M-Cal and M-Ma).

From the result Table 5.18, it is evident that Event 3 has a small RMSE value, small volume error and the coefficient of efficiency (E) is nearly equal to one. These results indicate a high degree of correlation between the computed and observed hydrographs. Hence, Event 3 was selected for sensitivity analyses from Reach-I, as detailed in Section 5.3.

5.2.2 Reach-II

The estimated catchment characteristics and parameters for Reach-II are contained in Tables 5.19 to 5.22.

Table 5.19 Hydraulic parameters for Reach-II using the MC-E method

Reach	Event	V_{av} [m.s^{-1}]	V_w [m.s^{-1}]	R [m]	y [m]	S [%]	n
II	1	1.35	1.66	0.82	1.23	0.55	0.05
	2	1.39	1.70	0.86	1.28	0.55	0.05
	3	1.38	1.69	0.85	1.27	0.55	0.05
	4	1.34	1.64	0.81	1.21	0.55	0.05

Table 5.20 Hydraulic parameters for Reach-II using the MC-X method

Reach	Event	V_{av} [m.s^{-1}]	V_w [m.s^{-1}]	R [m]	y [m]	S [%]	n
II	1	1.40	1.72	0.87	1.30	0.55	0.05
	2	1.48	1.80	0.93	1.40	0.55	0.05
	3	1.48	1.80	0.93	1.40	0.55	0.05
	4	1.51	1.85	0.97	1.45	0.55	0.05

Table 5.21 Estimated parameters for Reach-II using the MC-E method

Reach	Event	ΔL [m]	Δt [s]	A [m^2]	W [m]	Q_0 [m^3.s^{-1}]	K [s]	X	C_0	C_1	C_2
II	1	7777	5400	20.20	24.62	27.32	4698	0.49	0.99	0.08	-0.06
	2	7777	5400	22.58	26.39	31.39	4569	0.49	0.99	0.09	-0.08
	3	7777	5400	21.92	25.91	30.26	4603	0.49	0.99	0.09	-0.07
	4	7777	5400	19.44	24.04	26.04	4743	0.49	0.99	0.07	-0.06

Table 5.22 Estimated parameters for Reach-II using the MC-X method

Reach	Event	ΔL [m]	Δt [s]	A [m^2]	W [m]	Q_0 [m^3.s^{-1}]	K [s]	X	C_0	C_1	C_2
II	1	7777	5400	16.90	19.50	27.32	4531	0.49	0.98	0.10	-0.08
	2	7777	5400	19.60	21.00	31.39	4312	0.49	0.98	0.12	-0.10
	3	7777	5400	19.60	21.00	30.26	4312	0.49	0.98	0.12	-0.10
	4	7777	5400	21.03	21.75	26.04	4213	0.49	0.99	0.13	-0.12

The computed and observed hydrographs from the application of the MC-E and the MC-X methods for Reach-II are shown in Figures 5.18 to 5.21.

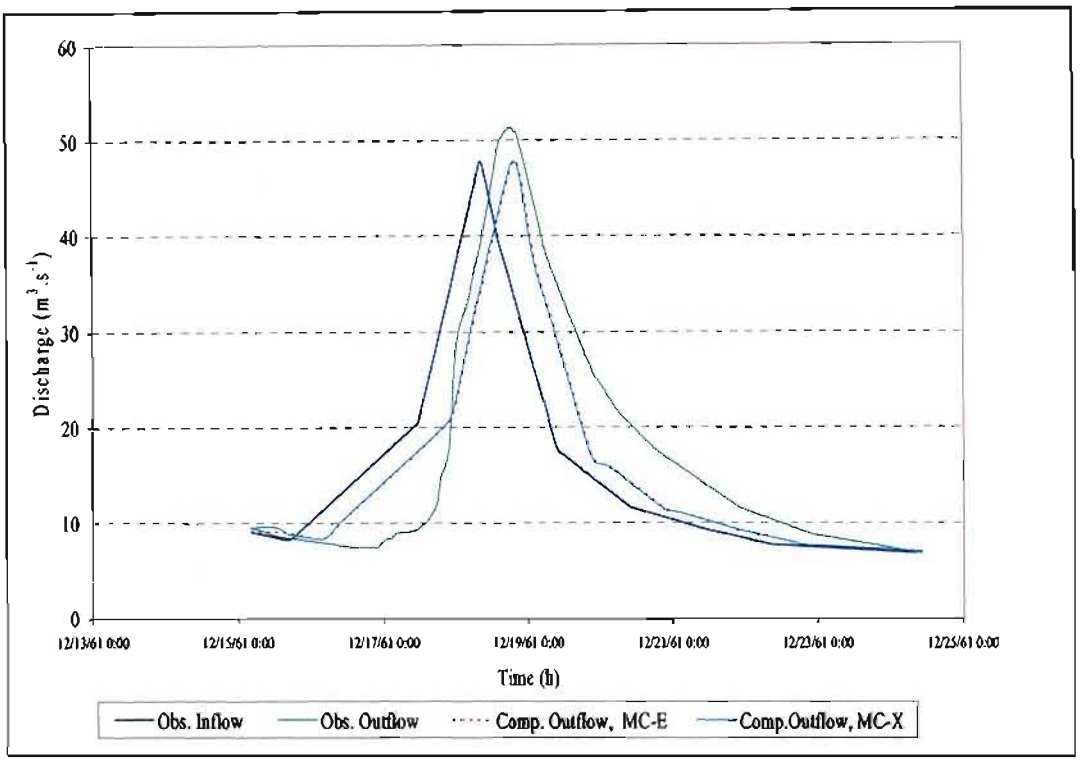

Figure 5.18 Observed and computed hydrographs of Event-1 in Reach-II

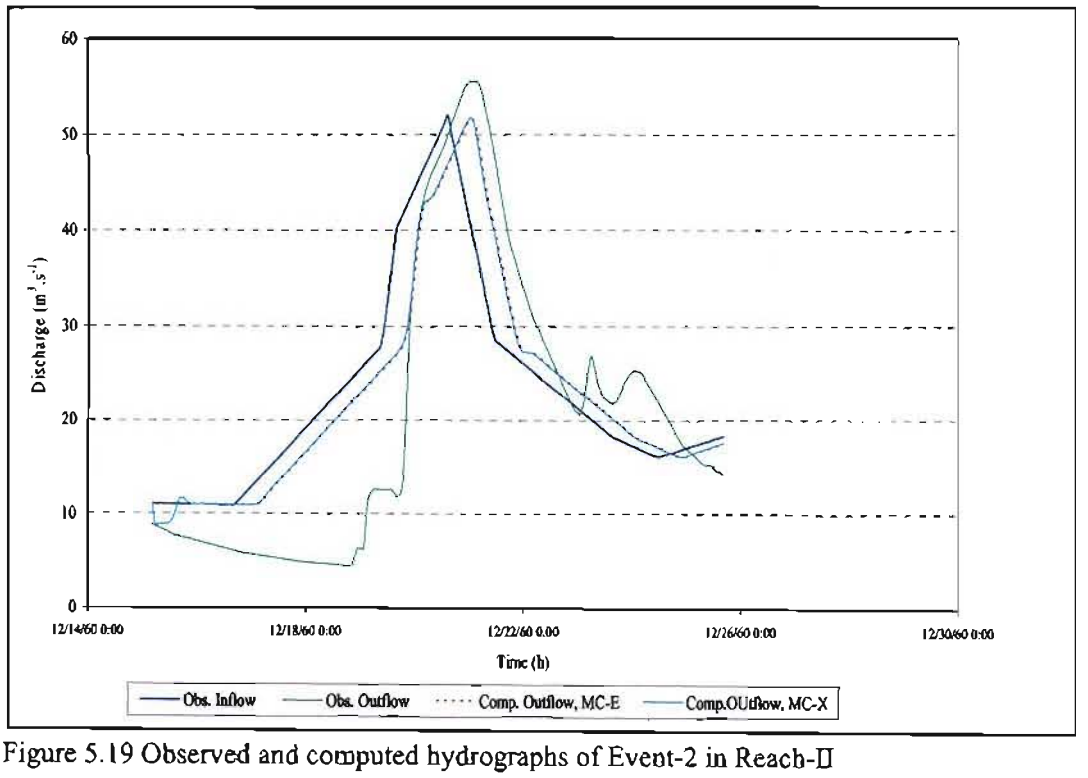

Figure 5.19 Observed and computed hydrographs of Event-2 in Reach-II

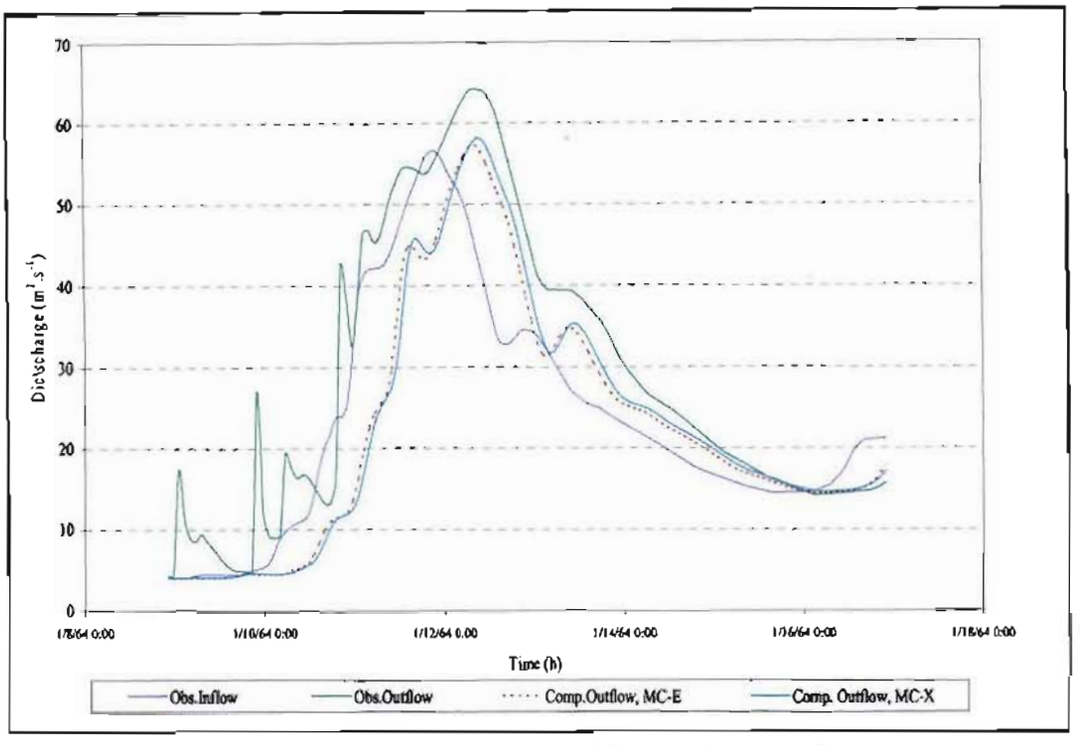

Figure 5.20 Observed and computed hydrographs of Event-3 in Reach-II

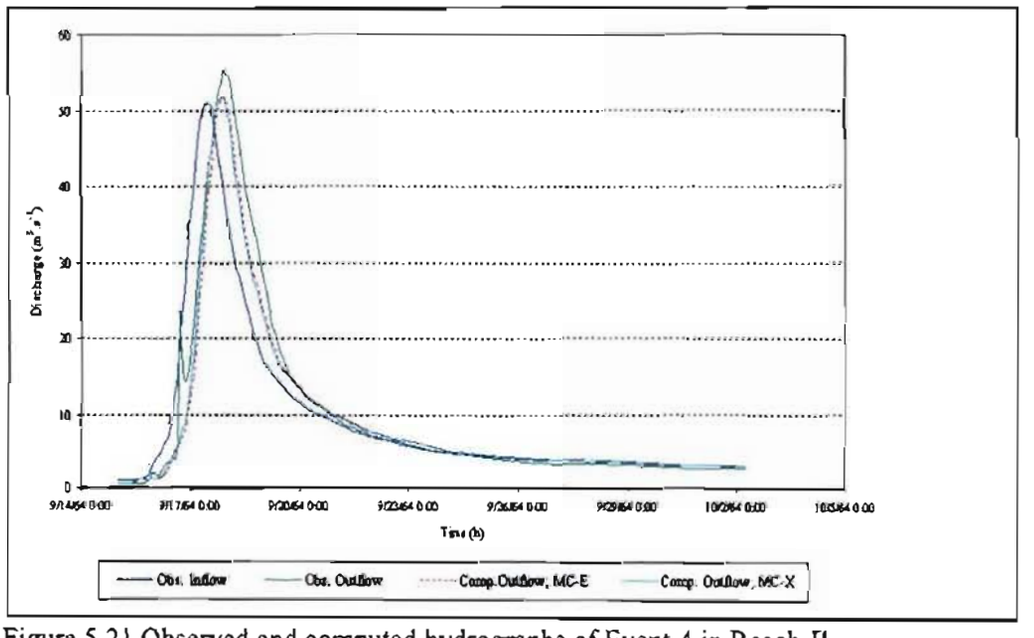

Figure 5.21 Observed and computed hydrographs of Event-4 in Reach-II

The results of flood routing analyses using the MC-E and the MC-X methods for Reach-II are contained in Tables 5.23 and 5.24.

Table 5.23 Results for Reach-II using the MC-E method

Reach	Event	Obs Peak outflow [$m^3.s^{-1}$]	Comp Peak [$m^3.s^{-1}$]	Peak Flow Error [%]	Peak timing Error [%]	RMSE [$m^3.s^{-1}$]	E	Obs Volume [mcm]	Comp Volume [mcm]	Volume Error [%]
II	1	51.25	47.87	-6.60	1.65	4.52	0.87	13.63	12.36	-9.31
	2	55.52	51.69	-6.90	0.00	7.40	0.82	18.54	20.70	11.68
	3	64.22	57.22	-10.89	0.00	8.98	0.74	19.87	15.62	-21.38
	4	55.40	51.77	-6.55	0.00	2.02	0.97	14.39	13.76	-4.33

Table 5.24 Results for Reach-II using the MC-X method

Reach	Event	Obs Peak outflow [$m^3.s^{-1}$]	Comp Peak [$m^3.s^{-1}$]	Peak flow Error [%]	Peak timing Error [%]	RMSE [$m^3.s^{-1}$]	E	Obs Volume [mcm]	Comp Volume [mcm]	Volume Error [%]
II	1	51.25	47.65	-7.02	1.65	4.58	0.86	13.63	12.37	-9.20
	2	55.52	51.60	-7.06	0.00	7.51	0.81	18.54	20.64	11.36
	3	64.22	57.14	-11.02	0.00	8.78	0.75	19.87	15.66	-21.17
	4	55.40	51.70	-6.66	0.00	2.07	0.97	14.39	13.77	-4.28

The depth of flow and the Muskingum parameters in both methods are nearly equal, showing no difference in the computed hydrographs.

As shown in Tables 5.23 and 5.24, Event 4 resulted in a relatively small RMSE and large coefficient of efficiency (E) values. Hence, Event 4 was selected for sensitivity analysis in Reach-II, as shown in Section 5.3. The other events have errors of less than 22% for the statistics considered

5.2.3 Reach-III

The estimated catchment characteristics and parameters for Reach-III are contained in Tables 5.25 to 5.28.

Table 5.25 Hydraulic parameters for Reach-III using the MC-E method

Reach	Event	V_{av} [$m.s^{-1}$]	V_w [$m.s^{-1}$]	R [m]	y [m]	S [%]	n
III	1	0.85	1.04	1.08	1.62	0.12	0.04
	2	0.91	1.11	1.20	1.80	0.12	0.04
	3	0.88	1.07	1.14	1.71	0.12	0.04
	4	0.78	0.97	0.94	1.42	0.12	0.04

Table 5.26 Hydraulic parameters for Reach-III using the MC-X method

Reach	Event	V_{av} [m.s^{-1}]	V_o [m.s^{-1}]	R [m]	y [m]	S [%]	n
III	1	0.84	1.03	1.07	1.60	0.12	0.04
	2	0.91	1.11	1.20	1.80	0.12	0.04
	3	0.88	1.07	1.13	1.70	0.12	0.04
	4	0.79	0.96	0.97	1.45	0.12	0.04

Table 5.27 Estimated parameters for Reach-III using the MC-E method

Reach	Event	ΔL[m]	Δt [s]	A [m^2]	W [m]	Q_o [m^3.s^{-1}]	K [s]	X	C_0	C_1	C_2
III	1	4000	9000	21.85	20.25	18.49	3862	0.41	0.90	0.43	-0.33
	2	4000	9000	28.97	24.16	26.31	5998	0.44	0.91	0.24	-0.14
	3	10000	9000	25.15	22.10	22.09	9317	0.46	0.92	0.02	0.05
	4	10000	9000	15.32	16.21	11.89	10547	0.47	0.93	-0.04	0.11

Table 5.28 Estimated parameters for Reach-III using the MC-X method

Reach	Event	ΔL[m]	Δt [s]	A [m^2]	W [m]	Q_o [m^3.s^{-1}]	K [s]	X	C_0	C_1	C_2
III	1	4000	9000	17.07	16.00	18.49	3891	0.38	0.87	0.44	-0.30
	2	4000	9000	21.60	18.00	26.31	5996	0.42	0.88	0.25	-0.13
	3	10000	9000	25.22	17.00	22.09	9343	0.45	0.90	0.03	0.07
	4	10000	9000	15.09	14.50	11.89	10388	0.46	0.93	-0.03	0.11

The computed and observed hydrographs from the application of the MC-E and MC-X methods for Reach-III are shown in Figures 5.22 to 5.25.

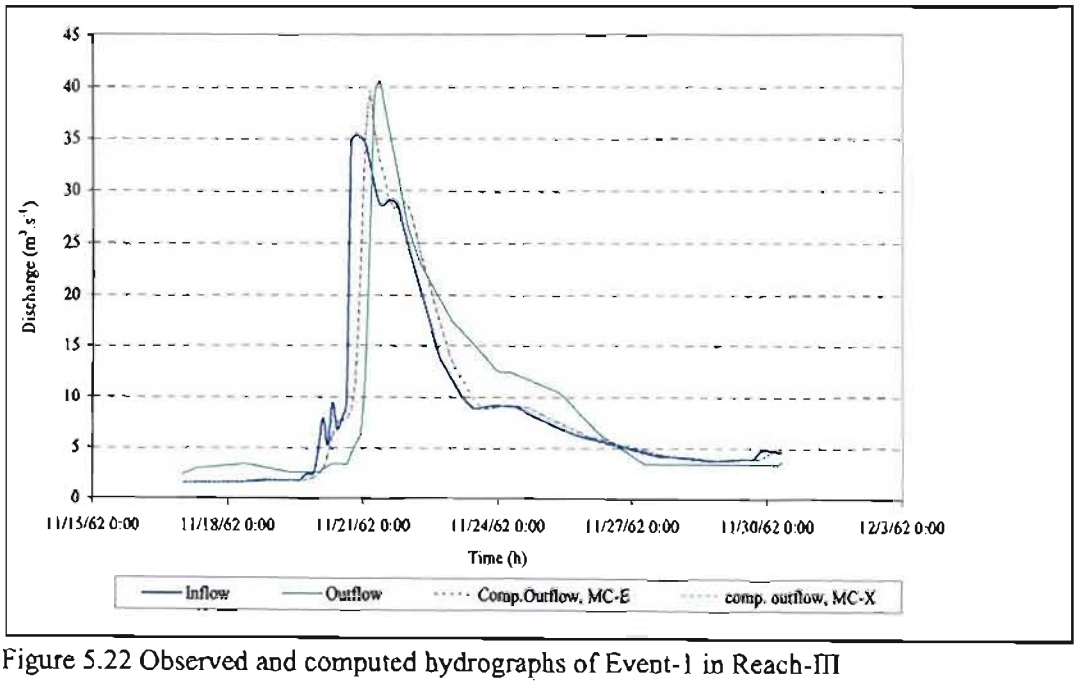

Figure 5.22 Observed and computed hydrographs of Event-1 in Reach-III

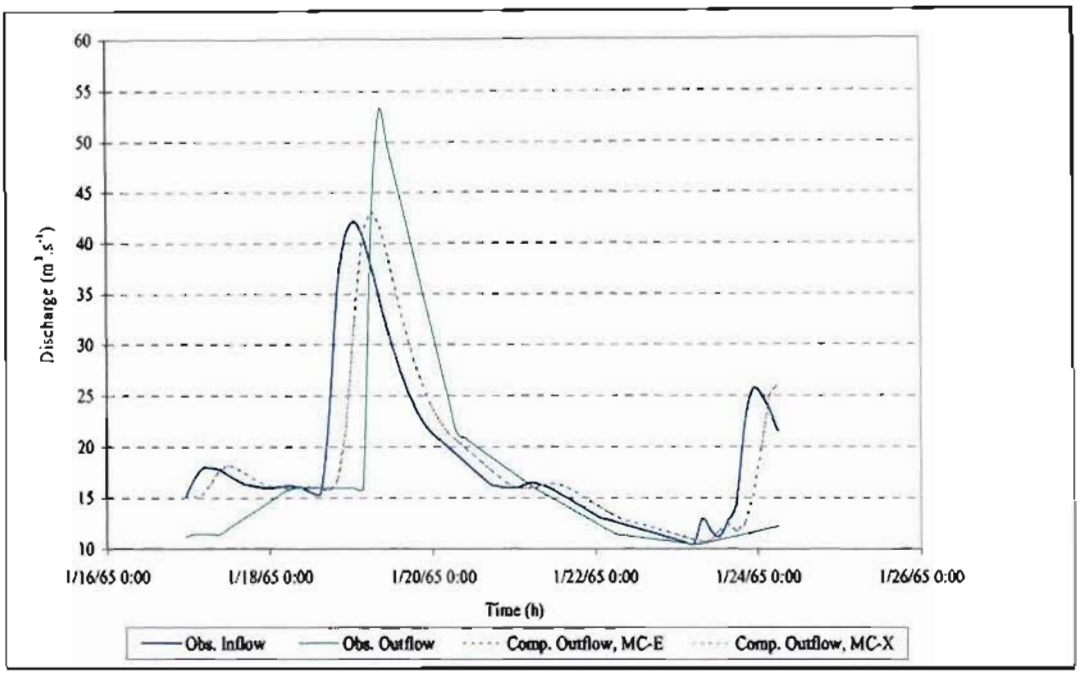

Figure 5.23 Observed and computed hydrographs of Event-2 in Reach-III

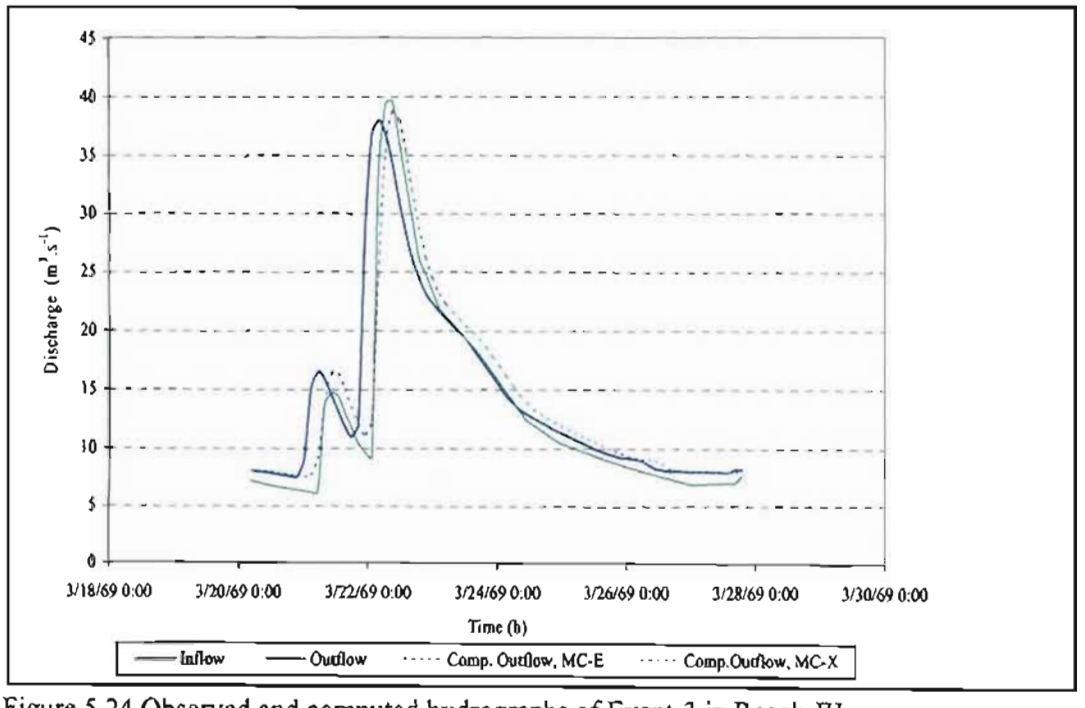

Figure 5.24 Observed and computed hydrographs of Event-3 in Reach-III

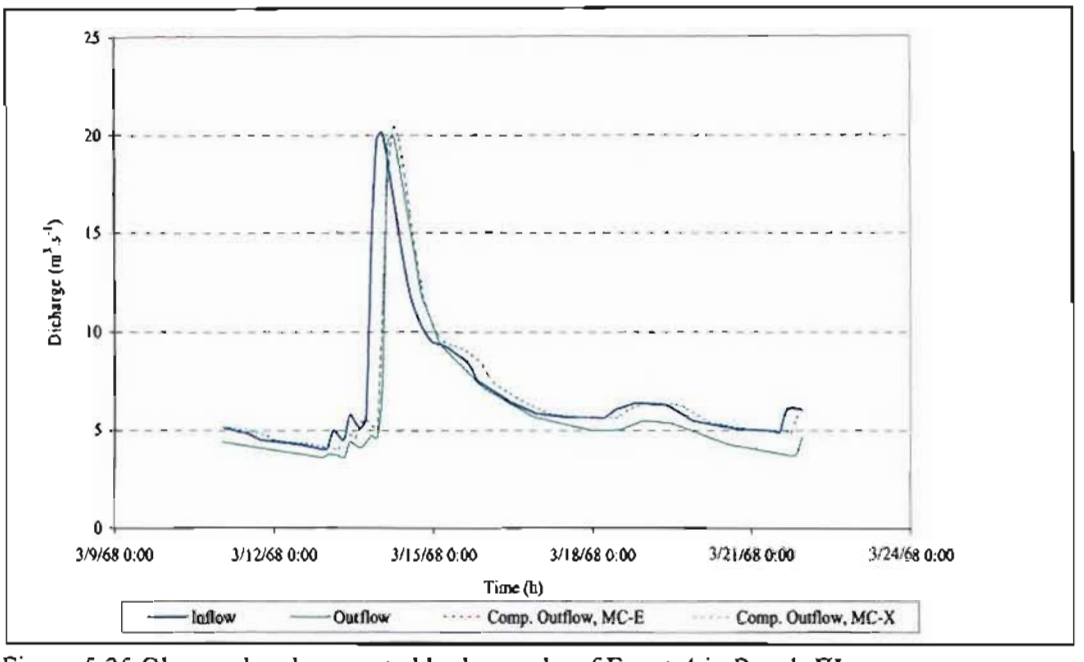

Figure 5.25 Observed and computed hydrographs of Event-4 in Reach-III

The results of flood routing analyses using the MC-E and the MC-X methods in Reach-III are contained in Tables 5.29 and 5.30.

Table 5.29 Results for Reach-III using the MC-E method

Reach	Event	Obs Peak outflow [$m^3.s^{-1}$]	Comp Peak [$m^3.s^{-1}$]	Peak flow Error [%]	Peak timing Error [%]	RMSE [$m^3.s^{-1}$]	E	Obs Volume [mcm]	Comp Volume [mcm]	Volume Error [%]
III	1	40.65	39.62	-2.52	2.38	3.70	0.82	10.34	9.71	-6.15
	2	52.97	43.14	-18.55	0.00	5.86	0.64	11.08	11.66	5.28
	3	39.64	38.74	-2.27	0.00	1.77	0.95	8.72	9.45	8.37
	4	19.97	20.36	1.94	0.00	0.88	0.93	5.67	6.36	12.25

Table 5.30 Results for Reach-III using the MC-X method

Reach	Event	Obs Peak outflow [$m^3.s^{-1}$]	Comp Peak [$m^3.s^{-1}$]	Peak flow Error [%]	Peak timing Error [%]	RMSE [$m^3.s^{-1}$]	E	Obs Volume [mcm]	Comp Volume [mcm]	Volume Error [%]
III	1	40.65	39.20	-3.56	2.38	3.67	0.82	10.34	9.71	-6.15
	2	52.97	42.92	-18.97	0.00	5.85	0.64	11.08	11.66	5.29
	3	39.64	38.53	-2.80	0.00	1.78	0.95	8.72	9.45	8.37
	4	19.97	20.37	1.98	0.00	0.88	0.93	5.67	6.36	12.26

As shown in Tables 5.29 and 5.30 for the MC-E and the MC-X methods, large volume errors were obtained for Event 4. Generally, the result obtained from all of the events show that the

computed hydrographs from both methods are similar to the observed hydrographs, with errors of less than 20% for the statistics considered.

As shown in Tables 5.29 and 5.30, Event 3 resulted in a relatively small RMSE and large coefficient of efficiency (E) values. Hence, Event 3 was selected for sensitivity analysis in Reach-III, as shown in Section 5.3.

5.2.4 Section conclusion

As observed in Figures 5.15 to 5.25 and Tables 5.16 to 5.30, the results of computed hydrographs using both empirically estimated parameters and parameters estimated from an assumed cross-section resulted in acceptable results when compared to the observed hydrographs, with errors of less than 26 % for the statistics considered. Hence, it is concluded that the methods can be applied in ungauged catchments.

The addition of lateral inflow in the simulated hydrographs was not sufficient adequate when compared to the observed outflow. As the length of a reach increases the possibilities of tributary inflows also increases. Hence, in large catchments the tributary flow should be added separately.

Since the ungauged flood routing methods utilise empirical formulae, the results may not be equal to the calibrated flood routing methods. The results indicate that the ungauged flood routing methods have estimated the simulated hydrographs with reasonable results when compared to the calibrated method. Hence it is concluded that the methods can be applied in situations when there are no observed data sets in the catchments.

From the events analysed, Event 3 in Reach-I, Event 4 in Reach-II and Event 3 in Reach–III were selected for sensitivity analyses using MC-E method.

5.3 Sensitivity Analyses

There are various limitations of the Muskingum-Cunge flood routing method and its assumptions which were outlined in Sections 2.1 and 2.2 The Muskingum method has

different responses to variations in physical catchment parameters such as reach slope, roughness coefficients and channel geometry used in the model. The statistical analysis of computed hydrographs with the observed hydrographs describes the model performance with regards to specific input variables to the model. Variations in roughness coefficients, reach slope and channel geometry influence the computed volume, peak flow rate and timing of the hydrographs. Hence, the sensitivity of the computed hydrographs to a 50% variation of the variables was analysed. The model sensitivity analyses were undertaken using the three selected events. A 50% variation was used in the sensitivity analysis as this is the typical error that could occur in the estimation of these variables in practice.

The three selected events have a large flow rate with small lag time (Reach–I), medium peak flow rate with large lag time and additional lateral inflows (Reach-II) as well as a small peak flow rate with medium lag time (Reach-III).

Changing the catchment flow variables changes the K and X parameters. Hence, the variation in the outflow hydrographs is due to the change in both the K and X parameters.

5.3.1 Sensitivity analysis for the coefficient of roughness (n)

The values for the roughness coefficient of the river reaches used in this study were subjectively estimated from field observations. The seasonal variation, subjectivity and other errors may change the estimation of the roughness coefficient which could influence the simulated hydrographs (Section 2.9.3). To analyse the effect of error in the estimation of the roughness coefficient, hydrographs with a 50% variation in the roughness coefficient were computed for the three events while keeping the other variables constant.

Increasing the roughness coefficient by 50% increases the value of the K parameter and decreases the value of X parameter. From the results for Reaches-I, II and III, it is observed that a 50% increase in the roughness coefficient, increases the peak error by 0.19 %.. Decreasing the roughness coefficient by 50%, decreases the computed peak error by 1% in Reach-I; increases the peak error by 0.0% in Reach-II and decreases the peak flow by 0.13% in Reach–III. The variation of response to the same variable change between the reaches may be explained by the fact that the increase or decrease of resistance affects the lower flows

more than higher flows. The lateral inflow into the main reach may also have an effect on the variation of roughness coefficients in Reach–II and Reach-III.

Figures 5.26 to 5.29 show the effect of variation of roughness coefficient on peak flow, shape and volume of hydrographs for the selected three events.

From the results obtained, it is evident that the performance of the MC-E method is insensitive to the value of the roughness coefficient used, i.e. a 50% variation in the roughness coefficient resulted in a change of less than 1% error for all the performance statistics considered.

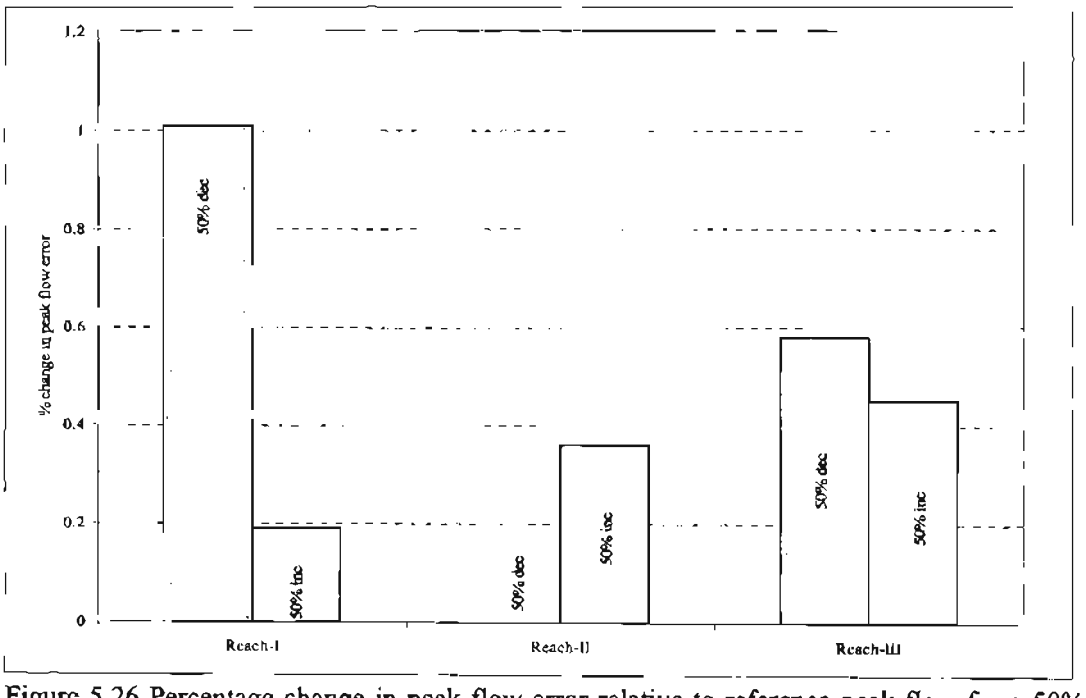

Figure 5.26 Percentage change in peak flow error relative to reference peak flow for a 50% increase and decrease in the roughness coefficient

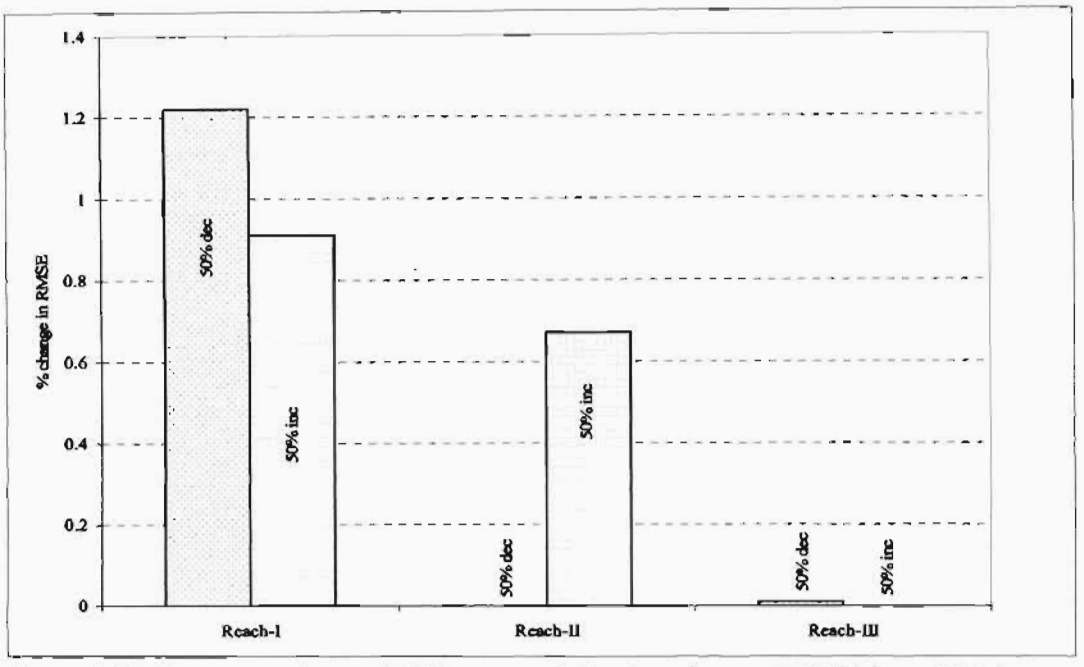

Figure 5.27 Percentage change RMSE error relative to reference RMSE for a 50% increase and decrease in the roughness coefficient

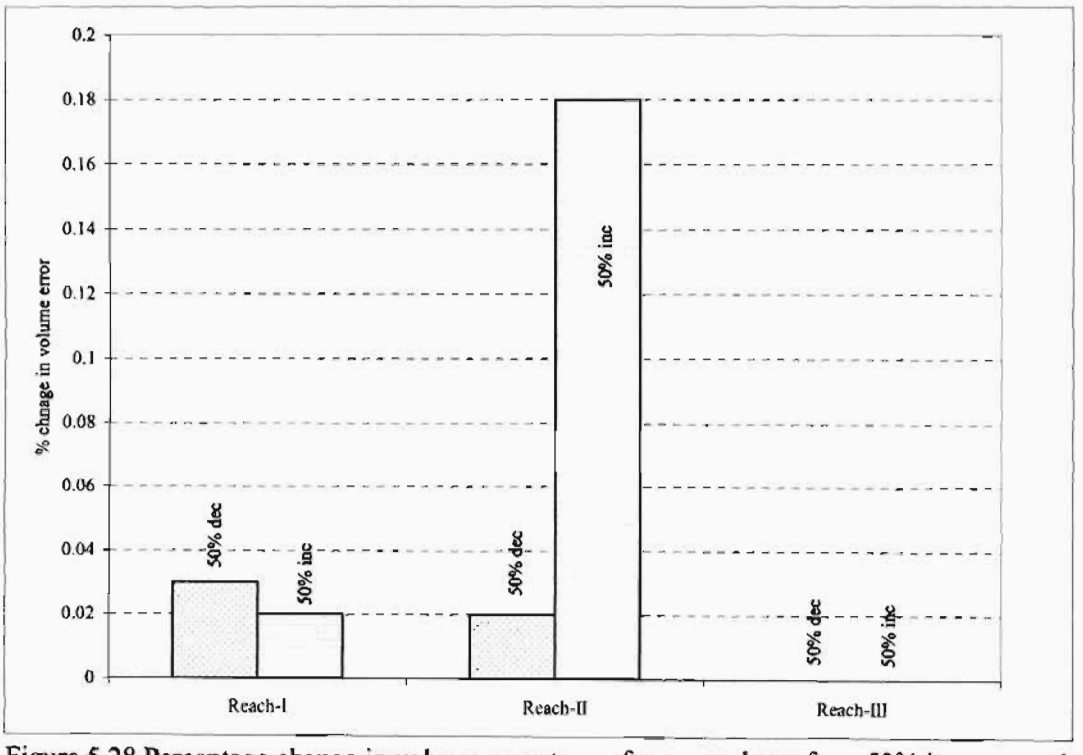

Figure 5.28 Percentage change in volume error to a reference volume for a 50% increase and decrease in the roughness coefficient

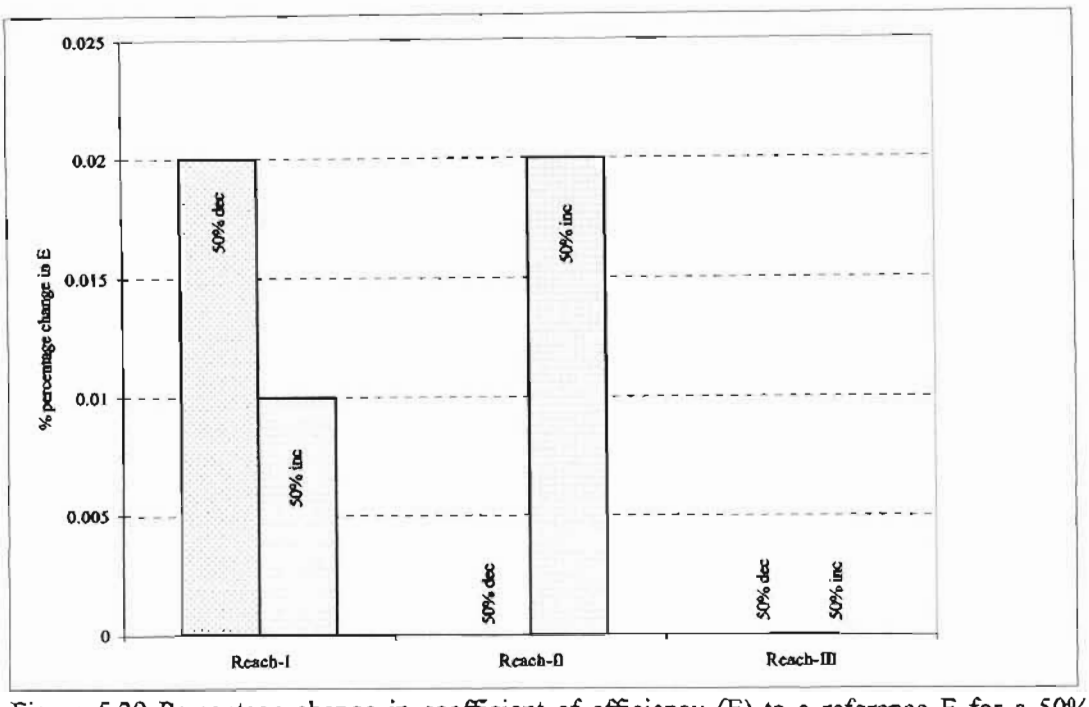

Figure 5.29 Percentage change in coefficient of efficiency (E) to a reference E for a 50% increase and decrease in the roughness coefficient

5.3.2 Sensitivity analysis for the slope (S)

It is evident from the sensitivity analysis that changing the slope affects the K and X parameters differently. When slope increases, the K parameter decreases and the X parameter increases.

Figures 5.30 to 5.33 show the effect of variation of reach slope on peak flow, shape and volume of the hydrographs for the three selected events. In general, increasing the slope of a river reach increases the velocity of flow. As a result, there will be a decrease in lag time that apparently increases the magnitude of peak discharge.

The analyses for varying the slope by 50% it is shown that effect on the relative error for all performance statistics considered is less than 2%. Hence, variation of a slope of 50% has little effect when routing is performed.

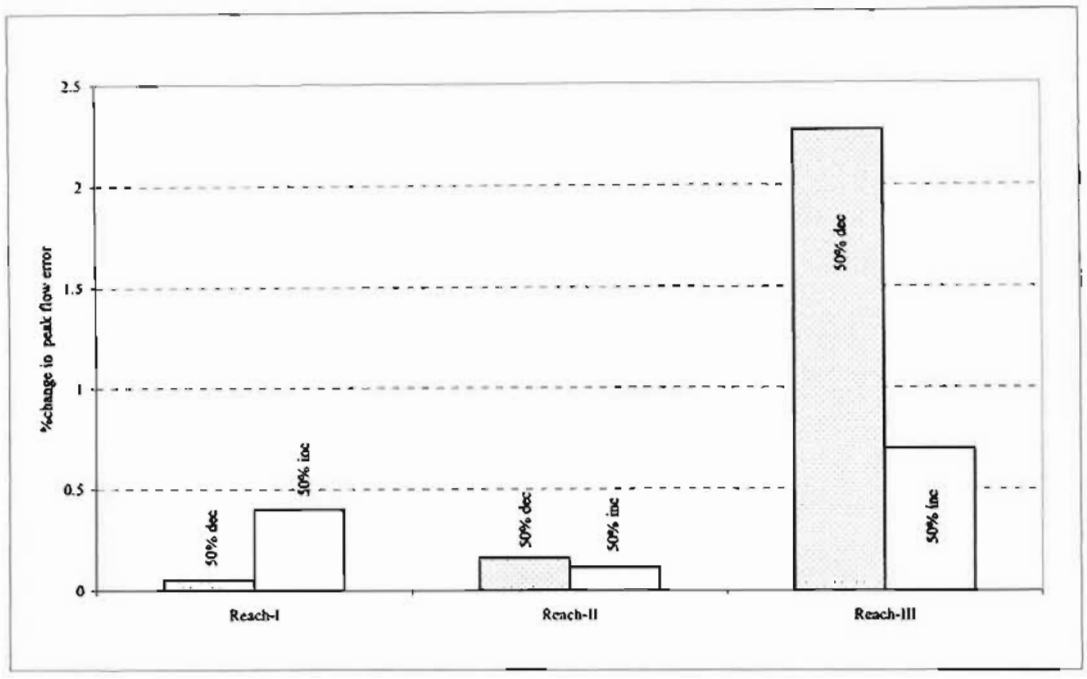

Figure 5.30 Percentage change in peak flow error relative to reference peak flow for 50%increase and decrease in the channel slope

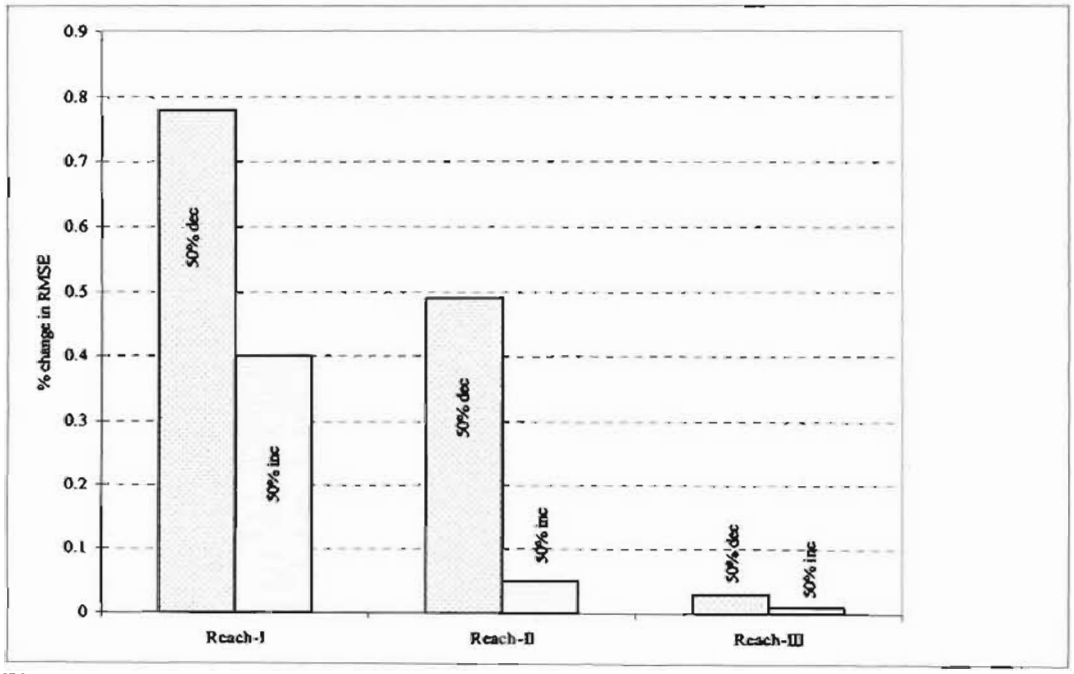

Figure 5.31 Percentage change in RMSE error relative to reference RMSE for a 50% increase and decrease in the channel slope

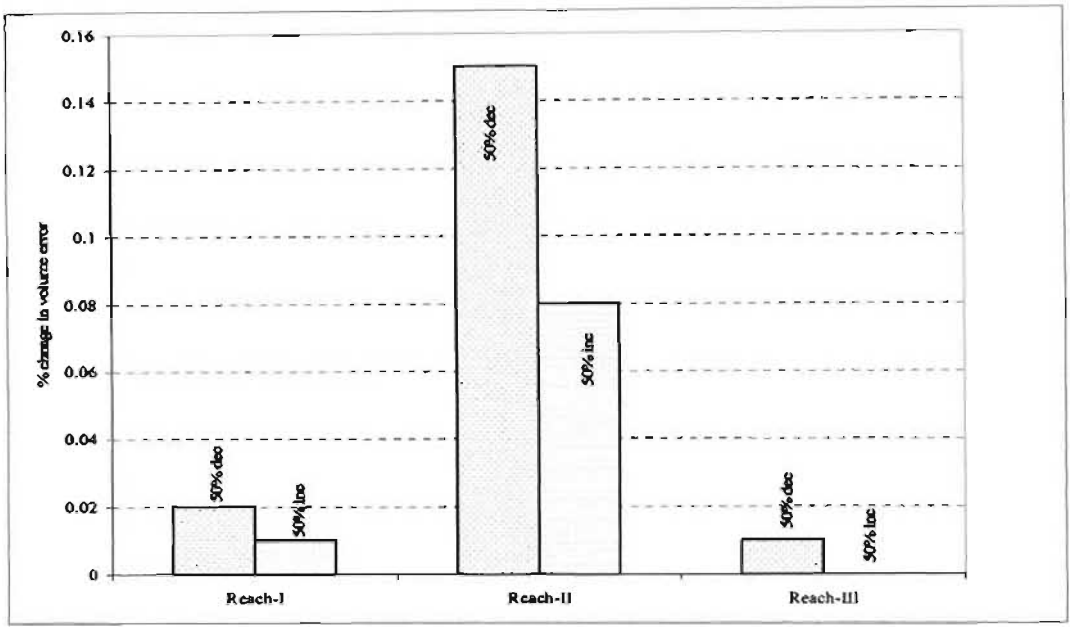

Figure 5.32 Percentage change in volume error to a reference volume for a 50% increase and decrease in the channel slope

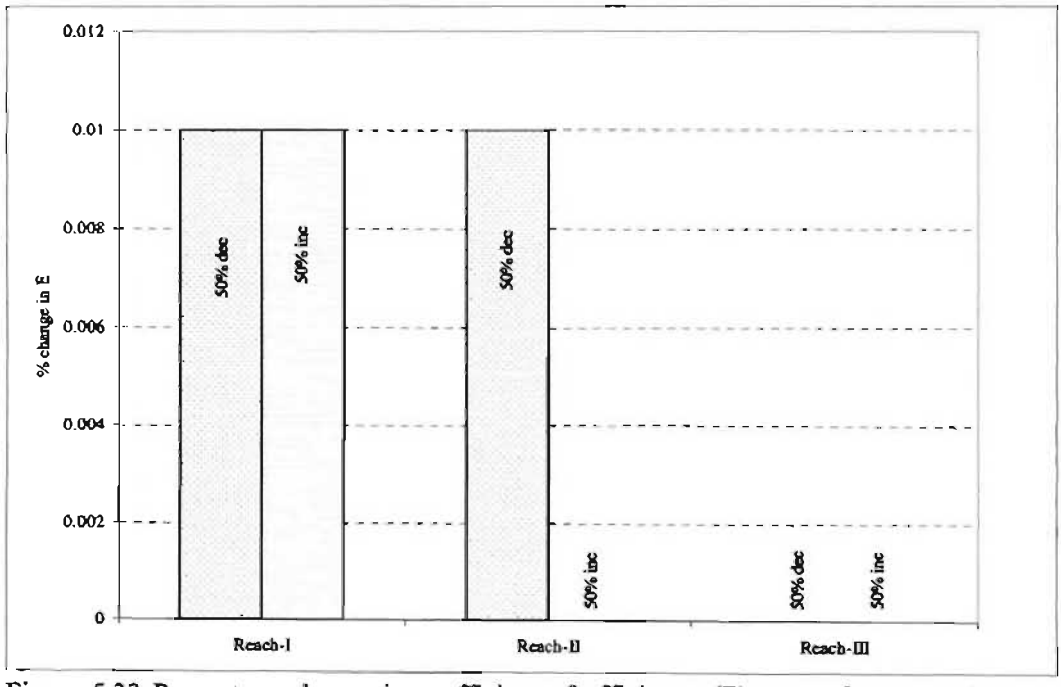

Figure 5.33 Percentage change in coefficient of efficiency (E) to a reference E for a 50% increase and decrease in the channel slope

5.3.3 Sensitivity analysis for the channel geometry

Changing the geometry of the channel section is expected to affect both the K and X parameters. As contained in Table 4.1 (Section 4), the ratio of the kinematic wave velocity (celerity) to average velocity for wide rectangular channels is larger than for triangular and parabolic section channels. The ratio of celerity to velocity for a triangular section is larger than that of parabolic section channel. From the sensitivity analysis it was observed that the changes in the peak flow errors are lowest for a triangular section. Figures 5.34 to 5.37 show the effect of variation in channel geometry from a parabolic section on changes in peak flow, shape and volume of hydrographs for the selected three events.

The sensitivity of flow to channel geometry shows that there is a decrease in the RMSE and an increase in the coefficients of efficiency (E), when there is a change in geometry from rectangular to parabolic and to triangular section.

These results show that different assumed geometrical shapes have an effect on the computed hydrographs. However, the statistics of performance vary by less than 1% and hence it is concluded the selection of cross-sectional shape is not important for flood routing using the MC-E method.

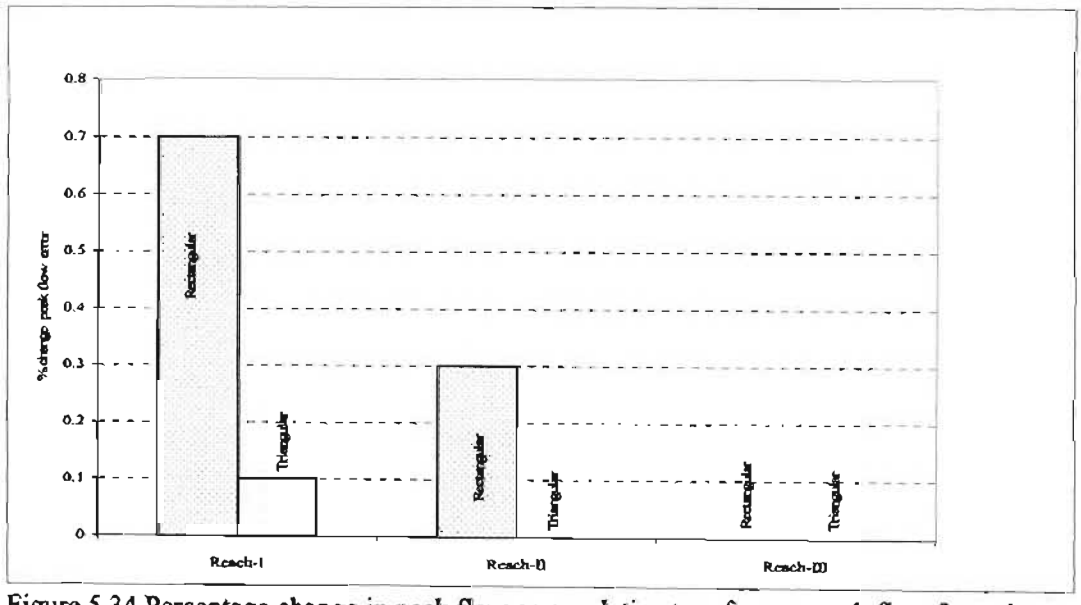

Figure 5.34 Percentage change in peak flow error relative to reference peak flow for a change in the channel geometry

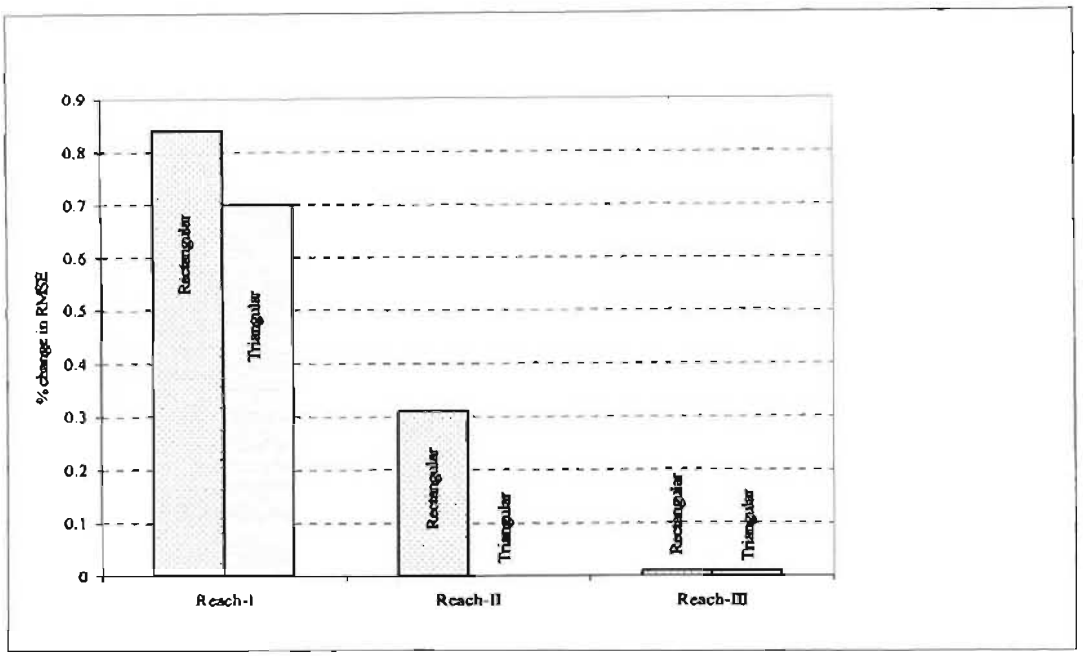

Figure 5.35 Percentage change in RMSE error relative to reference RMSE for a change in the channel geometry

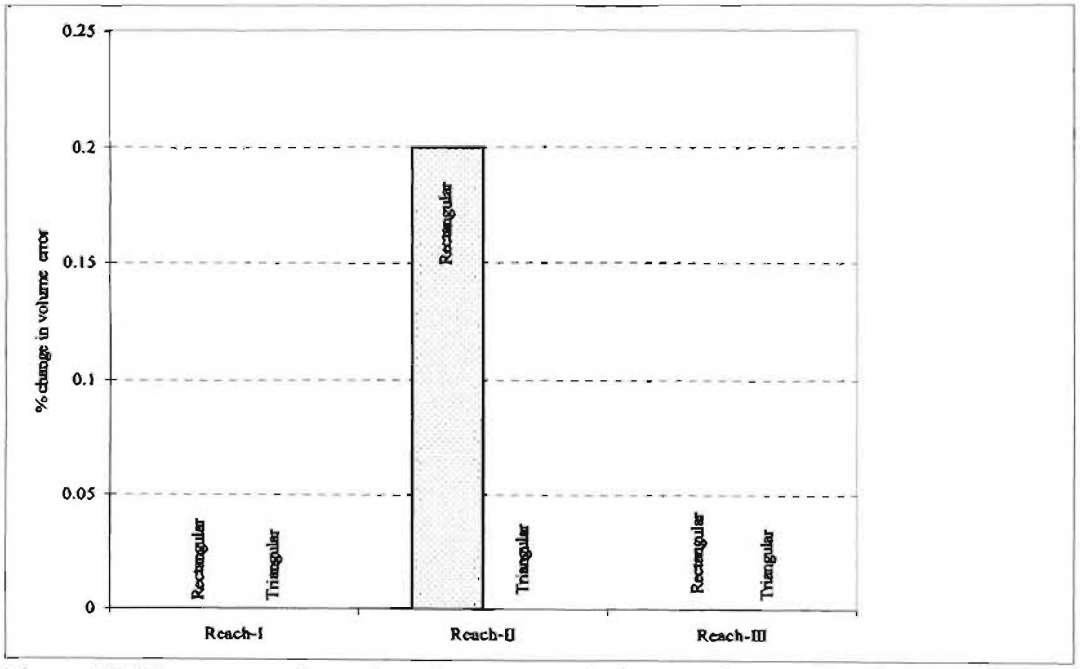

Figure 5.36 Percentage change in volume error relative to reference volume for a change in the channel geometry

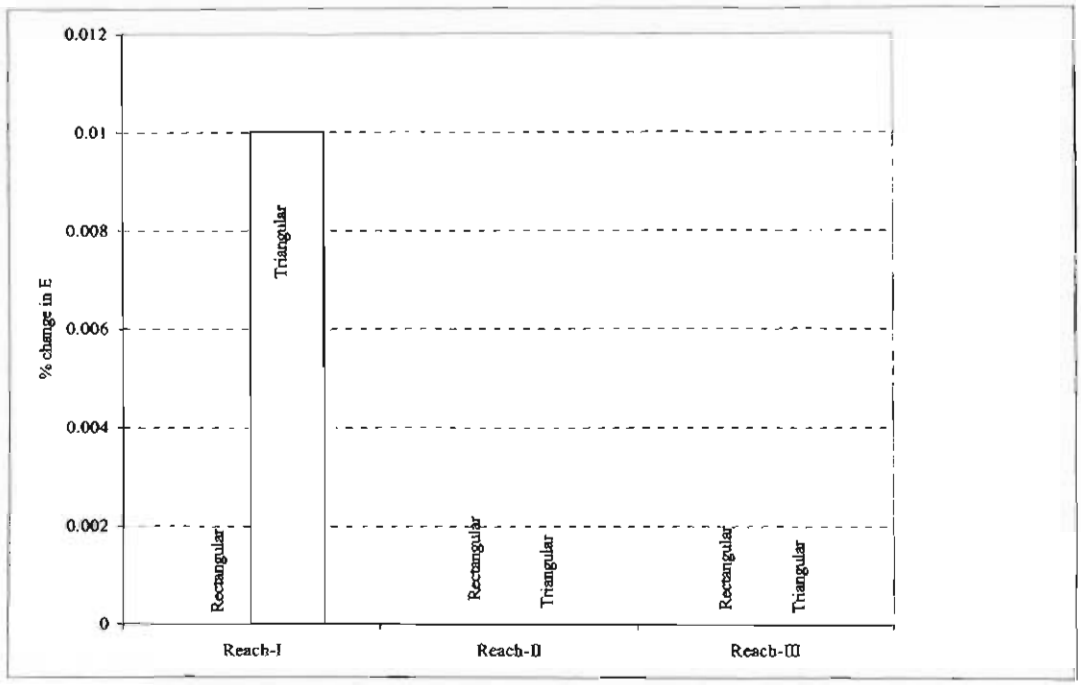

Figure 5.37 Percentage change in coefficient of efficiency (E) to a reference E for a change in the channel geometry

6. DISCUSSION AND CONCLUSIONS

Hydrological flood routing techniques are widely accepted and are extensively used in engineering practice. The ability to predict the changing magnitude and celerity of a flood wave as it propagates along rivers or through reservoirs makes flood routing important in designing hydraulic structure and in assessing the adequacy of measures for flood protection. However, in practice, only a limited number of gauging stations are available, and even measured or gauged runoff data are frequently unreliable. To establish gauging stations is an expensive task and on-going maintenance and service costs are also significant.

As it is conducted in this study, the factors considered when selecting suitable gauging stations for streamflow records include the availability and quality of data, and the suitability of the river reach to estimate flood routing parameters using Muskingum methods. In this study, reaches of different lengths were selected to assess the influence of river length in the application of flood routing methods. From an inspection of the flow data, it was evident that some of the observed hydrographs had unrealistic records, which might be due to technical problems or to incorrect data acquisition. Hence, the quality of data was carefully examined before selecting events for calibrating the Muskingum methods of flood routing.

From the analysis of both M-Cal and M-Ma methods, the results displayed reasonably similar volume and shape compared to the observed hydrographs. Since, Reach-II and Reach-III are long reaches, lateral inflows were added to the flood routing method. However, the addition of lateral inflow to the computed hydrographs in Reach–II and Reach-III was not sufficient to obtain the observed peaks, but did results in outflow peak discharges, which were larger than the inflow peak discharges, as evident in the observed data. Since, the addition of lateral inflow as used in this study considers only flows that are derived from the same rainfall event that resulted in the hydrographs, the under simulation of lateral inflow may be attributed to inflow from other catchments caused by different rainfall events.

As it is observed in this study, the computed hydrographs using the M-Ma method are a better fit to the observed outflow hydrographs for those that have good quality of data and a uniformly increasing discharge than the hydrographs computed using the M-Cal method. However, both methods produced acceptable results with errors of less than 20% for most

statistics considered. Both methods performed better for shorter reaches where the effect of lateral inflow is not significant. However, the parameters of M-Ma method only derived from observed hydrographs and it is not possible to apply M-Ma method in ungauged catchments. The parameters of Muskingum-Cunge method can be derived from reach and flow characteristics. Hence, the Muskingum-Cunge method, with empirically estimated parameters (MC-E), and Muskingum-Cunge method, with variables estimated from assumed section (MC-X), was applied in ungauged catchments.

From the results obtained, it was generally found that the estimated values of the flow variables in both the MC-E and the MC-X methods were nearly equal in this study, which resulted in similar computed outflow hydrographs. The computed outflow hydrographs using both the MC-E and MC-X methods have acceptable errors for the peak flow magnitude, peak timing, volume and have small RMSE values. In addition, the coefficients of model efficiency (E) are also near to one in most cases, which indicates that the hydrograph shapes are very similar to the observed hydrographs. Hence, it can be concluded that the MC-E and MC-X methods can be applied in ungauged reaches where observed data sets are unavailable.

As noted in the previous sections, the selection of an assumed section requires an in-field inspection to select representative section to use for the estimation of variables in the MC-X method. The selection is a subjective procedure, which could result in different computed hydrographs to different scenarios in the same reach. On the other hand, although the parameters of MC-E method can be estimated from empirical equations, the method is not subjective and result in the same computed hydrographs for different scenarios in the same reach. Hence, it is recommended that the MC-E method should be applied to route floods in ungauged catchments.

From the sensitivity analysis, it is evident that the performance of the MC-E method is insensitive to the accurate estimation of the roughness coefficient and a 50% variation in the roughness coefficient resulted in a change of less than 1% error for all the performance statistics considered. Similarly, the performance was found to be insensitive to channel geometry.

Hence, from this study, it can be concluded that Muskingum-Cunge flood routing method, with parameters estimated using the MC-E method, can be used to route hydrographs in

ungauged reaches in the Thukela catchments and it is postulated that the method can be used to route floods in other ungauged rivers in South Africa.

7. RECOMMENDATIONS

In the methodology used, errors may be inherent in a number of the steps performed. For example, the original observed flow data were converted from stage height to discharge assuming steady state flow conditions and the slope of the rivers extracted from a digital elevation model was averaged and does not consider sinks and waterfalls along the river course. In addition the calculation of travel time using hydrographs, the approximation of hydraulic radius, the roughness coefficient and slope extraction from digital elevation model, as stated in the methodology section of the study, might also introduce further errors. The assumptions made in estimating variables and the subjectivity while interpreting and collecting data in the field were other factors that affected the routing procedure.

It was assumed that the reaches used in this study were uniform. However, the three reaches used (Klip and the Mooi Rivers) have varying widths and cross-sections and do meander as well as having different vegetation cover within the reach. The discharge is related to the channel dimensions using empirical formulae that were developed for different river conditions. Furthermore, the linearity assumption of the Muskingum-Cunge method along the river reach might also introduce errors in the computed hydrographs. Considering all the above assumptions made in this study to route floods in ungauged catchments, the following recommendations are made:

(i) The empirical formulae and base roughness coefficients should be checked at a regional level and be related to historical flow records to verify the empirical formulae.

(ii) The slope of a reach and roughness coefficient requires practical experience to determine realistically. Hence, the estimated slope and roughness should be checked against the practical scenarios.

(iii) The computed hydrographs do not fit the observed hydrographs as well in longer reaches (i.e. Reach-II and Reach-III) compared to a short reach (Reach-I). This may be explained by the inadequate estimation of lateral inflows to the main stream. Hence, lateral flow to the main stream requires a regional level study to estimate the coefficients, such as β.

(iv) Overbank flow cannot be simulated by the Muskingum-Cunge method. Therefore, these cases need further studies or modifications to consider floods that spill over the banks.

(v) The methods are not applicable to steeply rising hydrographs. Hence, further research needs to be conducted to apply the Muskingum method to flows with high velocities in ungauged catchments.

8. REFERENCES

Aldama, AA. 1990. Least-squares parameter estimation for Muskingum flood routing. *Journal of Hydraulic Engineering,* 116 (4): 580-586.

Aldridge, BN and Garret, JM. 1973. *Roughness coefficients for stream channels in Arizon*a: Report No. (-.) US Geological Survey in collaboration with Arizona Highway Department, Arizona, USA.

Angus, GR. 1987. *A distributed version of the ACRU model.* Unpublished MSc Eng Dissertation, Department of Agricultural Engineering, University of Natal, Pietermaritzburg, RSA.

Arcement, GJ, Jr and Schneider, VR. 1989. Guide for Selecting Manning's Roughness Coefficients for Natural Channels and Flood Plains. [Internet]. Oklahoma Technical Press, Okalahoma, USA. Available from: http://www.fhwa.dot.gov/bridge/wsp2339.pdf. [Accessed 15 July 2004].

Barfield, BJ Warner, RC and Haan, CT. 1981. Applied Hydrology and Sedimentology for Distributed Areas. Oklahoma Technical Press, Oklahoma, USA.

Bauer, SW and Midgley, DC. 1974. *A simple procedure for synthesising direct runoff hydrographs.* Report No. 1/74. Hydrological Research Unit of Department of Civil Engineering, University of Witwatersrand, Johannesburg, RSA.

Bauer, SW. 1975. *Multiple Muskingum flood routing including flow losses and reservoir storages.* Report No. 3/75. Hydrological Research Unit of Department of Civil Engineering, University of Witwatersrand, Johannesburg, RSA.

Blackburn, J and Hicks, FE. 2001. Combined flood routing and flood level forecasting. *Proceedings of the 15th Canadian Hydro Technical Conference,* Canadian Society for Civil Engineering, Victoria British Columbia, Canada, 345-350.

Bray, DI. 1982. Regime equations for mobile Gravel-bed Rivers. In: - ed. RD Hey, JC Bathurst and C R Thronne *Gravel bed rivers,* Ch. 19. John Wiley and Sons. New York, USA, 517-552.

Caldecott, RE. 1989. *A distributed model for hydrograph simulation and routing.* Unpublished MSc Eng Dissertation, Department of Agricultural Engineering, University of Natal, Pietermaritzburg, RSA.

Charlton, FG, Brown, PH and Benson, RW. 1978. *The hydraulic geometry of some gravel bed rivers in Britain.* Report No. IT 180, Hydraulics Research Station, Wallingford, UK.

Choudhury, P, Shrivastava, RK and Narulkar, SM. 2002. Flood routing in river networks using equivalent Muskingum inflow. *Journal of Hydrologic Engineering* 7(6): 413-419.

Chow, VT. 1959. *Open Channel Hydraulics*, McGraw-Hill, New York, USA.

Chow, VT, Maidment DR and Mays, LW. 1988. *Applied Hydrology*. McGraw-Hill, New York, USA.

Clark, PB and Davies SMA. 1988. Application of regime theory to wadi channels in desert conditions. In: (ed.) White, WR, *International Conference on River Regime:* Paper B3. Hydraulics Research Limited, Wallingford, UK, 67-82.

Cowan, WL. 1956. Estimating hydraulic roughness coefficients. *Journal of Agricultural Engineering*, 37 (7): 473-475.

Cunge JA. 1969. On the subject of a flood propagation method. *Journal of Hydraulics Research,* 7 (-): 205-230.

DWAF 2003. Hydrological Information Systems. [Internet]. Department of Water Affairs and Forestry, Pretoria, RSA. Available from: http://www.dwaf.gov.za/hydrology/cgi-bin/his/cgihis.exe/station [Accessed 13 April 2004].

Encyclopaedia of Nationmaster 2004. Thukela River. [Internet]. Encyclopaedia, Free Software Foundation Inc. Boston, USA. Available from: http://www.nationmaster.com/encyclopedia/Tugela-River. [Accessed 19 May 2004].

ESRI 2000. Environmental System Research Institute, GIS and Mapping software package, California, USA.

Etcheverry, BA. 1915. *Irrigation Practice and Engineering, Vol. II Conveyance of Water.* McGraw-Hill, New York, USA.

Feng, P and Xiaofang, R. 1999. Method of flood routing for multibranch rivers. *Journal of Hydraulic Engineering,* 125 (3): 271-276.

France, PW. 1985. Hydrologic routing with a microcomputer. *Advanced Engineering Software*, 7 (1): 8-12.

Fread, DL. 1981 Flood routing: a synopsis of past, present, and future capability. *Proceedings of international symposium on rainfall-runoff modelling*, Mississippi State University, Mississippi, USA, 521-541.

Fread DL. 1998. NWS FLDWAV model theoretical description. [Internet]. Hydrologic Research Laboratory Office of Hydrology, National Weather Service (NWS) Maryland, USA. Available from: http://www.nws.noaa.gov/oh/hrl/rvrmech/documentation/fldwav_doc.pdf [Accessed 10 April 2005].

Fread, DL. 1993. Flow routing. In: (ed.) Maidment, DR, *Hand Book of Hydrology*. Ch. 10. McGraw-Hill, New York, USA, 1-36.

Garg, SK. 1992. *Irrigation Engineering and Hydraulics Structures*, Khanna Publishers, Delhi, India

Gelegenis, JJ and Sergio, ES. 2000. Analysis of Muskingum equation based flood routing schemes. *Journal of Hydrologic Engineering,* 5 (1):102-105.

Gill, MA. 1978. Flood routing by the Muskingum method. *Journal of Hydrology,* 36: 353-363.

Gill, MA. 1992. Numerical solution of Muskingum equation. *Journal of Hydraulic Engineering,* 118 (5): 804-809.

Green, IRA and Stephenson, D. 1985. *Comparison of Urban Drainage Models for Use in South Africa*. Report No. 115/6/86.Water Researc Commission, Pretoria, RSA.

Haktanir, T and Ozmen, H. 1997. Comparison of hydraulic and hydrologic routing on three long reservoirs. *Journal of Hydraulic Engineering,* 123 (2): 153-156.

Heggen, RJ. 1984. Univariate least squares Muskingum flood routing. *Water Resources Bulletin*, 20 (1):103-107.

Herbst, PH. 1968. *Flood Estimation for Ungauged Catchments*. Report No. 46. Division of Hydrology, Department of Water Affairs, Pretoria, RSA.

Hey, RD and Thorne, CR. 1986. Stable channels with mobile gravel Beds, *Journal of Hydraulic Engineering*, ASCE, 112 (8): 671-689.

Kellerhals, R. 1976. Stable channels with gravel paved beds. *Journal of Waterways and Harbours Division,* 102 (7): 813-829.

KenBohuslay, PE.2004. Hydraulic design manual. [Internet]. Texas Department of Transportation Design Division. Texas, USA, Available from: http://manuals.dot.state.tx.us/dynaweb/colbridg/hyd/@Generic__BookTextView/8;cs=default;ts=default. [Accessed 4 May 2004].

Klaassen, GJ and Vermeer, K.1988. *Channel Characteristics of the Braiding Jamuna River, Bangladesh.* Delft Hydraulics, The Netherlands. In: ed. White, WR, *International Conference on River Regime.* Paper E1. Hydraulics Research Limited, Wallingford, UK, 173-189.

Koegelenberg, FH, Lategang, MT, Mulder, D J, Reinders, FB, Stimie, CM and Viljoen, PD. 1997. Channels. In: (ed.) Kegelenberg, FH, *Irrigation Design Manual*, Ch.7. Institute for Agricultural Engineering, Silverton, RSA, 1-26.

Kundzewicz, ZW and Strupczewski, WG. 1982. Approximate translation in the Muskingum model. *Journal of Hydrological Sciences*, 27 (-): 19-17.

Kundzewicz, ZW. 2002. Prediction in ungauged basins; A systemic perspective. [Internet]. Research Centre for Agricultural and Forest Environment, Polish academy of Sciences, Bukowska, Poland. Available from: http://www.cig.ensmp.fr/~iahs/PUBs/Brasilia-apers/Kundzewicz.pdf [Accessed 10 June 2003].

KZN Tourist Map. 2003. 1:100 000 KZN Tourist Map. AC BRABY & Tourism KZN, Pinetown, RSA.

Lacey, G. 1930. Stable channels in alluvium, *Minutes of Proceedings of Institute of Civil Eng*, 229 (-):259-292.

Lacey, G. 1947. A general theory of flow in alluvium, *Journal supplement*, Institute of Civil Eng., No. 8, paper 5518, 425-451.

Land & Water Australia. 2004. Stream roughness-Cowan method. [Internet]. The river team, Canberra, Australia. Available from: http://www.rivers.gov.au/roughness/cowan.htm. [Accessed 1 July 2004].

Lawler, EA. 1964. Flood routing, In: (ed.) *Handbook of Applied Hydrology*. Section 25-II. River Division, US Army Corps of Engineers, Ohio, USA, 35-58.

Limerinos, JT.1970. Determination of the Manning coefficient from measured bed roughness in natural channels. US Geological Survey Water Supply Paper No.1898-B. California Department of Water Resources, California, USA.

Linsley, RK, Kohler, MA and Paulus, JLH. 1982. *Hydrology for Engineers*. McGraw-Hill New York, USA.

Linsley, RK, Kohler, MA and Paulus, JLH. 1988. *Hydrology for Engineers*. McGraw-Hill New York, USA.

Moramarco, T and Singh, VP. 2001. Simple method for relating local stage and remote discharge. *Journal of Hydrologic Engineering*, 6 (1): 78-81.

McCarthy, GT. 1938. The unit hydrograph and flood routing. In: (ed.) US Army Corps of Engineers, *Proceedings of Conference of North Atlantic Division*. .US Engineers Office. Providence, USA.

Mohan, S. 1997. Parameter estimation of non-linear Muskingum models using genetic algorithm. *Journal of Hydraulic Engineering*, 123 (2):137-142.

Muthiah, P, O'Connell, PE and Raju, KGR. 2001. Field application of a variable-parameter Muskingum method. *Journal of Hydrologic Engineering*, 6 (3):196-207.

Mutreja, KN. 1986. *Applied Hydrology*. Tata McGraw-Hill, New Delhi, India.

Nash, JE and Sutcliffe, JV. 1970. River flow forecasting through conceptual models. Part I –A discussion of principles. *Journal of Hydrology*, 10 (2):82-290.

NERC. 1975. Flood routing studies. Report No. V-III, Natural Environment Research Council, London, UK.

Nixon, M. 1959. A study of bankfull discharge of the rivers in England and Wales, *Proceedings of the Institution of Civil Engineers*, 12 (-): 157-174.

NRCS. 1972. Flood Routing, [Internet], Natural Resources Conservation Service, US Department of Agriculture, Beltsville, USA. Available from: ftp://ftp.wcc.nrcs.usda.gov/downloads/hydrology_hydraulics/neh630/630ch17.pdf [Accessed 20 April 2003].

O'Donnell, T. 1985. A direct Three–Parameter Muskingum Procedure incorporating lateral inflow. *Hydrological Sciences*, 30 (4): 497-495.

O'Donnell, TP, CP and Woods, RA. 1988. An improved three-parameter Muskingum routing procedure. *Journal of Hydraulic Engineering*, 114 (5): 516-529.

Perumal, M and Raju, KGR. 1998. Variable-parameter stage-hydrograph routing method. I: Theory. *Journal of Hydrologic Engineering*, 3 (2):109-114.

Pitman, WV and Stern, JA. 1981. *Design flood determination in SWA-Namibia*: Report No. 14/81.University of Witwatersrand, Johannesburg, RSA.

Ponce, VM. 1989. *Engineering Hydrology*. Prentice-Hall Inc., New Jersey, USA.

Ponce, VM and Yevjevich, V. 1978. Muskingum-Cunge method with variable parameters. *Journal of the Hydraulics Division*, 104 (12): 1663-1667.

Ponce, VM, Lohani, AK. and Scheyhing, C. 1996. Analytical verification of Muskingum-Cunge routing. *Journal of Hydrology Amsterdam*, 174 (-): 235-241.

Punmia, BC and Pande, B B L. 1981. *Irrigation and Water Power Engineering*, Standard Publishers Distributors, Delhi, India.

Reed, DW. 1984. A *review of British floods forecasting practice*. Report. No. 90. Institute of Hydrology, Willington, UK.

SAICEHS. 2001. Quality Flow Measurements at Mine Sites [Internet]. Science Applications International Corporation Environment and Health Science Group, Environment Protection Agency, Idaho Falls, USA. Available from http://www.earthwardconsulting.com/library/600R01043Complete.pdf. [Accessed 24 June 2004].

Savenije, HHG. 2003. The width of a bankfull channel; Lacey's formula explained. *Journal of Hydrology* 276 (2003): 176-183.

Shaw, EM. 1994. *Hydrology in Practice*. TJ press (Padstow) LTD, Cornwall, UK.

Shen, HW and Julien, PY. 1993. Erosion and Sediment Transport. In: (ed.) Maidment, DR, Hand *Book of Hydrology,* Ch. 12. McGraw-Hill, New York, USA, 1-61.

Schulze, RE, Lynch, SD, Smithers, JC, Pike, A, and Schmidt, EJ. 1995. Statistical output from ACRU. In: (ed.) Schulze, RE, *Hydrology and Agrohydrology: A Text to Accompany the ACRU 3.00 Agro hydrological Modelling System*, AT Ch. 21. Water Research Commission, Pretoria, RSA, 1-35.

Schulze, RE, Howe, BJ, Lynch, SD, Maharaj, M, Melvile -Thomson, B. 1997. South African Atlas of Agrohydrology and-Climatology. Water Research Commission, Pretoria, RSA.

Schulze, RE and Taylor, V. 2002. Hydrology for Environment, life and policy [Internet]. Basin Initiative Thukela Catchment KZN, South Africa. Available from: http://www.riob.org/ag2002/Thukela.htm [Accessed 12 April 2004].

Simons, DB and Albertson, ML 1963. Uniform water conveyance Channels in alluvial material. TASAE, 128 (3399).

Singh, VP and McCann, RC. 1980. Some notes on Muskingum method of flood routing. *Journal of Hydrology*, 48: 343-361.

Singh, VP. 1988. *Rainfall-Runoff Modeling*. Prentice Hall, New Jersey, USA.

Singh, VP and Woolhiser, AD. 2002. Mathematical modelling of watershed hydrology. *Journal of Hydrologic Engineering,* 7 (4): 270-292.

Smithers, JC and Caldecott, RE. 1993. Development and verification of hydrograph routing in a daily simulation model. *Water SA,* 19 (3): 263 - 267.

Smithers, JC and Caldecott, RE. 1995. Hydrograph Routing. In: (ed.) Schulze, RE, *Hydrology and Agrohydrology: A Text to Accompany the ACRU 3.00 Agrohydrological Modelling System.* AT Ch. 13. Water Research Commission, Pretoria, RSA, 1-10.

Smithers, JC. 2003. Convert varying increment time series to fixed increment time series FORTRAN program. School of Bioresources Engineering and Environmental Hydrology, University of KwaZulu-Natal, Pietermaritzburg, RSA

South Africa Map 1989. 1:50 000 South Africa Map. Chief Directorate: Surveys and land Information, Pretoria, RSA.

SPSS11 2003. Statistical Software Package, Chicago, USA.

Thukela Basin Consultants 2001. *Thukela Water Project Feasibility Study Engineering Investigations Main Report.* Report No. PBV000-00-3199. Department of Water Affairs and Forestry, Pretoria, RSA.

Tung, YK. 1985. River flood routing by non-linear Muskingum method. *Journal of Hydraulic Engineering*, 111 (12): 1447-1460.

US Army Corps of Engineers 1993. River Hydraulics. [Internet]. US Army Corps of Engineers Manual 1110-1-1416, Washington, DC, USA. Available from: http://www.usace.army.mil/inet/usace-docs/eng-manuals/em1110-2-416/entire.pdf. [Accessed 12 April 2004].

US Army Corps of Engineers 1994a. Engineering Design and Flood-Runoff Analysis [Internet]. US Army Corps of Engineers Manual 1110-2-1417, Washington DC, USA. Available from: http://www.usace.army.mil/inet/usace-docs/eng-manuals/em1110-2-1417/c-9.pdf. [Accessed 15 April 2003].

US Army Corps of Engineers 1994b. Methods for Predicting n Values for the Manning Equation [Internet], US Army Corps of Engineers Manual 1110-2-1601, Washington DC, USA. Available from: http://www.rivers.gov.au/roughness/docs/MethodsforPredictingManningsn.pdf. [Accessed 2 July 2004].

Viessman, W, Lewis, GL and Knapp, JW. 1989. *Introduction to Hydrology.* Harper and Row, New York, USA.

Wilson, BN and Ruffin, JR. 1988. Comparison of physically based Muskingum methods. *Transactions of ASAE,* 31 (-): 91-97.

Wilson, EM. 1990. *Engineering Hydrology.* MacMillan, Hong Kong, China.

9. APPENDICES

Appendix A

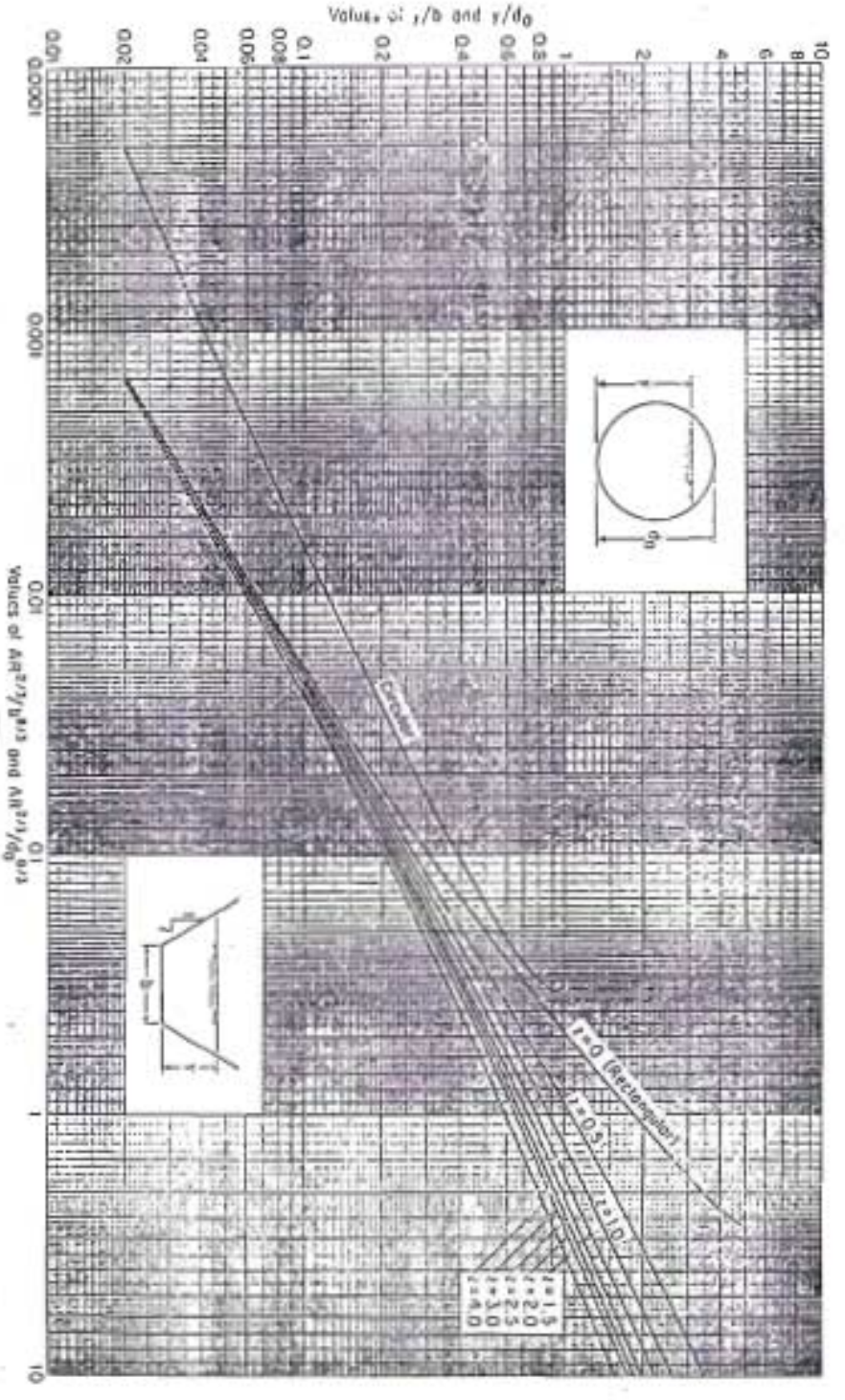

Figure A.1 Curves for determining the normal depth (Chow, 1959)

Table A.1 Geometrical properties of general channel shapes (Koegelenberg *et al.*, 1997)

Sketches	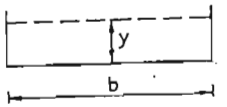	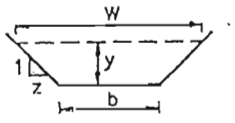	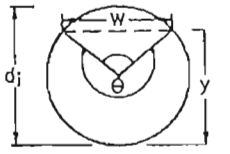	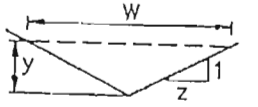	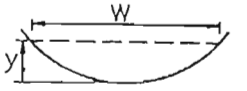
Cross sectional shape	**Rectangular**	**Trapezoidal**	**Circular (> ½ full)**	**Triangular**	**Parabolic**
Area (A)	by	$(b + zy)\,y$	$\frac{d_i^2}{8}\left(2\pi - \frac{\pi\theta}{180} + \sin\theta\right)$	zy^2	$\frac{2yW}{3}$
Wetted perimeter (P)	$b + 2y$	$b + 2y\sqrt{1 + z^2}$	$\frac{\pi d_i\,(360 - \theta)}{360}$	$2y\sqrt{z^2 + 1}$	$W + \frac{8y^2}{3W}$
Top width (W)	b	$b + 2zy$	$(\sin\frac{\theta}{2})\,d_i$	$2zy$	$\frac{3A}{2y}$
Hydraulic radius (R)	$\frac{by}{b + 2y}$	$\frac{(b + zy)y}{b + 2y\sqrt{1 + z^2}}$	$\frac{45d_i}{\pi(360-\theta)}\left[2\pi - \frac{\pi\theta}{180} + \sin\theta\right]$	$\frac{zy}{2\sqrt{z^2 + 1}}$	$\frac{2yW^2}{3W^2 + 8y^2}$
Hydraulic mean depth (D_m)	y	$\frac{(b + zy)y}{b + 2zy}$	$2\pi - \frac{\pi\theta}{180} - \sin\theta$	$\frac{y}{2}$	$\frac{2y}{3}$

NB: θ is measured in degrees